ROLE OF C-TERMINUS OF HSC70 INTERACTING PROTEIN IN DETERMINING NEURONAL FATE IN ACUTE INJURY

By

Jeannette N. Stankowski

Dissertation

Submitted to the Faculty of the

Graduate School of Vanderbilt University

in partial fulfillment of the requirements

for the degree of

DOCTOR OF PHILOSOPHY

in

Neuroscience

May, 2011

Nashville, Tennessee

Approved:

Professor BethAnn McLaughlin

Professor Pat R. Levitt

Professor Brian E. Wadzinski

Professor Deborah G. Murdock

ACKNOWLEDGEMENTS

This work would not have been possible without the guidance and support of my mentor Dr. BethAnn McLaughlin. From the day I started in the McLaughlin lab, Dr. McLaughlin encouraged me to take on new and challenging tasks, to think critically and to be innovative and creative. It is due to Dr. McLaughlin's guidance and her leading by example as an excellent scientist that has allowed me to develop into the successful and confident scientist that I am now. Dr. McLaughlin never hesitated to take time out of her busy schedule to teach me new scientific techniques and to discuss my project and new scientific concepts and ideas. These one-on-one learning opportunities were what I valued most and further underlined Dr. McLaughlin's outstanding qualifications as a mentor. It was, and still is, obvious that the success and overall well-being of her graduate students is dear to Dr. McLaughlin's heart. I cannot thank Dr. McLaughlin enough for constantly supporting and motivating me on my path to become not only a better scientist but also a better person and I will always keep these past five years in wonderful memory.

Moreover, I would like to thank all members of the McLaughlin lab, past and present. It has been a true honor and pleasure to work with everyone, and I cannot thank the McLaughlin lab members enough for all their support throughout my time in Graduate School. Specifically, I would like to thank Amy Palubinsky and Jacquelynn Brown, not only for being outstanding colleagues with whom I could work on projects and discuss results, ideas and concepts, but also for being amazing friends. I am very

grateful to Amy and Jacquelynn for their constant support and encouragement, and for making daily research a wonderful and exciting endeavor.

My thesis committee played an integral role throughout my scientific education at Vanderbilt. I greatly appreciate the willingness of Drs. Pat Levitt, Brian Wadzinski and Deborah Murdock to provide help and support. Their guidance allowed me to investigate my thesis project from several different, interesting and exciting angles, and ultimately made my thesis project stronger. My committee always encouraged me to strive toward becoming a better scientist, and I am extremely grateful for their faith in my ability to work hard and conduct great science. I will always remember our committee meetings as a positive and vibrant part of my training.

I would also like to thank several very important collaborators at Vanderbilt, whose input and expertise was integral to my scientific education. Drs. Gregg Stanwood, Daniel Liebler and Jiang Cai opened their doors to me and my thesis project and never hesitated to discuss new ideas with me, and personally taught me new experimental techniques which further strengthened my project. I am extremely grateful for all their time and help and for giving me the opportunity to learn from them.

The NeuroStroke group at Vanderbilt University also played a crucial role in my scientific education. Drs. Howard Kirshner, Anne O'Duffy, Derek Riebau and former member Dr. Rishi Gupta helped me to better understand the existing gap between basic scientific research and the clinical realities of stroke care. Our monthly stroke meetings as well as individual conversations significantly broadened my knowledge about the complexity of stroke pathology as well as new cutting edge therapeutics and treatments that are used for stroke treatment.

I am also extremely grateful for all the support provided by the Neuroscience Graduate Group. Drs. Mark Wallace and Douglas McMahon were extremely supportive throughout my career at Vanderbilt, and I appreciate their time to speak to me about my scientific progress and their care of me as a Neuroscience graduate student. I know that I could have not chosen a better graduate group, and I would also like to express my special thanks to Steve Edminster, Shirin Polous, Mary Michael-Woolman and Rosalind Johnson not only for always having time to answer my many questions, but also for being amazing friends. I would also like to thank my dear friends Ms. Gail Ingle, Evan Cohen, Colin Stanwood and Amelia Stanwood. The support I received from them was more than I could have ever asked for. During good and bad times, I was able to rely on them, share my excitement with them and have a caring shoulder to lean on. I know that I would have not been able to get this far without their hugs, support and smiles. Ms. Gail, Evan, Colin and Amelia were more than just friends to me – they were my little American family and I am so grateful that I had the honor to meet each and every one of them.

My family has played a tremendous role during my time in Graduate School. My parents, Ilona and Marek Stankowski, as well as my sister Isabella Stankowski, were always there for me and constantly encouraged and supported my each and every move. They always listened to me talk about my project and shared my undeniable excitement about CHIP with me. Their patience and love motivated me to pursue my dreams. I am extremely grateful, blessed and proud to have such an outstanding family. Moreover, I would like to thank my grandparents, Margot and Günther Gaida as well as Ewa and Czesław Stankowski. My grandparents always believed in me and supported my scientific endeavors to the fullest. Opa Günther constantly stressed the importance of a

great education to Isabella and I, and he always encouraged us to work hard in order to reach our goals. My grandparents were always interested in my research project, and they frequently told me of their faith in me to make great advancements in health treatments. One of the last things Oma Ewa said before she lost her year-long battle against Parkinson's disease was "Jeannette will find the cure for Parkinson's disease." Oma Ewa's final words of encouragement redoubled my passion for science and I am tremendously appreciative of all that Vanderbilt did to allow me to reach my goals. I know that my grandparents are constantly by my side and that they are incredibly proud of their 'Sonnenschein'.

This work was financially supported by NIH grants NS050396 (BM) and the Vanderbilt Neuroscience predoctoral training Fellowship T32ES014668 (JS). Statistical and graphical support was provided by P30HD15052 (Vanderbilt Kennedy Center).

TABLE OF CONTENTS

Page

LIST OF TABLES

Table **Page**

LIST OF FIGURES

LIST OF ABBREVIATIONS

4-HNE	4-hydroxy-2-nonenal
AD	Anoxic depolarizations
AMPA	α-amino-3-hydroxy-5-methyl-4-isoxazolepiopionic acid
BAG-1	Bcl-2-associated athanogene 1
BAG-2	Bcl-2-associated athanogene 2
Bax	Bcl-associated X protein
BSA	Bovine serum albumin
CBF	Cerebral blood flow
CHIP	C-terminus of HSC70 interacting protein
CNS	Central nervous system
COX IV	Cytochrome c oxidase
C-terminus	Carboxy terminus
DAPI	4,6-diamidino-2-phenylindole
DIV	Days *in vitro*
DMEM	Dulbecco's modified eagle medium
DMSO	Dimethyl sulfoxide
DNPH	2,4-dinitrophenylhydrazine
DNP	Dinitrophenyl
DR	Derivatization reaction
DTT	Dithiothreitol
EDTA	Ethylenediaminetetraacetic acid

EGTA	Ethyl glycol tetraacetic acid
ER	Endoplasmic reticulum
ETC	Electron transport chain
FBS	Fetal bovine serum
Fk2	Antibody against mono – and polyubiquitinated proteins
GAPDH	Glyceraldehyde 3-phosphate dehydrogenase
GCL	Glutamate cysteine ligase
GFAP	Glial fibrillary acidic protein
GFP	Green fluorescent protein
GPx	Glutathione peroxidase
GS	Glutathione synthase
GSSG	Glutathione dissulfide
GSH	Glutathione
H_2O_2	Hydrogen peroxide
HBSS	Hank's balanced salt solution
HEPES	4-(2-hydroxyethyl)-1-piperazineethaanesulfonic acid
Het	Heterozygous
HIP	HSC70 interacting protein
$HOCl^-$	Hypochlorous acid
HOP	HSC70 organizing protein
HPLC	High performance liquid chromatography
HRP	Horseradish peroxidase
HSC70	Heat shock cognate 70

HSF1	Heat shock factor 1
HSP	Heat shock protein
HSP40	Heat shock protein 40
HSP70	Heat shock protein 70
HSP72	Heat shock protein 72
HSP90	Heat shock protein 90
HSPBP1	HSP70 binding protein 1
IgG	Immunoglobulin G
K48	Lysine 48
KO	Knockout
LC3	Autophagy protein
LDH	Lactate dehydrogenase
MEM	Minimum essential medium
MG132	Z-Leu-Leu-Leu-al
MTT	3-(4,5-dimethylthiazol-2-yl)-2,5-diphenyltetrazolium bromide
NaCl	Sodium chloride
NC	Negative control
NeuN	Neuronal nuclei
NINDS	National Institute of Neurological Disorders and Stroke
NMDA	*N*-methyl-D-aspartate
nNOS	Nitric oxide synthase
NP-40	Nonyl phenoxypolyethoxylethanol
N-terminus	Amino terminus

NXY-095	Disodium 2,4-disulfophenyl-N-tert-butinitrone
O_2	Oxygen
$O_2^{\bullet-}$	Superoxide radical
OE	Overexpressing
OGD	Oxygen glucose deprivation
$OH^{\bullet}$	Hydroxyl radical
$ONOO^-$	Peroxynitrite
PBS	Phosphate buffer saline
PCR	Polymerase chain reaction
PI	Propidium iodide
PID	Peri-infarct depolarizations
PINK1	PTEN induced putative kinase 1
PMI	Post-mortem interval
PVDF	Polyvinylidene difluoride
RING	Really interesting new gene
ROS	Reactive oxygen species
RT	Room temperature
SAINT	Stroke-Acute ischemic NXY treatment
SDS	Sodium dodecyl sulfate
SEM	Standard error of the mean
siRNA	Small interfering RNA
SOD	Superoxide dismutase
Suc-LLVY-AMC	Suc-Leu-Leu-Val-Tyr-AMC

TBS	Tris-buffered saline
TBST	Tris-buffered saline/Tween 20
TIA	Transient ischemic attack
t-PA	Tissue-plasminogen activator
TPR	Tetratricopeptide repeat domain
UPP	Ubiquitin proteasome pathway
VDAC	Voltage-dependent anion channel
WT	Wild type

CHAPTER I

INTRODUCTION

Stroke

Stroke is the most serious and debilitating neurological disorder in the United States. It is the third leading cause of death in this country after cancer and heart disease (Lloyd-Jones et al., 2009). Moreover, stroke is the leading cause of severe, long-term adult disability, accounting for $68.9 billion in health care costs and economic losses in the US in 2009 alone (Lloyd-Jones et al., 2009). The most recent statistical update by the American Heart Association Statistics Committee and Stroke Statistics Subcommittee underscores these somber statistics citing that approximately 795,000 people in the US experience a new or recurrent stroke, of which 610,000 cases are first attacks (Lloyd-Jones et al., 2009).

Stroke subtypes

Strokes are predominately ischemic in nature, comprising 87% of all strokes (Lloyd-Jones et al., 2009) (**FIGURE 1.1**). An ischemic stroke is defined as the presence of a thrombosis, stenosis, embolism or systemic-hypoperfusion leading to the obstruction of blood flow to the brain, thereby decreasing the amounts of oxygen and glucose reaching this organ (Doyle et al., 2008). Of all patients suffering from ischemic stroke, 70% present with a cerebral artery occlusion (Kidwell et al., 2004). The remaining 13% of all strokes are hemorrhagic in nature (**FIGURE 1.1**), resulting from the rupture of a

blood vessel in the brain and subsequently leading to the leakage of blood into the surrounding brain tissue (Winkler et al., 2001).

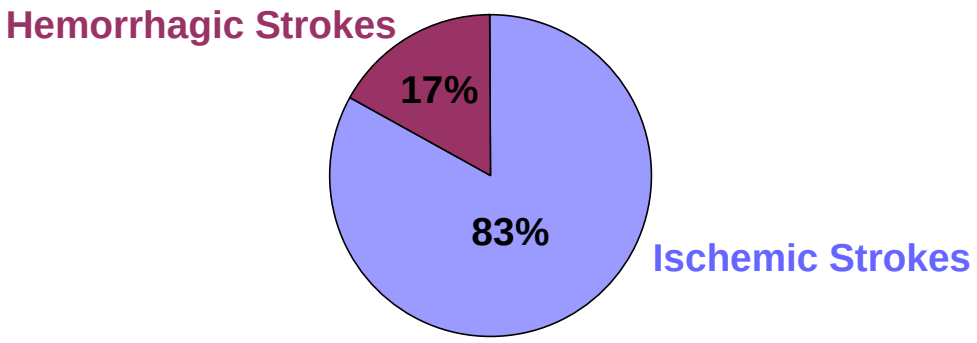

FIGURE 1.1: Statistical analysis of stroke subtypes. Out of all strokes, 83% are ischemic in nature, indicating that the presence of an embolism, plaque, stenosis or hypoperfusion results in the obstruction of blood flow to the brain. The remaining 17% are hemorrhagic in nature, resulting from the rupture of a blood vessel in the brain and subsequently leading to the leakage of blood into the surrounding brain tissue.

While the numbers of strokes are massive, these do not take into account the incidence of silent strokes. Silent strokes are defined as lesions that are comparable to cerebral infarcts and hemorrhages from a neuroimaging and neuropathological perspective, yet they do not show the characteristic clinical symptoms associated with symptomatic stroke (Leary et al., 2003). Despite the lack of clinical symptoms, silent strokes are associated with substantial neurological, medical and psychiatric deficits (Leary et al., 2003). It is suggested that the number of silent stroke incidences increases with age, and statistical analyses from 1998 revealed that in the United States, 9,040,000 cases of silent strokes were ischemic in nature, while 1,940,000 cases were hemorrhagic in nature (Leary et al., 2003). Furthermore, to accurately assess annual stroke incidences, one would also have to include patients experiencing transient ischemic attacks (TIAs)

(Leary et al., 2003), which are defined as "a sudden, focal neurological deficit that lasts for less that 24 hours" (Albers et al., 2002). Unlike symptomatic strokes, TIAs do not result in permanent brain damage (Albers et al., 2002). Taken together, these numbers and facts not only underscore that the actual annual stroke burden is highly underestimated, but also point to a pressing need to even better understand the biology underlying stroke. Improved identification of candidates that are at high risk for either symptomatic or asymptomatic stroke would enable more accurate and efficient treatment with appropriate therapeutics at the earliest possible time point, with the ultimate goal of preventing the occurrence of an actual stroke.

Stroke treatment – Lost in translation?

Research aimed at identifying and understanding molecular pathways involved in neuronal death following ischemic stroke has advanced at an impressive rate uncovering a myriad of complex cellular processes that trigger cell death. Processes leading to neuronal death following ischemic stroke include ionic imbalance, peri-infarct depolarization, glutamate mediated excitotoxicity, oxidative stress and apoptosis (Doyle et al., 2008, Mehta et al., 2007, Onteniente et al., 2003) (**FIGURE 1.2**). Notably, the same fundamental processes cut across the boundaries of other neurological diseases including Parkinson's, Alzheimer's and Huntington's diseases (Choi, 1992, Greene et al., 1996).

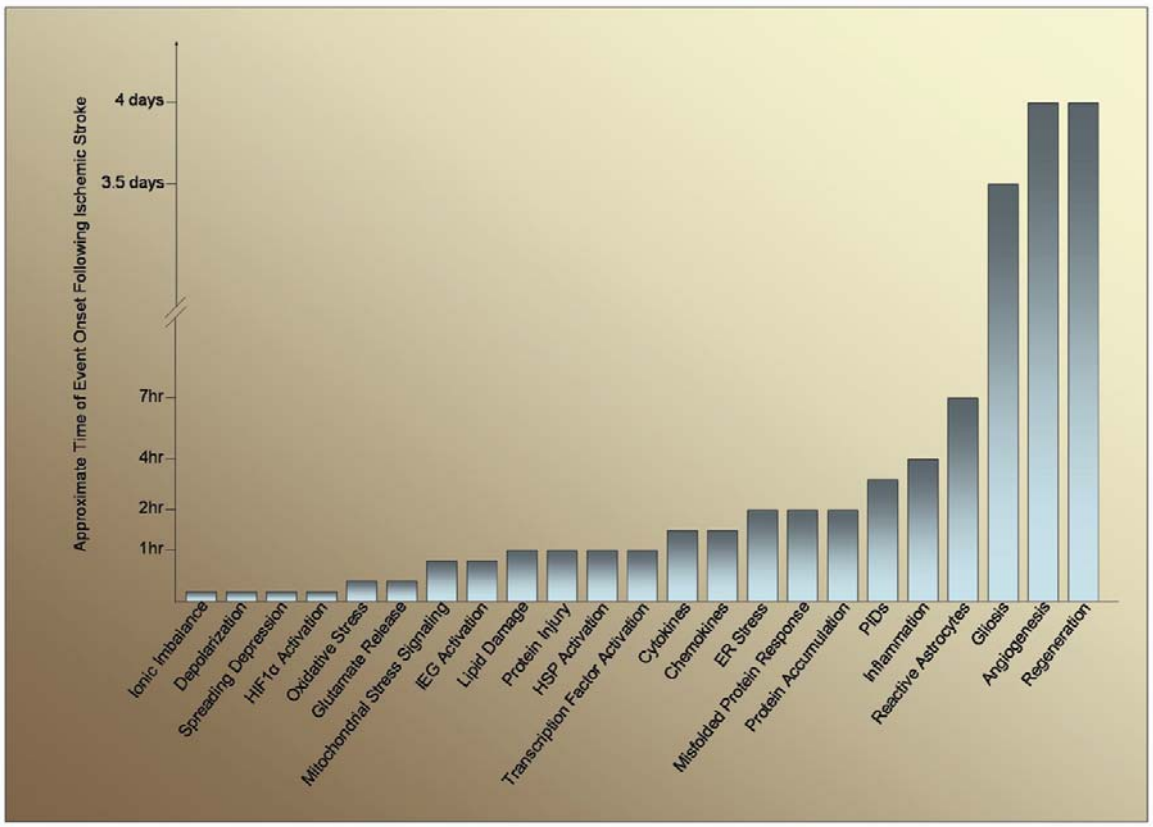

FIGURE 1.2: Approximate timeline of molecular pathway onsets following ischemic stroke. Obstruction of blood flow to the brain via the presence of a thrombosis, embolism or systemic-hypoperfusion results in a drastic reduction in ATP production with ultimately leads to the initiation of the depicted ischemic cascade which ultimately results in neuronal death.

Despite our wealth of knowledge regarding the pathology of delayed neuronal death following ischemic stroke, clinical trials aimed at blocking these events have been extremely disappointing. We have failed to develop any safe and effective neurotherapeutics that can prevent stroke-induced cell death. Of the more than 100 agents that were assessed in Phase I-III clinical trials, only one pharmacological agent has been approved by the Food and Drug Administration for use in acute ischemic stroke: the thrombolytic tissue-plasminogen activator (t-PA) (Johnston, 2006). t-PA dissolves blood

clots and re-establishes blood flow to the tissue downstream of the occluded cerebral artery (Armstead et al., 2006, Johnston, 2006). When administered intravenously within the first three hours of stroke onset, t-PA can dramatically improve clinical outcome (Liberatore et al., 2003, Lopez-Atalaya et al., 2008). This tight time window has recently been expanded to 4.5 hours (Gupta et al., 2006, Lansberg & Schrooten et al., 2009). In spite of the promise of t-PA, less than 3% of eligible patients receive thrombolytic therapy. This huge clinical gap has been attributed to the lack in awareness and education regarding t-PA as well as the failure of patients to arrive at hospitals within the therapeutic time window (Armstead et al., 2006). While there are clear benefits of t-PA, studies have, however, shown that prolonged or delayed use of t-PA is not without risk. Due to its function as a serine protease, t-PA can cross the blood-brain barrier, destroy the brain parenchyma and thereby contribute to the increased risk of intracranial hemorrhage that is observed in these stroke patients (Armstead et al., 2006, Lansberg & Bluhmki et al., 2009, Lansberg & Schrooten et al., 2009, Liberatore et al., 2003, Marler, 1995).

While the goal of t-PA therapy is to re-establish circulation to an ischemic area, a multitude of studies has been conducted with the goal to identify bona fide neuroprotective agents which block neurodegeneration in the hours to days following stroke. The National Institute of Neurological Disorders and Stroke (NINDS) invested more than $200 million on stroke clinical trials from 1977-2002 (Marler, 2002). While many of these drugs were successful in preclinical stroke models, not a single therapy has proven to decrease morbidity and mortality in the clinical setting (Doyle et al., 2008). This issue has been extensively reviewed in an attempt to identify potential areas that

may have contributed to the startling failure to translate successful results obtained in basic science laboratories into the clinical setting. Amongst these, the appropriateness of experimental animals as well as commonly used *in vitro* stroke models has been criticized (O'Collins et al., 2006). With regard to experimental animals, there is a lack of model systems aside from rodents, and within rodent systems themselves, there is a deficiency in data from aging and diseased animals (O'Collins et al., 2006, Savitz et al., 2007). Moreover, data evaluating long-term neurological outcomes, complex behaviors and lasting benefits of treatments are also absent from current preclinical studies (Savitz et al., 2007). In the context of *in vitro* model systems of stroke, many preclinical trials focus on the role of a single molecular pathway governing cell fate, whereas a plethora of events are elicited in this heterogeneous disease (**FIGURE 1.2**) (O'Collins et al., 2006). More to the point perhaps, is the average lag of 7 years between the initial scientific findings obtained from *in vivo* and *in vitro* models and the actual onset of clinical trials, thereby further complicating the transition from bench to bedside (Johnston, 2006).

Stroke pathology and molecular events elicited following ischemic stroke

Despite the apparent failure to translate basic science results into the clinical setting, the few drugs available for use against stroke-induced cell death emerged from the knowledge gained from basic science research using *in vivo* and *in vitro* model systems of stroke. It is due to these results that scientists and clinicians were able to formulate and develop effective approaches aimed not only at preventing disease, but also at treating a multitude of human diseases (Lenfant, 2003). As a result, basic science research needs to advance further in the quest to either identify novel, safe and effective

therapeutics for the use in ischemic stroke, or to improve the current understanding of previously identified agents in order to determine why certain agents failed in the clinical setting. To underline potential sites for neurotherapeutic intervention, major molecular events elicited following stroke will be chronologically examined in this chapter.

Changes in energy metabolism following ischemic stroke

Under normoxic conditions, neurons conduct electrical impulses in the form of action potentials, a process dependent upon Na^+, K^+ and Ca^{2+} homeostasis. Fully 50-60% of the total ATP synthesized in the brain is used for the maintenance of these electrochemical concentration gradients (Erecinska et al., 1994). During ischemic stroke, obstruction of cerebral blood flow (CBF) to the brain and the subsequent lack of oxygen and glucose supply results in a drastic reduction in aerobic ATP production. Using *in vivo* rat models of transient ischemia, studies have demonstrated that total ATP levels drop precipitously within 2 minutes following the insult (Doyle et al., 2008, Erecinska et al., 1994, Lipton, 1999, Onteniente et al., 2003). Moreover, glucose levels drop to 50% of baseline values and ATP levels drop to approximately 25% of normal values in the ischemic core, which is the brain region of maximum and irreversible damage (Lipton, 1999). The use of *in vivo* rat model systems of ischemic stroke have furthermore demonstrated that ATP levels in the core remain decreased between 5min and 4hr after the ischemic insult and return to approximately two-thirds of basal values upon reperfusion (Lipton, 1999).

In contrast, within the penumbra, the brain region surrounding the core where neurons are functionally impaired yet potentially salvageable, glucose utilization initially

increases at early time points, but falls to about 50% of normal values by 3.5hr. Notably, ATP levels in the ischemic penumbra rapidly drop to about 50-70% of basal levels (Lipton, 1999) resulting in the inability of neurons to maintain their ionic homeostasis (Doyle et al., 2008). The subsequent intracellular increase in Na^+ and decrease in K^+ leads to the depolarization of neuronal membranes (Onteniente et al., 2003). In the ischemic core, this sudden and profound loss of membrane potential is termed anoxic depolarization, an event which is characterized by neuronal death following the opening of voltage gated Ca^{2+} channels and rapid influx of Ca^{2+} into neurons (Jarvis et al., 2001, Joshi et al., 2001, Mehta et al., 2007, Onteniente et al., 2003). The core propagates spontaneous electrical waves known as peri-infarct depolarizations (PIDs) to the penumbra, leading to a rapid cycling of de- and repolarizations within these neurons (Fabricius et al., 2006, Mehta et al., 2007, Onteniente et al., 2003). While anoxic depolarizations occur within minutes following the initial insult, recurring PIDs occur in the penumbra 3-4hr following stroke, setting the stage for further degeneration (Joshi et al., 2001, Onteniente et al., 2003).

Glutamate release and excitotoxicity

The initial loss of ATP and the resulting inability of molecular pumps to maintain ionic gradients across the neuronal membrane ultimately results in the depolarization of neurons, an event which is accompanied by the influx of Ca^{2+} into neurons via voltage gated Ca^{2+} channels (Mehta et al., 2007). Ca^{2+} triggers the release of neurotransmitters, notably glutamate, which is the major excitotoxic neurotransmitter in the CNS (Kandel et al., 1999). The use of *in vivo* brain microdialysis studies has shown that under

physiological conditions, cytosolic glutamate concentrations reach up to 10mM, while synaptic glutamate concentrations range between 1-5μM (Doyle et al., 2008, Lipton, 1999, Matsumoto et al., 1996, Mehta et al., 2007). Following ischemic stroke, glutamate levels can reach concentrations that are up to 100 times higher than under basal conditions (Kanthan et al., 1995). Moreover, regions rich in glutamatergic innervation such as the cortex and hippocampus are some of the most vulnerable to ischemic stroke (Benveniste et al., 1984).

The presence of sodium-dependent glutamate transporters in pre- and postsynaptic membranes is directly involved in the regulation of cellular signaling by assuring the maintenance of appropriate glutamate gradients across the plasma membrane as well as proper clearing of glutamate from the synaptic cleft (Doyle et al., 2008). The rise in cytosolic Na^+ concentrations following ischemic stroke results in the reversal of glutamate transporters, allowing glutamate to flow from the cytosol into the synaptic cleft down its concentration gradient (Doyle et al., 2008). The reversal of the activity of the glutamate transporters prevents the reuptake of glutamate into the cell, thus allowing extracellular glutamate concentrations to reach neurotoxic levels (Doyle et al., 2008). Using microdialysis in animal models of transient ischemia, Benveniste and colleagues demonstrated that extracellular glutamate concentrations in the hippocampus start to rise within the first 1-2min following the insult and can reach concentrations ranging between 16 and 30μM within 15min upon transient ischemia (Benveniste et al., 1984). The presence of high levels of glutamate within the synaptic cleft results in massive overactivation of ionotropic glutamate receptors, including the *N*-methyl-D-aspartate (NMDA) and the α-amino-3-hydroxy-5-methyl-4-isoxazolepropionic acid (AMPA)

receptors. The pathological overstimulation of these receptors in combination with downstream activation of cell death signaling pathways is commonly referred to as "excitotoxicity" (Brouns et al., 2009, Choi, 1992, Greene et al., 1996, Martin et al., 1998). NMDA receptors are the prominent route of Ca^{2+} influx during glutamatergic transmission. Opening of these ligand gated channels results in potentially neurotoxic increases in intracellular Ca^{2+} levels (Mehta et al., 2007). While Ca^{2+} is involved in the regulation of a variety of adaptive cellular processes including cell growth, differentiation and enzyme function, high intracellular Ca^{2+} levels can promote the activation of cellular cascades leading to cell death (Mehta et al., 2007, Onteniente et al., 2003).

In contrast to NMDA receptors, AMPA receptors are impermeable to Ca^{2+} by virtue of their GluR2 subunit. Interestingly, studies using the oxygen glucose deprivation (OGD) paradigm as an *in vitro* model to investigate brain ischemia demonstrated that both mRNA and protein levels of the GluR2 subunit are substantially reduced following ischemia and that the insertion of GluR2-lacking AMPA receptors into the postsynaptic membrane is promoted, thereby further increasing Ca^{2+} influx (Gorter et al., 1997, Liu et al., 2006, Noh et al., 2005, Pellegrini-Giampietro et al., 1992).

The sustained increase in intracellular Ca^{2+} levels results in the initiation of a plethora of cytosolic and nuclear events. These include generation of reactive oxygen species (ROS) and activation of Ca^{2+}-dependent enzymes, such as calpains, endonucleases, phospholipase A, cyclooxygenases and neuronal nitric oxide synthase (nNOS) which govern extensive cellular damage (Goll et al., 2003, Lipton, 1999, Mehta et al., 2007). For instance, the activation of both the micromolar-Ca^{2+} requiring calpain (μ-calpain) and the millimolar-Ca^{2+} requiring calpain (m-calpains) has been associated

with the pathology of ischemic stroke (Goll et al., 2003), as these proteases are involved in activating apoptosis via their ability to cleave and activate caspase-9 (Goll et al., 2003). Moreover, calpains have also been shown to increase mitochondrial permeability transition activities, thereby leading to mitochondrial damage and the initiation of programmed cell death (Arrington et al., 2006, Lipton, 1999, Polster et al., 2005). Other targets of calpains include cytoskeletal proteins, such as MAP2, tubulin and spectrin, leading to the disruption of cytoskeletal networks and resulting in cell death (Lipton, 1999). In addition to apoptosis, morphological changes characteristic of necrotic and autophagic cell death have been noted to be involved in neuronal death following ischemic stroke (Adhami et al., 2006, Chu, 2008, Garcia et al., 1995, Martin et al., 1998, Sairanen et al., 2006, Unal-Cevik et al., 2004).

Oxidative Stress

Oxygen (O_2) is an essential element for the survival of all aerobic species. It is involved in a variety of processes including respiration and production of energy in the form of ATP by means of the mitochondrial electron transport chain. While the importance of oxygen for survival is indisputable, the risks harbored by this element and the fact that aerobic species are solely able to survive in the presence of oxygen due to the evolution of antioxidant systems are often times disguised. The dangers and damaging effects of oxygen lie in the generation of oxygen radicals, a process which predominantly occurs during oxidative energy metabolism in the mitochondria (Halliwell et al., 2007, Kleinhans et al., 2006).

By definition, a free radical is any molecule that contains an unpaired electron in its outermost orbital and is therefore capable of oxidizing other molecules (Gilgun-Sherki et al., 2002, Halliwell et al., 2007, Lambert et al., 2009). In its ground state, O_2 has two unpaired electrons available, rendering it suitable to oxidize other molecules (Halliwell et al., 2007, Hoidal, 2001). Reactions involving O_2 can result in the generation of reactive oxygen species (ROS), including superoxide radicals ($O_2^{\bullet -}$) and hydroxyl radicals ($OH^{\bullet}$), as well as non-radicals, including hydrogen peroxide (H_2O_2), and peroxynitrites ($ONOO^-$) (Halliwell et al., 2007, Lambert et al., 2009).

While low concentrations of ROS are essential for normal cellular function, the rapid and excessive generation of ROS along with a decrease in the detoxifying activities of intracellular antioxidants poses a danger for cellular survival as ROS can damage macromolecular structures including proteins, lipids and nucleic acids (Droge, 2002, Halliwell et al., 2007, Hancock et al., 2001, Lambert et al., 2009, Sykes et al., 2007). The imbalance between pro – and antioxidants is commonly referred to as "oxidative stress" and has been shown to be elicited following ischemic stroke as well as the subsequent reperfusion of brain tissue (Bolanos et al., 2009, Halliwell et al., 2007). Due to its high oxygen consumption and abundant lipid content, the brain is particularly susceptible to attack by ROS, which ultimately interferes with normal physiological brain function (Das et al., 2007, Pari et al., 2004).

Cellular sources of ROS

ROS are primarily generated during aerobic cellular respiration at the mitochondrial electron transport chain (ETC) (Droge, 2002, Kleinhans et al., 2006,

Lambert et al., 2009). Normally, electrons are transferred by a system of electron carriers to O_2, the final electron acceptor in the chain, in order to form H_2O. A significant proportion of electrons, however, "leaks" from intermediate electron carriers of the ETC directly onto oxygen, thereby resulting in the generation of superoxide radicals ($O_2^{\bullet -}$) (Halliwell, 1992, Page et al., 2010). About <5% of the total electron flow through the ETC accounts for electron leakage under physiological conditions (Halliwell, 1992), resulting in the formation of 2 billion $O_2^{\bullet -}$ and H_2O_2 molecules per cell per day in humans (Hoidal, 2001).

Targets of ROS: lipids, DNA, proteins

Reactive oxygen species can cause serious damage to all cellular macromolecules including proteins, lipids and nucleic acids (DNA and RNA). Damage by ROS has been associated with ischemic stroke, neurodegenerative diseases, diabetes and inflammatory diseases (Halliwell, 1992, Halliwell et al., 2007, Maisonneuve et al., 2009, Szeto, 2006). As a result, understanding the mode of action of ROS on macromolecules is of utmost importance in order to identify targets for therapeutic intervention.

Attack of DNA by ROS does not only result in damage to the purine and pyrimide bases and the deoxyribose sugars of DNA, but it also leads to strand breakage and interferes with processes including DNA repair, replication and transcription (Halliwell et al., 2007, Monaghan et al., 2009). The process of oxidative damage to lipids is commonly referred to as lipid peroxidation and has dramatic consequences for the structure, fluidity and function of biological membranes (Fam et al., 2003, Halliwell et al., 2007, Milne et al., 2005, Montine et al., 2004, Musiek et al., 2005). Moreover, lipid

peroxidation also results in the formation of biologically active byproducts, such as isoprostanes, cytotoxic aldehydes and hydrocarbons, which can subsequently damage other cellular components (Fam et al., 2003, Halliwell et al., 2007, Mehta et al., 2007, Milne et al., 2005, Monaghan et al., 2009, Montine et al., 2004).

Protein damage by ROS

With regard to the attack of ROS on proteins, it has to be noted that in contrast to the traditional notion that damage to proteins by ROS is random and non-specific, it has become increasingly clear that protein adduction by ROS is a highly selective and specific process (Halliwell et al., 2007, Liebler, 2008, Maisonneuve et al., 2009). 80% of all proteins are adducted at a single cysteine residue (Liebler, 2008), and amino acid residues, such as cysteines, methionines, histidines, arginines and lysines, are particularly prone to adduction by ROS (Dennehy et al., 2005, Halliwell et al., 2007, Liebler, 2008). Moreover, it has been shown that structural features of proteins, the presence of a transition metal as part of the protein structure and the proximity of a protein to the site of ROS generation also play important roles in conferring susceptibility of proteins to damage by ROS (Liebler, 2008, Maisonneuve et al., 2009).

Given that proteins are involved in a variety of cellular processes, including, amongst others, catalysis of cellular reactions, signal transductions, protein transport and receptor function, loss of protein function due to damage by ROS can have a large impact on overall cellular function (Dalle-Donne et al., 2003, Halliwell et al., 2007, Maisonneuve et al., 2009). Attack of proteins by ROS can be multimodal. On the one hand, proteins can be directly attacked by ROS, while on the other hand, damage to

proteins can be of secondary nature via attack of end-products of lipid peroxidation (Halliwell et al., 2007, Liebler, 2008).

A common biochemical marker of protein oxidation is the formation of carbonyl groups (aldehydes and ketones) on protein side chains. Carbonyl groups are composed of a carbon atom double-bonded to an oxygen atom, and are primarily formed on proline, arginine, lysine and threonine side chains (Dalle-Donne et al., 2003, Levine et al., 1990, Levine et al., 1994, Robinson et al., 1999, Shacter et al., 1994). Moreover, reactive aldehydes govern the formation of carbonyl groups on protein side chains including lysines, cysteines and histidines (Dalle-Donne et al., 2003, Maisonneuve et al., 2009). Protein adduction can irreversibly alter a proteins' structure and function and result in the accumulation of oxidatively modified proteins, a common pathological hallmark observed in neurological diseases (Halliwell et al., 2007, Liebler, 2008). In Chapter III we discussed how these attributes allowed us not only to determine total levels of oxidized proteins following acute oxidative injury, but also to identify the specific protein targets of oxidative stress.

Cellular antioxidant systems

Cells are equipped with robust cellular antioxidant defense mechanisms to aid in the scavenging and removal of ROS. An antioxidant is "any substance that significantly delays or prevents oxidation of that substrate" (Halliwell et al., 2007). There are a wide variety of antioxidants, including those that are synthesized *in vivo*, such as glutathione, catalase and superoxide dismutase (SOD), and those that are supplemented to the body

from the diet, such as ascorbic acid (Vitamin C) and alpha-tocopherol (Vitamin E) (Halliwell et al., 2007, Hancock et al., 2001).

The low molecular weight antioxidant glutathione (GSH) is, however, the most abundant cellular antioxidant with concentrations ranging between 0.5 and 10mM (Maher, 2005). This tripeptide is synthesized from glutamate, cysteine and glycine via the enzymatic activities of glutamate cysteine ligase (GCL) and glutathione synthase (GS) (Halliwell et al., 2007, Maher, 2005). Glutathione peroxidases (GPx) aid in the removal of H_2O_2 in a process that results in the oxidation of GSH, and the generation of H_2O and glutathione disulfide (GSSG) as reaction products. In whole cell extracts, the percentage of GSSG to GSH lies between 1 and 3%, while in mitochondria this percentage is elevated and ranges between 9-25% (Lenton et al., 1999). GSSG can be converted back to GSH with the help of glutathione reductase (Halliwell et al., 2007, Maher, 2005) and GSH can also scavenge a wide variety of other ROS, including $OH^{\bullet}$, hypochlorous acid ($HOCl^{-}$) and peroxynitrite ($ONOO^{-}$) (Halliwell et al., 2007).

Cellular Strategies to Handle Protein Stress – Molecular Chaperones

Despite the highly efficient role of cellular antioxidants in protecting macromolecular structures from the damaging effects of ROS, protein damage may still occur. When ROS overrun cellular defenses, cells rely on tightly regulated endogenous surveillance systems to remove injured proteins. These systems are specialized not only in maintaining and controlling proper protein structure and quality, but also in aiding to repair and restore proper protein function (Hohfeld et al., 2001, Kaarniranta et al., 2002, Voisine et al., 2010). At the core of the cellular surveillance system, or protein quality

control, lie molecular chaperones which are highly conserved, abundantly expressed proteins that are present in all cell types, tissues and subcellular compartments (Voisine et al., 2010). Expression levels of molecular chaperones can be regulated by a wide range of physiological and environmental stressors, yet a core group of sentinel molecules are also constitutively expressed in order to maintain protein homeostasis (Bukau et al., 2006, Douglas et al., 2010, Ellis et al., 1991, Voisine et al., 2010).

Heat Shock Proteins (HSPs)

The heat shock protein (HSP) molecular chaperones form the backbone of the protein sentinel system. They are highly conserved, abundantly expressed proteins with diverse functions, including the assembly of multi-protein complexes, transport of nascent polypeptides and regulation of protein folding (Hohfeld et al., 2001, Kiang et al., 1998, Nollen et al., 2002). Heat shock proteins can be divided into two main classes. The first class is composed of HSPs that are constitutively expressed in the tissue and are referred to as cognate proteins, while the second class is composed of HSPs that are synthesized immediately following stress and are referred to as inducible proteins (Snoeckx et al., 2001). The molecular chaperone heat shock protein 70 (HSP70) is the major stress inducible cytosolic chaperone and is upregulated with thermal stress, oxidative injury, and following acute and chronic injury (Cyr et al., 2002, Hohfeld et al., 2001). The HSP70 family has been broadly recognized for its neuroprotective properties which have been attributed to the binding and sequestering of activated caspases and other cell death proteins by HSP70 as well as to its ability to actively refold damaged substrates (Arndt et al., 2007, Beere et al., 2001, McLaughlin et al., 2003).

HSP70 operates as part of a multi-protein complex where associated co-chaperones alter the function of the complex (**FIGURE 1.3**) (Arndt et al., 2007, Hohfeld et al., 2001, Qian et al., 2006). For example, the E3 ubiquitin ligase C-terminus of HSC70 interacting protein (CHIP) competes with heat shock cognate 70 (HSC70) organizing protein (HOP) for C-terminal HSP70 binding, while Bcl-2-associated athanogene 1 (BAG-1) competes with HSC70 interacting protein (HIP) for N-terminal HSP70 binding (Arndt et al., 2007, Hohfeld et al., 2001). The formation of the HIP/HSP70/HOP complex is thought to direct HSP70 activity towards client protein refolding, whereas the CHIP/HSP70/BAG-1 complex promotes client protein ubiquitination and subsequent proteasomal degradation (**FIGURE 1.3**) (Arndt et al., 2007, Hohfeld et al., 2001).

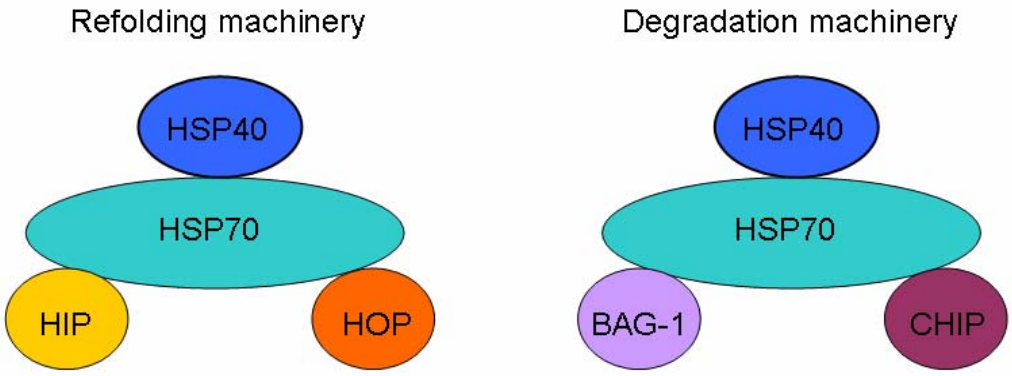

FIGURE 1.3: Schematic presentation of the co-chaperone networks that interact with HSP70 to govern protein triage decisions. The interaction of HSP70 with the co-chaperones HIP and HOP results in the refolding of a protein substrate, while HSP70‘s interaction with BAG-1 and CHIP governs proteasomal protein degradation.

It has become increasingly clear that HSP70's association with different co-chaperone networks also governs HSP70's ATPase activity, which is located at the N-terminus of the HSP70 protein (Nollen et al., 2002). That is, the binding of HIP and HOP to HSP70 results in the activation of HSP70's ATPase activity, promoting the ADP-bound, high-substrate affinity state of HSP70, thereby supporting the refolding of the client protein. In contrast, binding of BAG-1 and CHIP to HSP70 inhibits the hydrolytic activity of HSP70's ATPase domain, resulting in the ATP-bound, low-substrate affinity state of HSP70, promoting the proteasomal degradation of the client protein (Kampinga et al., 2003). Therefore, one would predict that in a state where ATP is limiting, such as in ischemic stroke, HSP70's activity is directed toward the refolding of protein substrates as opposed to the tagging of client proteins for subsequent proteasomal degradation.

C-terminus of HSC70 interacting protein (CHIP)

CHIP discovery and distribution

C-terminus of HSC70 interacting protein (CHIP) is a dual function co-chaperone/E3 ubiquitin ligase with a molecular weight of 34.8kDa (Ballinger et al., 1999, Qian et al., 2006). Using full-length hCHIP fused to the GAL4 DNA-binding domain as the bait, CHIP was first identified in 1999 during a yeast-2-hybrid screen aimed at the identification of additional proteins that contain a tetratricopeptide repeat (TPR) domain (Ballinger et al., 1999). The TPR domain is a 34-amino-acid protein-protein interaction motif that is involved in a variety of cellular functions including protein transport, development, transcription and mitosis (Ballinger et al., 1999). Using Northern blot analysis to determine CHIP's distribution in human tissue as well as its presence in a

multitude of commonly used *in vitro* tissue culture systems, Ballinger and colleagues demonstrated that CHIP expression is highest in adult striated muscle and heart, but it is also present in brain, placenta, liver, kidneys and lung. Moreover, CHIP is expressed in most human cell lines and primary cultures (Ballinger et al., 1999).

CHIP structure and function

In addition to the discovery of CHIP, Ballinger and colleagues not only delineated parts of the protein structure of CHIP, but also determined the function of some of these protein domains (Ballinger et al., 1999). From a structural perspective, the CHIP protein can be divided into three main domains: the N-terminal TPR domain, the mixed charged region and the C-terminal U-box domain (**FIGURE 1.4**) (Ballinger et al., 1999, Jiang et al., 2001, Murata et al., 2001). The N-terminal TPR domain of the CHIP protein governs CHIP's interaction with HSC70, HSP70 and heat shock protein 90 (HSP90) (Ballinger et al., 1999). The highly mixed charged region of CHIP is required for CHIP dimerization and proper CHIP function (Nikolay et al., 2004). The C-terminal U-box domain harbors the E3 ligase activity of CHIP, indicating a role of CHIP in the ubiquitination of protein substrates thereby targeting them for their subsequent proteasomal degradation (**FIGURE 1.4**) (Jiang et al., 2001, Murata et al., 2001). Moreover, it has become evident that CHIP has autoubiquitination capabilities which are independent of the ubiquitination status of client proteins (Jiang et al., 2001, Murata et al., 2001). Ultimately, it is through the E3 ligase activity of the U-box and CHIP's ability to interact with molecular chaperones that CHIP has been coined as the link between two of the most opposing

cellular systems, namely the molecular chaperone system and the ubiquitin proteasome pathway (McDonough et al., 2003).

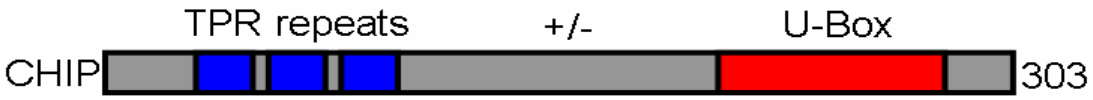

FIGURE 1.4: Protein domain arrangement of CHIP. The CHIP protein is composed of three domains. The N-terminal tetratricorepeat domain governs CHIP's interaction with main members of the heat shock protein family. The mixed charged region is required for CHIP dimerization. The C-terminal U-box domain governs CHIP's E3 ubiquitin ligase activities.

As previously mentioned, the co-chaperone CHIP interacts with main members of the HSP family by means of its N-terminal TPR domain. The importance of this interaction is that the association of CHIP with HSP70 is crucial in governing the fate of client proteins due to CHIP's ability to inhibit HSP70's ATPase activity. This interaction decreases the time HSP70 is associated with the client substrate thereby enhancing the rapid ubiquitination of the client protein by CHIP (Kampinga et al., 2003). In addition to being involved in regulating HSP70's folding cycle, CHIP also controls HSP70 expression itself (Kim et al., 2005). Qian and colleagues demonstrated that CHIP can not only enhance HSP70 induction during times of stress, but also decrease HSP70 expression levels during recovery (Qian et al., 2006). These processes are predominantly governed by CHIP's interaction with heat shock factor 1 (HSF1), both of which translocate from the cytoplasm into the nucleus following stress where they govern the

synthesis of inducible heat shock proteins (Anderson et al., 2009, Dai et al., 2003, Kim et al., 2005).

CHIP substrates and its implication in human diseases

In addition to CHIP's role in governing HSP70 folding activities and expression levels, CHIP also functions as an E3 ubiquitin ligase, thereby mediating the tagging of damaged proteins for their subsequent proteasomal degradation. In the last decade, a wide range of studies were aimed at identifying endogenous substrates of CHIP. It is now known, that CHIP is responsible for the degradation of over 40 proteins including tau, α-synuclein, ataxin-3, p53, huntingtin and the cystic fibrosis transmembrane conductance regulator (Arndt et al., 2007, Rosser et al., 2007), all of which are associated with diseases including Parkinson's, Alzheimer's and Huntington's as well as cystic fibrosis and cancer (Arndt et al., 2007, Rosser et al., 2007).

Acute overexpression of CHIP can increase cellular survival *in vitro* via CHIP's ability to aid in the removal of damaged proteins, thereby decreasing proteotoxic stress in chronic neurological diseases (Arndt et al., 2007, Dickey et al., 2007, Rosser et al., 2007). Specifically, in an elegant study, Imai and co-workers demonstrated that CHIP can compensate for the loss of function of the proteotypic E3 ligase Parkin, a protein where mutations are associated with an autosomal recessive form of Parkinson's disease (Imai et al., 2002). These results imply that although E3 ubiquitin ligases are highly specific with respect to the client proteins they interact with, a certain degree of redundancy exists (Morishima et al., 2008). This redundancy resulted in a strong push in the Parkinson's disease field to develop drugs and therapies to increase CHIP expression as a means to

block Parkinson's disease induced neuronal dysfunction and death. This work was, however, premature given that the E3 ligase activity of Parkin is highly limited and the long-term consequences of increased CHIP expression on cell death were unknown.

Ubiquitin and the Proteasome

Ubiquitin

Given CHIP's function as an E3 ubiquitin ligase, it is involved in tagging damaged proteins for their subsequent proteasomal degradation via the attachment of an ubiquitin chain (Jiang et al., 2001, McLaughlin et al., 2005, Murata et al., 2001). The attachment of ubiquitin molecules to a damaged protein is governed by the sequential interaction of the E1 activating, E2 conjugating and E3 ligating enzymes (Goldberg, 2005, Herrmann et al., 2007, McLaughlin et al., 2005). While there are a handful of E1 enzymes and a few dozen E2 enzymes, there are 500-1000 E3 ligases present in eukaryotic cells (McLaughlin et al., 2005). This large number of E3 ligases underscores that the specificity of the ubiquitin proteasome pathway (UPP) occurs at the levels of the E3 ligases (Goldberg, 2005, Herrmann et al., 2007, McLaughlin et al., 2005). Moreover, while the involvement of several of the seven lysine residues of ubiquitin have been associated with a variety of cellular functions, ubiquitin's lysine residue 48 (K48) governs the targeting of damaged proteins for their subsequent proteasomal degradation (Herrmann et al., 2007, McLaughlin et al., 2005).

The proteasome

Once ubiquitinated, proteins are processed to the next step in the UPP, namely the proteasome (Jiang et al., 2001, Murata et al., 2001). The 26S proteasome has a molecular weight of approximately 2.5MDa and is composed of a 20S core subunit with 19S regulatory subunits attached to each side (Hanna et al., 2007). This ATP-dependent, multi-subunit complex is located throughout the cytosol and in the nucleus, and it is the major intracellular non-lysosomal proteolytic system essential for the rapid elimination of damaged proteins (Coux et al., 1996, Herrmann et al., 2007, McLaughlin et al., 2005).

Given the UPP's role in removing damaged proteins from the cell, a multitude of studies have focused on investigating its role in disease states, as the accumulation of damaged proteins is a common pathological hallmark of many human diseases including ischemic stroke, Parkinson's disease and Alzheimer's disease (Goldberg, 2003, Hegde et al., 2007, McLaughlin et al., 2005). Studies in the field of ischemic stroke demonstrate a loss in proteasome activity within 10min following the insult, leading to the accumulation of damaged and ubiquitinated proteins in the CNS (McLaughlin et al., 2005). Moreover, the use of electron microscopy allowed for the identification of the precise location of protein aggregates, demonstrating an accumulation of damaged proteins in the soma, dendrites and axons of neurons following ischemic injury (Hu et al., 2000, McLaughlin et al., 2005). In contrast, studies in the field of chronic neurodegenerative diseases suggest that an impairment of the UPP may be involved in the development of disease pathology (Hegde et al., 2007). For instance, in the case of Parkinson's disease, mutations in the E3 ubiquitin ligase Parkin have been associated with the onset of an autosomal recessive form of the disease (Imai et al., 2002). These mutations abolish the E3 ligase activity of

Parkin, preventing the proper ubiquitination of damaged proteins for their subsequent proteasomal degradation, and ultimately leading to the accumulation of damaged proteins and neuronal death (McLaughlin et al., 2005). Results like these not only demonstrate the importance of the proper function of the UPP for cellular function and survival, but also underscore the complexity of this pathway and the crucial role it plays in the CNS.

CHIP – To Be or Not to Be?

The overexpression of CHIP has been shown to be neuroprotective in animal and cell culture models of chronic neurodegenerative disorders, an effect which has been attributed to CHIP's E3 ligase activity by which damaged proteins are tagged for proteasomal degradation (Imai et al., 2002, Sahara et al., 2005). As a result, increasing CHIP expression appears to be a reasonable target for neurotherapeutic intervention in chronic neurodegenerative diseases. However, CHIP's role in determining cell fate in acute neurological disorders has not been assessed. Moreover, studies investigating the ability of the brain to control expression levels of this dual function co-chaperone/E3 ubiquitin ligase under stress have been lacking. In order to address these questions, the following hypothesis and specific aims were proposed and results in the here presented thesis were aimed at answering these questions:

Rationale

Due to the fact that the molecular events elicited following ischemic stroke are also commonly observed in chronic neurodegenerative diseases, including Parkinson's and Alzheimer's disease (Choi, 1992, Greene et al., 1996), and the fact that acute CHIP

upregulation has been associated with increased cellular survival in the context of these diseases (Arndt et al., 2007, Dickey & Patterson et al., 2007, Imai et al., 2002, Rosser et al., 2007), we sought to determine if CHIP is altered in acute ischemic stroke and examine the consequences of altering CHIP expression on responsiveness to oxidative stress.

Hypothesis

We hypothesized that the increase in CHIP levels observed in our post-mortem human tissue samples is a means of neurons to enhance the removal of damaged proteins from the cellular environment and to increase survival as a result.

Specific Aims of the Thesis

1) Is CHIP expression regulated in response to acute neuronal ischemic injury?
2) What are the consequences of CHIP overexpression in governing neural fate following acute injury?
3) Who are the proteins targets of oxidative stress in the presence of different levels of CHIP?
4) What are the effects of CHIP on neural survival?

CHAPTER II

C-TERMINUS OF HSC70 INTERACTING PROTEIN INCREASES FOLLOWING STROKE AND IMPAIRS SURVIVAL AGAINST ACUTE OXIDATIVE STRESS

Abstract

Overexpression of the E3 ubiquitin ligase CHIP has been associated with increased survival in models of chronic neurodegenerative diseases. CHIP has also been shown to compensate for the loss of function of the E3 ligase Parkin, of which mutations are associated with autosomal recessive forms of Parkinson's disease. The role of CHIP in acute neurological diseases, however, remained unclear. Using post-mortem human tissue samples, we provide the first evidence that cortical CHIP expression is increased following ischemic stroke. Oxygen glucose deprivation (OGD) *in vitro* led to rapid protein oxidation, antioxidant depletion, proteasome dysfunction and a significant increase in CHIP expression. To determine if CHIP upregulation enhances neural survival, we overexpressed CHIP *in vitro* and evaluated cell fate 24hr following acute oxidative stress. Surprisingly, CHIP overexpressing cells fared worse against oxidative injury, accumulated more ubiquitinated and oxidized proteins and experienced decreased proteasome activity. Conversely, using siRNA to decrease CHIP expression in primary neuronal cultures improved survival against oxidative stress, suggesting that increase in CHIP observed following stroke-like injuries is likely correlated with diminished survival and may negatively impact the neuroprotective potential of HSP70.

Introduction

Strokes are predominately ischemic in nature, comprising 87% of all stroke cases (Lloyd-Jones et al., 2009). The risk of ischemic stroke increases dramatically in individuals who are diagnosed with hypertension, cardiovascular disease, diabetes and dyslipidemia, as well as in individuals who are obese, physically inactive and smoke (Lloyd-Jones et al., 2009). Despite the efforts to educate the public about stroke risk factors and to encourage people to improve their health, stroke remains the third leading cause of death in this country and the leading cause of serious, long-term adult disability (Lloyd-Jones et al., 2009).

In the last 30 years, numerous studies aimed at understanding and identifying endogenous cellular and molecular responses elicited following stroke were performed in an attempt to develop safe and effective neurotherapeutics. In the course of this work, we have increasingly come to appreciate that HSP70 and CHIP are critical regulators of neuronal cell fate following injury. CHIP is a multifunctional ubiquitin ligase and its overexpression has been shown to afford neuroprotection by enhancing HSP70's client degradation activity (Dickey & Patterson et al., 2007). Other functions of CHIP include an ability to act as an autonomous molecular chaperone blocking proteotoxic stress (Rosser et al., 2007) as well as a regulator of HSP70 expression (Qian et al., 2006). CHIP is also capable of impeding cell death associated with severe endoplasmic reticulum (ER) stress (Imai et al., 2002), suggesting that CHIP overexpression may positively influence survival against chronic stress. While HSP70 induction is a common feature of chronic and acute neurological injuries, alterations in CHIP expression following stress have not been evaluated in acute human neurological disorders.

Moreover, the ability of CHIP to alter cell survival following acute ischemic stress has not been assessed.

In this work, we provide the first evidence that CHIP is upregulated in post-mortem tissue from patients following TIA or stroke, and we also examined the effects of chronic CHIP overexpression on neural survival following acute oxidative injury *in vitro*. We demonstrate that chronic upregulation of CHIP is associated with a loss of proteasome activity and increased levels of ubiquitinated and oxidized proteins in neural cells following acute oxidative stress. Cells which had high levels of CHIP also had decreased survival in response to oxidative stress, while decreasing CHIP expression resulted in increased neuronal survival following acute oxidative injury. These data suggest that long-term elevations of CHIP may be deleterious to survival and a poor therapeutic strategy to enhance neuronal outcome in the context of acute neurological disease or as a means to decrease cell stress in those at high risk of stroke.

Materials and Methods

Reagents

XT-MOPS running buffer, Tris/Glycine transfer buffer, Criterion Bis-Tris gels and prestained kaleidoscope molecular weight markers were purchased from Bio-Rad Laboratories (Hercules, CA). Membrane blocking solution was from Zymed (San Francisco, CA). Western Lightning Chemiluminescence Reagent Plus was from Perkin Elmer Life Sciences, Inc. (Boston, MA) and Hybond P polyvinylidene difluoride (PVDF) membranes from GE Healthcare (Piscataway, NJ). Gel Code Blue Stain Reagent was obtained from Thermo Scientific (Rockford, IL).

For Western blots and immunofluorescence, mouse monoclonal antibody to ubiquitinated proteins (Clone Fk2, PW8810) was purchased from Biomol (Plymouth Meeting, PA). Rabbit CHIP (PC711) antibody was purchased from Calbiochem (San Diego, CA). Rabbit HSP40 polyclonal antibody (SPA-400), rabbit HSP70 (HSP72) polyclonal antibody (SPA-811), and rabbit HSC70 polyclonal antibody (SPA-816) were purchased from Assay Designs (Ann Arbor, MI). The mouse c-myc (9E10) monoclonal antibody (sc-40) was purchased from Santa Cruz Biotechnology Inc. (Santa Cruz, CA). The mouse GAPDH monoclonal antibody (AM4300) was purchased from Applied Biosystems/Ambion (Austin, TX).

For tissue culture, fetal bovine serum (FBS) was purchased from Hyclone (Logan, UT) and Penicillin/Streptomycin was obtained from Cambrex Bio Science (Walkersville, MD). Dulbecco's Modified Eagle Medium (DMEM, 11995) with high glucose, Minimum Essential Medium (MEM, 51200), 0.25% Trypsin – EDTA 1x, trypan blue

stain 0.4%, and hygromycin B in PBS 50mg/ml were purchased from Invitrogen (Carlsbad, CA).

Unless otherwise stated, all other chemicals were purchased from Sigma-Aldrich (St. Louis, MO).

Post-mortem tissue

Dr. Rashad Nagra of the VA West Los Angeles Healthcare Center kindly provided human post-mortem samples of cerebral cortex from the Human Brain and Spinal Fluid Resource Center. Three patient categories were developed based on neuropathological diagnosis and available clinical data. Control cerebral cortical samples were obtained from subjects with no history of neurological disease and where cause of death was cancer without evidence of metastasis of the brain (prostate, breast, bladder and non-Hodgkin's lymphoma) *(see **TABLE 2.1** for patient data and post-mortem interval (PMI)).* Transient ischemic attacks (TIAs) or subacute stroke category was compiled using patients who had a clinical history of TIAs, but the cause of death in these patients was associated with other diseases (chronic obstructive pulmonary disease, diabetes mellitus, and congestive heart failure) or accidental death. These specimens had no cortical neuropathological lesions that were classified as being larger than microinfarctions or injury to the vasculature. Thickening of the vascular walls in both small and large vessels was evident in several samples. Sections were matched for dissection region with subjects in the stroke category. The stroke category was comprised of patients who had suffered non-hemorrhagic strokes associated with occlusion of the middle cerebral artery based on at least two of the following findings:

clinical manifestations, imaging, or post-mortem placement of plaques/emboli. The average patient age was 74.3 ± 2.94 years, and the average PMI was equal to or less than 15h.

	HSB Number	Sex	Diagnosis	Age	Average Age	PMI	Average PMI
Control	3565	M	Cardiomyopathy	76		11	
Control	3346	F	Congestive heart failure	91		10	
Control	3371	M	Lung Cancer	52		16	
Control	3397	F	Breast cancer	73		20	
Control	3406	F	Congestive heart failure	72	*73*	20	*15*
Stroke	1714b	F	Stroke; hypertension	80		3	
Stroke	2113	M	Massive right frontal stroke	82		4	
Stroke	2264	M	Stroke; diabetes mellitus	61		10	
Stroke	3968	F	Stroke, middle cerebral artery	81		14	
Stroke	3132	M	Large cerebral infarction	53	71	20	10
TIA	2435b	F	TIA; Mild supranuclear palsy	76		7	
TIA	1947	F	TIA; Alzheimer's disease	78		9	
TIA	1718	F	TIA; dementia	75		10	
TIA	3333	F	Strokes, Mini; COPD	89		19	
TIA	2528b	F	Cerebral vascular infarction, chronic	76	*79*	20	*13*

TABLE 2.1: Human tissue diagnosis and post-mortem interval (PMI).

Primary neuronal cell culture

Primary cortical cultures were prepared from embryonic day 18 Sprague-Dawley rats as previously described (McLaughlin & Nelson & Erecinska et al., 1998) with adaptations. Briefly, cortices were dissociated and the resultant cell suspension was adjusted to 335,000-350,000 cells/ml. Cells were plated 2ml/well in 6-well tissue culture plates containing one 25mm poly-L-ornithine-coated coverslip per well. Cells were maintained at 37ºC, 5% CO_2 in growth media composed of a volume to volume mixture

of 84% Ham's F12-nutrients (11765, Sigma-Aldrich, St. Louis, MO), 8% FBS, 24U/ml penicillin, 24µg/ml streptomycin, and 80µM L-glutamine. Glial proliferation was inhibited after two days in culture with 1-2µM cytosine arabinoside, after which cultures were maintained in Neurobasal medium (Gibco) containing B27 and NS21 supplements (Chen et al., 2008), penicillin and streptomycin.

Neuronal oxygen glucose deprivation (OGD)

Oxygen glucose deprivation experiments were preformed when cells were at least two weeks old (14-20 DIV), at which time point neurons represent at least 95% of these cultures as assessed by NeuN and GFAP staining (McLaughlin & Nelson & Silver et al., 1998). OGD was performed essentially as described (Gonzalez-Zulueta et al., 2000) by complete exchange of media with deoxygenated, glucose-free Earle's balanced salt solution (150mM NaCl, 2.8mM KCl, 1mM $CaCl_2$ and 10mM HEPES; pH 7.3), bubbled with 10% H_2/85% N_2/5% CO_2. Cultures were exposed to hypoxia in an anaerobic chamber (Billups-Rothberg) for various durations of time (5-90min) at 37ºC. Upon OGD termination, cells were washed with MEM/BSA/HEPES (0.01% BSA and 25mM HEPES) and maintained in MEM/BSA/HEPES/2xN2 (0.01% BSA, 25mM HEPES and 2xN2) until cell viability was determined 18-24hr later using a lactate dehydrogenase (LDH)-based *in vitro* toxicity assay kit. Toxicity data were represented as averaged raw LDH values. As a positive control for inducing total neuronal degeneration, cultures were exposed to 100µM NMDA and 10µM glycine in MEM/BSA/HEPES/2xN2 for 60min as we have previously described (McLaughlin et al., 2003). Data were analyzed

by two-way ANOVA followed by Bonferroni *post hoc* analysis to assess significant deviations from control.

Protein extracts from primary neurons were prepared 24hr following exposure to OGD as previously described (McLaughlin et al., 2003). In brief, plates were placed on ice and cells were washed twice with ice cold 1xPBS. Cells were then scraped from the dish using a rubber policeman in 350µl TNEB (50mM Tris-HCl, 2mM EDTA, 100mM NaCl and 1% NP-40; pH 7.8) with added protease inhibitor cocktail. Of this suspension, 50µl was saved for protein determination, 150µl were resuspended in an equal volume of Laemmeli Buffer with ß-mercaptoethanol, heated to 95ºC for 10min, and stored at -20ºC, and the remaining 150µl were added into a new Eppendorf tube containing dithiothreitol (50mM) (DTT; D9779, Sigma-Aldrich, St. Louis, MO) for the determination of total oxidized proteins as described in the *OxyBlot methodology* below. Immunoblots probing for HSC70, HSP70, HSP40, CHIP, Fk2 and GAPDH were processed as described below.

GSH and oxidized glutathione measurement by high-performance liquid chromatography

To determine the consequences of OGD on antioxidant defenses, intracellular glutathione (GSH) concentrations were measured by high-performance liquid chromatography (HPLC) as previously described (Wang et al., 2008). Briefly, mature neuronal cultures (14-21 DIV) underwent OGD as described above. Upon treatment termination, cultures were extracted with 5% perchloric acid/0.2M boric acid. Acid-soluble thiols were derivatized with iodoacetic acid and dansyl chloride and were analyzed by HPLC using a propylamine column (YMC Pack, NH2, Waters, Milford, MA) and an automated HPLC system (Alliance 2695, Waters). The GSH and oxidized

glutathione (GSSG) concentrations were normalized to the protein contents of the samples measured by the Bradford assay (Bio-Rad, Hercules, CA).

Determination of total oxidized protein levels using the OxyBlot methodology

The OxyBlot Protein Oxidation Detection Kit was purchased from Chemicon International (Temecula, CA). For the determination of total oxidized protein levels, neural or neuronal cells were harvested as described below or above, respectively. To prevent protein oxidation from occurring after cell harvest, 50mM DTT was added to aliquots designated for the OxyBlot procedure and cell lysates were divided for the derivatization reaction containing 2,4-dinitrophenylhydrazine and for the negative control reaction containing derivatization control solution. Samples were stored at 4ºC and run within seven days of protein derivatization. Equal protein concentrations were separated using 4-12% Criterion Bis-Tris gels and processed as described in the *Immunoblotting* section below. Antibodies specific for the detection of oxidized proteins were provided by the manufacturer. Data represent results from at least three independent experiments.

Oxidative stress model of neural injury in HT-22 cells

HT-22 cells were derived from the immortalized H4 hippocampal murine neuroblastoma cell line, and were a generous gift from Pamela Maher (Salk Institute). This neural cell line was chosen because HT-22 cells are an excellent, well-characterized model of neural oxidative injury (Maher, 2005, Stanciu et al., 2000, van Leyen et al., 2005). Due to the lack of functional glutamate receptors, these cells undergo oxidative stress induced toxicity upon exposure to glutamate, which blocks glutamate-cystine anti-

porters in the plasma membrane resulting in glutathione deficiency and oxidative cell death (van Leyen et al., 2005). HT-22 cells were maintained in Dulbecco's modified Eagle's medium (DMEM) with glutamine, supplemented with 10% FBS and penicillin/streptomycin (0.2%). The CHIP overexpressing cell line, CHIP-6B, which we refer to as CHIP OE, was derived by stable transfection with a full-length human CHIP cDNA with a myc-tag in a hygromycin resistant vector and has been previously described (Wang et al., 2005). Media for these HT-22 derived neural cells was supplemented with 50mg/ml hygromycin B. Cells were grown in 75cm^2 cell culture flasks at 37ºC with 5% CO_2 and passed by trypsinization when the cells' confluency reached 50-80% (Davis et al., 1994).

Immunoblotting

To determine the effect of chronic CHIP overexpression on expression levels of inducible molecular chaperones and levels of ubiquitinated proteins, we performed immunoblots on extracts from both neural cell lines that underwent oxidative injury. For the preparation of cell extracts, culture dishes were placed on ice and cells were scraped into the medium by using a rubber policeman as described above (McLaughlin et al., 2001). The cell suspension was centrifuged at 1,141 x *g* for 10min. The pellet was gently washed with ice cold 1xPBS, followed by its resuspension in 300µl of TNEB with added protease inhibitor cocktail. Fifty microliters of each sample were reserved for the spectrophotometrical determination of protein concentrations using a Bio-Rad D_c Protein Assay kit (Hercules, CA). The remaining cell lysate was added to sample buffer,

comprised of an equal volume of Laemmli Buffer (Bio-Rad, Hercules, CA) and ß-mercaptoethanol (1:19), heated to 95ºC for 10min and stored at -20ºC.

Equal protein concentrations were separated using 4-12% Criterion Bis-Tris gels, after which proteins were transferred to polyvinylidene difluoride (PVDF) membranes, and blocked in methanol for 5min at room temperature. Following 15min of drying, membranes were incubated at 4ºC overnight in their respective primary antibody, which was diluted in either 5% nonfat milk in Tris buffer saline (TBS) containing 0.1% Tween 20 (TBST) or Zymed blocking solution. Primary antibodies were used at the following concentrations: C-terminus of HSC70 interacting protein (CHIP; 1:500), the constitutive form of HSP70 (HSC70; 1:2000), heat shock protein 70 (HSP70; 1:1000), heat shock protein 40 (HSP40; 1:10,000), glyceraldehyde-3-phosphate dehydrogenase (GAPDH; 1:10,000), c-Myc (1:10,000) and antibody to ubiquitinated proteins (clone Fk2, 1:50,000). The following day, the primary antibody was removed, the membranes were washed 4 times with TBST for a total of 30min, and then incubated for 1hr at RT with a horseradish peroxidase (HRP)-conjugated anti-rabbit or anti-mouse secondary antibody. The membranes were then washed as above and placed into 2ml of ECL chemiluminescent substrate for 1min at room temperature. The membranes were then exposed to HyBlot CL Autoradiography Film (Denville Scientific Inc., Metuchen, NJ) (McLaughlin et al., 2001).

Semi quantitative analyses of immunoblots were performed and were noted per our previously described method by performing high resolution scans for densitometric quantification with Scion NIH IMAGE J. Values are expressed as mean increase above

control levels (± SEM) and statistical analysis was performed by using two-tailed *t* tests (McLaughlin et al., 2003).

Immunofluorescence

Cells were fixed in 10% formaldehyde and then permeabilized with 0.1% Triton X-100 as we have previously described (Du et al., 2002). Cells were then blocked with 8% Bovine serum albumin (BSA) diluted in 1xPBS and incubated in Fk2 (1:200) primary antibody diluted in 1% BSA overnight at 4°C. Cells were then washed with 1xPBS for a total of 30min and incubated in the dark in cy-3 anti-mouse (Fk2) secondary antibody (1:500) for 60min at RT. Cells were counterstained with DAPI to visualize nuclei (Ravagnan et al., 2001). After 25min of additional washes, coverslips were mounted and fluorescence was visualized with a Zeiss Axioplan microscope equipped with an Apotome optical sectioning filter as previously described (Musiek et al., 2006). Cells that were loaded with propidium iodide (PI) were fixed in 10% formaldehyde, permeabilized with 0.1% Triton X-100 and counterstained with DAPI to visualize nuclei (Ravagnan et al., 2001). Following 25min of additional washes, coverslips were mounted and fluorescence was visualized as described above.

Proteasome measurements

To determine the consequences of chronic CHIP overexpression on protein turnover, the chymotrypsin-like activity of the proteasome was measured by means of fluorogenic peptide substrates. Both neural lines were plated at a density of 100,000 cells per well in 6-well plates, and incubated at 37ºC with 5% CO_2 overnight. The following

day, cells were exposed to glutamate (3mM) to induce oxidative stress or MG132 (10μM) to inhibit proteasome activity (van Leyen et al., 2005). Oxidative stress was terminated by placing culture dishes on ice and scraping cells into culture media with a rubber policeman. The cell suspension was centrifuged at 1,141 x *g* and 4ºC for 10min. After removal of the supernatant, the pellet was washed carefully with ice cold 1xPBS, followed by its resuspension in 400μl lysis buffer (10mM Tris-HCl, 0.5mM DTT, 5mM ATP, 0.035% SDS and 5mM $MgCl_2$, pH 7.8). Fifty microliters of each sample were reserved for a protein assay and the remaining 350μl were used to determine proteasome activity. Addition of 40μM Suc-LLVY-AMC to each sample was followed by a 30min incubation in a 37ºC water bath. The reaction was terminated by adding 13μl ethanol and 87.5μl ddH_2O to quench the substrate. One hundred microliter-aliquots from each sample were then added to a white 96-well plate (Corning Incorporated, Corning NY) in quadruplicate. Fluorescence was measured by using a SpectraFluorPlus plate reader (Tecan, Austria) at 360nm excitation, 465nm emission following a three second pre-measurement delay and a 40μs integration time. All data represent the mean ± SEM of at least three independent experiments.

For the assessment of the chymotrypsin-like activity of the proteasome in neuron enriched primary cultures, neurons were exposed to oxygen glucose deprivation and extracts were prepared by placing plates on ice, then carefully washing cells twice with ice cold 1xPBS and harvested as above in lysis buffer. Fifty microliters of each sample were reserved for a protein assay. The remaining 350μl was used for the assessment of the chymotrypsin-like activity of the proteasome as described above. All neuronal data represent the mean ± SEM of at least four to seven independent experiments.

Glutamate toxicity assay in neural cells

Both neural cell lines were plated at a density of 30,000 cells per well in 24-well plates and allowed to grow at 37ºC with 5% CO_2 overnight. The following day, cells were treated by exchanging the medium with 0.5ml media containing glutamate (1, 3, or 5mM) and glycine (10μM). Sorbitol (1M) solution was prepared in culture media to induce total cell death. Twenty-four hours following incubation at 37 ºC, cellular viability was photodocumented and assessed with an *in vitro* thiazolyl blue tetrazolium bromide (MTT) toxicology assay. MTT was dissolved in media comprised of Minimum Essential Medium, FBS (0.01%), and GlutaMAX (1%) (Hoyt et al., 2000). Reconstituted MTT was added directly to the wells in an amount that was equal to 10% of the media volume. Cultures were returned to the incubator for 4hr allowing reduction of tetrazolium salt by living cells. Cells were then solubilized by a 1:1 addition of solubilization solution (10% Triton X-100 plus 0.1N HCl in anhydrous isopropanol) and absorbance was measured using a SpectraFluor Plus plate reader (Tecan, Austria) at a wavelength of 590nm with a three second pre-measurement delay. All data represent the mean ± SEM of at least three independent experiments.

Transfections of neural cells and primary cortical neurons with CHIP siRNA

All siRNAs were obtained from QIAGEN Science (Valencia, CA). The CHIP siRNA sequence used for experiments in HT-22 cells was *5'-CCCACTTGTGGCAGTGTACTA-3'*. The CHIP siRNA sequence used for experiments in primary neuronal cultures was *5'-CCAGCTGGAGATGGAGAGTTA-3'*. Amaxa reagents

for the transfection of primary neurons and HT-22 cells using the nucleofector methodology were obtained from Lonza (Cologne, Germany).

Because of their high transfection efficiency (80-90%), we used HT-22 cells for the biochemical determination of optimal CHIP knock-down. CHIP siRNA transfected cells were harvested at 24-72h post transfection and cell extracts were prepared for immunoblotting as described above.

For the transfection of HT-22 cells, the Cell line Nucleofector Kit V (VCA-1001, Lonza, Cologne, Germany) was used following manufacturer's protocol. Briefly, HT-22 cells were grown to an 80% confluency, then trypsinized and centrifuged at 1,141 x *g* for 10min. The pellet was resuspended in 5ml plating media, cells were counted and adjusted to a final concentration of $1x10^6$ cells per nucleofection sample. Cells were compacted by centrifugation at 1.141 x *g* for 10min, and the pellet was resuspended in 100µl Cell Line Nucleofector solution. CHIP siRNA (25nM) and GFP (2µg) were added to 97.5µl of cell suspension and electroporated using Nucleofector program U-030. Cells were immediately placed in a 1:15 dilution of Hank's balanced salt solution (HBSS) and re-equilibrated to RT for 10min. 500µl of the cell suspension was transferred into each well of a 6-well plate containing 2ml of growth media. Transfected cells were allowed to grow overnight at 37ºC with 5% CO_2 after which transfection efficiency was assessed using a Zeiss Axiovert 25 microscope equipped with a fluorescent bulb. All experiments using CHIP siRNA were conducted 72hr following transfection, as pilot experiments revealed this to be the amount of time needed for optimal knock-down of CHIP expression (**FIGURE 2.1A**).

To assess the effect of CHIP knock-down on neuronal viability, primary cortical neurons were transfected with CHIP siRNA on the day of the dissection and cells were allowed to grow in culture for 72hr (3 DIV) before conducting experiments. *(See **FIGURE 2.1B** for verification of decreased neuronal CHIP expression induced by siRNA and electroporation optimized to 72hr)*. For transfections of primary neurons, the Rat Neuron Nucleofector Kit (VCA-1003, Lonza, Cologne, Germany) was used. To increase both neuronal survival following transfection and transfection efficiency, the manufacturer's protocol was modified as follows: the pellet formed following neuronal dissociation was washed with HBSS and carefully resuspended in 5ml HBSS. The cell suspension was equally divided into two 15ml conical tubes and cells were allowed to settle after which the supernatant was carefully removed. Cells designated for control conditions were resuspended in 1.5ml HBSS, whereas cells specified for nucleofection were resuspended in 100µl Rat Neuron Nucleofector solution. Cells were transfected as described above using the Nucleofector program O-03. Upon termination of the 10min re-equilibration period, 250µl of the cell suspension was plated into each well of a 6-well plate containing 2ml growth media composed of 84% Dulbecco's Modified Eagle's Medium (DMEM, 11960, Invitrogen, Carlsbad, CA), 8% Ham's F12-nutrients (11765, Sigma, St. Louis, MO), 8% fetal bovine serum, 24U/ml penicillin, 24µg/ml streptomycin, and 80µM L-glutamine and maintained at 37ºC with 5% CO_2. Twenty-four hours following transfection, cells underwent a complete growth media change into fresh media and transfection efficiency was examined as described above.

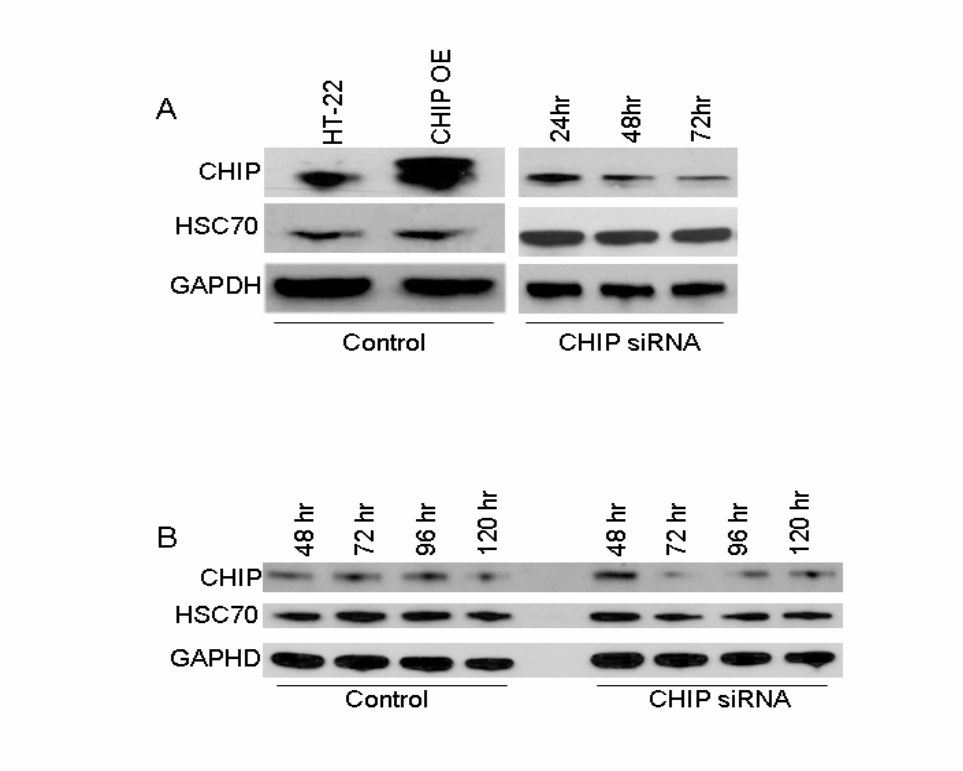

FIGURE 2.1: Optimal CHIP knock-down is achieved 72hr following transfection. A) HT-22 cells and B) young primary neurons were transfected with CHIP siRNA using the Nucleoporation methodology. Cells were harvested at various time points post transfection and proteins were separated on SDS-PAGE gels and probed with antibodies specific for CHIP, HSC70 or GAPDH. Optimal CHIP knock-down was achieved 72hr following transfection in both model systems. Comparable results were obtained in three additional independent experiments.

Induction of oxidative injury in primary cortical cultures

To determine if neurons had altered vulnerability to acute oxidative injury when CHIP expression was decreased, young primary neurons (3 DIV) were exposed to glutamate (3mM) for 9hr three days (72hr) following transfection with CHIP siRNA. Coverslips of CHIP siRNA transfected and control cortical cultures were transferred into a 24-well plate containing control or toxicity media. Oxidative injury was induced by exchanging the growth medium with 0.5ml MEM/BSA/HEPES media containing glutamate (3mM) and glycine (10μM). Staurosporin (0.5μM) was prepared in

MEM/BSA/HEPES and was used as a positive control for the induction of apoptosis. Upon treatment termination, cells were incubated with 0.5ml propidium iodide (10μM) (PI, P4170, Sigma-Aldrich, St. Louis, MO) diluted in MEM/BSA/HEPES for 10min at 37ºC with 5% CO_2 after which cells were fixed and counterstained with DAPI and mounted as described in the *Immunofluorescence* section above. Cell viability was assessed by counting the number of neurons that were positive for propidium iodide and that showed chromatin condensation using DAPI staining.

Quantification of cell death in siRNA transfected neurons

The percentage of propidium iodide positive cells in CHIP siRNA transfected and control primary cultures following induction of oxidative injury was determined by cell counting. Neurons undergoing cell death were identified by nuclei with chromatin condensation as well as by intense propidium iodide staining. Counts were performed by individuals blinded to the treatment conditions. Three to five fields of view per coverslip from a total of 10-12 coverslips per condition were quantified as we have previously described (Aizenman et al., 2000). All data represent the average ± SEM from at least three independent experiments. Statistical significance was determined by a two-tailed ANOVA and Bonferroni *post hoc* analysis.

Results

CHIP levels are increased in human tissue following hypoxic injury

The overexpression of CHIP has been shown to be neuroprotective in animal and cell culture models of chronic neurodegenerative disorders, an effect which has been attributed to CHIP's E3 ligase activity by which damaged proteins are targeted for proteasomal degradation (Imai et al., 2002, Sahara et al., 2005). To evaluate if CHIP was altered by acute central nervous system injury, we compared the expression profiles of CHIP as well as HSP70 and HSC70 in post-mortem human cerebral cortical tissue samples from individuals with no history of neurological injury (Control), with those who had a recent history of transient ischemic attacks (TIA) or those who suffered from a fatal ischemic stroke (Stroke) due to the occlusion of the middle cerebral artery (**FIGURE 2.2A**). Prior work has demonstrated that both the CHIP and HSP70 proteins are stable with post-mortem intervals (PMI) of up to 24hr (Sahara et al., 2005). Therefore, only samples with a PMI shorter than 23hr were included in this study. Patients were matched for PMI and gender with an average age of 74 (see **TABLE 2.1**).

Using a total sample size of 5 patients from each group, we observed a significant increase in HSP70 expression levels in the cerebral cortex in both TIA and stroke samples compared to control tissue (**FIGURE 2.2B**). The constitutively expressed form of the HSP70 family, HSC70, was not altered and was used as a loading control as previously described (McLaughlin et al., 2003). We also observed a significant increase in CHIP expression levels in both TIA and stroke tissue (**FIGURE 2.2B**).

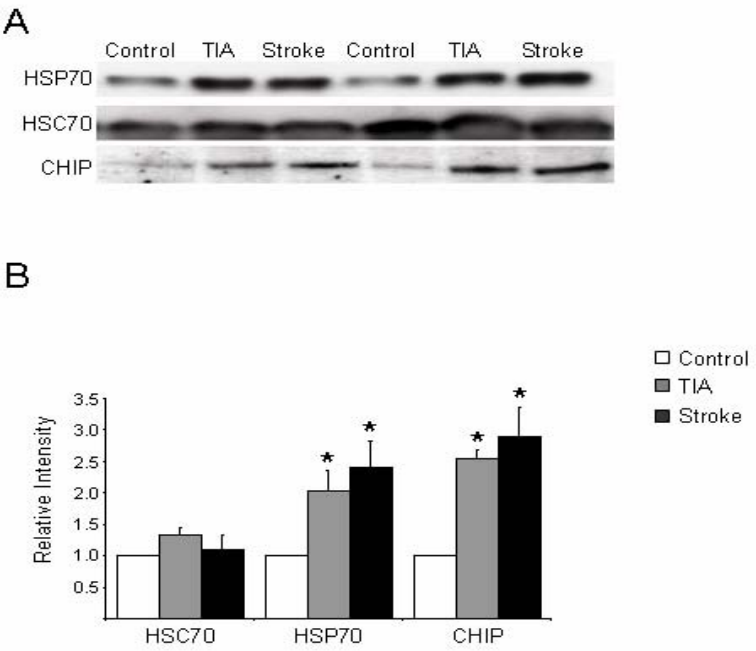

FIGURE 2.2: Hypoxic injury results in increased expression levels of HSP70 and CHIP in human tissue. A) Post-mortem specimens from patients who had experienced a fatal ischemic stroke of the middle cerebral artery (Stroke), history of transient ischemic attacks (TIA) or died from causes that were not associated with hypoxia, ischemia or neurologically compromised (Control) were probed for HSP70, the constitutively active chaperone HSC70 or CHIP. 20µg of protein were run in each lane and blots are representative of results obtained from 5 independent sample sets. B) Alterations in protein expression were quantified by performing high-resolution scans for densitometric quantification with Scion NIH IMAGE J. Equal protein loading was ensured by protein assays and equal expression of HSC70. Values are expressed as means (± SEM) of 5 independent sample groups. * denotes statistical significance compared to control as determined by two-tailed *t*-test with $p < 0.05$. *For detailed information on PMI, age, sex and cause of death, see **TABLE 2.1**.*

Glutathione levels are decreased and oxidative protein damage is increased following neuronal exposure to OGD

To determine if the observed upregulation of CHIP was neuroprotective in an acute injury setting, we moved to a more pliable *in vitro* model of stroke. Mature neuron enriched cultures were exposed to OGD for 5, 15 or 90min followed by a 24hr recovery period. Representative photomicrographs of neurons exposed to OGD for 5 and 15min demonstrate many healthy phase-bright neurons (**FIGURE 2.3A, B**). Neurite retraction

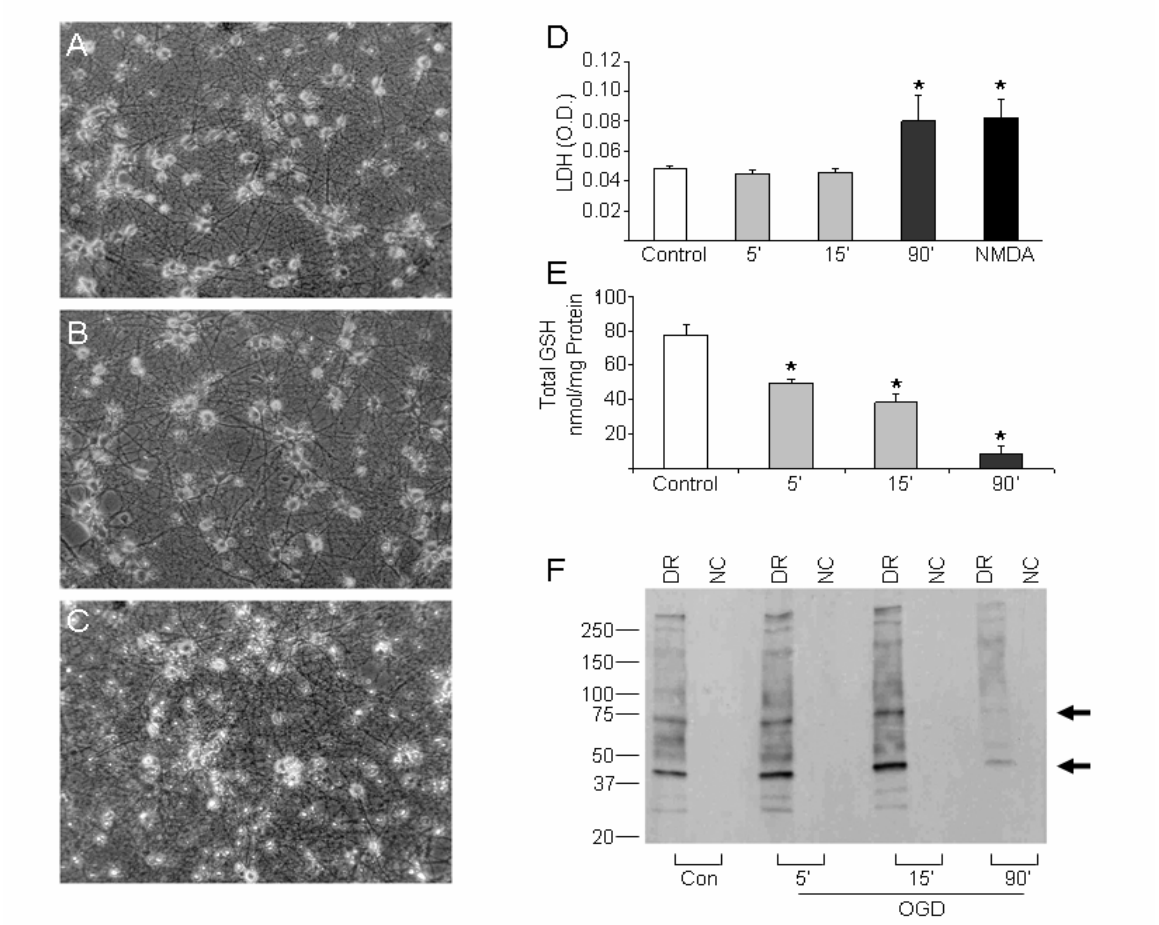

FIGURE 2.3: Neuronal exposure to OGD impairs antioxidant defenses and increases oxidative protein damage. Neuron enriched primary cultures were exposed to oxygen glucose deprivation (OGD) for 5-90min and cell survival was determined by visually inspecting cells under phase-bright microscopy. Representative photomicrographs of cultures 24hr after the termination of A) 5 min or B) 15 min of OGD demonstrate many healthy phase-bright neurons with elaborate processes. Neurons exposed to OGD for C) 90min show loss of phase-bright somas and neurite retraction 24h after OGD. D) Cell viability was furthermore assessed 24hr following OGD using an *in vitro* toxicology kit measuring the release of LDH from dead and dying neurons. Data demonstrate an increase in cell death as the duration of neuronal exposure to OGD increased. E) Total glutathione levels were measured by the HPLC methodology 24hr after termination of OGD. Results reveal a significant decrease in total glutathione levels following OGD. F) Oxidative protein damage was assessed using the OxyBlot methodology 24hr following termination of OGD. Levels of oxidized proteins increased following mild and modest OGD particularly in the 40kDa and 70kDa ranges (arrow), but decreased robustly following lethal OGD. All data is expressed as means (± SEM) of four to seven independent experiments run in duplicate. * represents $p < 0.05$ using a one-tailed ANOVA with Dunnett's *post hoc* analysis. DR, Derivatization Reaction; NC, Negative Control.

and a loss of phase-bright somas was evident following exposure to OGD for 90min (**FIGURE 2.3C**). These architectural changes were associated with a loss of viability as assessed by the release of the essential cytosolic enzyme lactate dehydrogenase (LDH). Neither 5 nor 15min OGD significantly increased LDH levels while 90min OGD induced cell death comparable to the 100% neurotoxicity observed in neurons that were exposed to 100μM NMDA/10μM glycine for 60min (**FIGURE 2.3D**) (McLaughlin et al., 2003). We decided to use 100μM NMDA to induce total cell death in our neuron enriched cultures, as previous studies have shown that exposure of neurons to 50μM NMDA for 5min is neurotoxic, while exposure to 100μM NMDA results in 100% cell death at 24hr (Choi, 1992, McNamara et al., 1990, von Engelhardt et al., 2007).

Enhanced generation of reactive oxygen species (ROS) due to oxidative stress has been implicated in the pathophysiology of many neurological disorders including ischemic stroke (Chan, 2001, Mehta et al., 2007). Cells are able to counteract the deleterious effects of ROS under normal conditions via the activity of cellular antioxidant defense mechanisms, including the main cellular antioxidant glutathione (Maher, 2005, Mehta et al., 2007). In order to assess if mild ischemic conditions were inducing antioxidant stress, we assessed total glutathione levels 24hr following 5, 15 or 90min of OGD. We observed a significant depletion of glutathione levels which was exacerbated with increasing OGD duration (**FIGURE 2.3E**).

We next assessed ROS damage to proteins by detection of protein carbonyl group formation (Dalle-Donne et al., 2003) and observed a moderate increase in total oxidized protein levels as well as an apparent increase in oxidation levels of proteins in the 40kDa

and 70kDa ranges (arrow; **FIGURE 2.3F**). We did not, however, observe an increase in protein oxidation at the 24hr time point following neuronal exposure to lethal ischemia (90'; **FIGURE 2.3F**). We believe that this result reflects the unrecoverable nature of this insult, inducing massive cell death within hours. This observation is supported by preliminary time course analyses using the OxyBlot methodology (3 and 6hr following OGD) where severe OGD resulted in increased protein carbonyl formation (data not shown).

Neuronal exposure to OGD increases protein ubiquitination, alters proteasome function and moderately increases CHIP expression *in vitro*

As an E3 ubiquitin ligase, CHIP plays an important role by intervening after protein dysfunction via its ability to ubiquitinate damaged proteins and targeting them for proteasomal degradation. Given the intensity of protein oxidation we observed in **FIGURE 2.3F**, we hypothesized that many of these oxidized proteins were likely to be tagged for proteasomal degradation. We therefore investigated if protein ubiquitination was altered following various durations of neuronal exposure to OGD. Using the Fk2 antibody, which detects mono– and polyubiquitinated proteins, we observed an increase in polyubiquitinated proteins, represented by a dark smear of higher molecular weight proteins 24hr after OGD. There was also a near complete loss of monoubiquitinated protein species following 90min OGD, indicating that the majority of the cellular ubiquitin has been recruited to damaged proteins (**FIGURE 2.4A**; arrow).

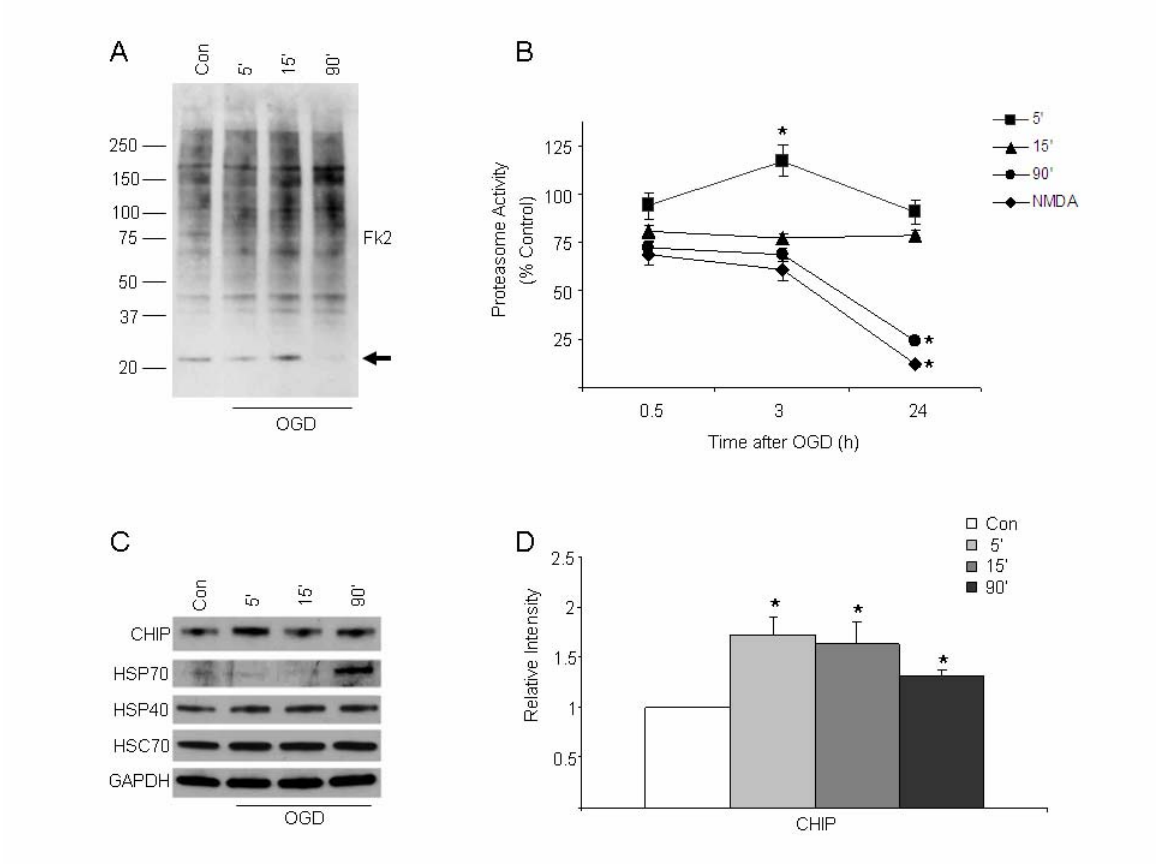

FIGURE 2.4: Neuronal OGD increases protein ubiquitination, alters proteasome function and moderately increases CHIP expression *in vitro.* Whole cell extracts of neuronal cultures were harvested 6hr following exposure to OGD. Proteins were separated by SDS-PAGE gels and probed with antibodies specific to mono- and polyubiquitinated proteins (Fk2). A) Protein polyubiquitination increased with prolonged exposure of neurons to OGD while a near complete loss of monoubiquitinated proteins is detected following lethal OGD (arrow). B) Primary cultures were exposed to OGD for 5-90min, harvested 30min, 3hr, or 24hr following OGD and proteasome activity was measured. Data represent the mean ± SEM for five independent experiments. * denotes statistical significance as determined by two-tailed *t*-test with $p < 0.05$. C) Cells harvested 24hr after OGD show that CHIP expression levels are significantly increased following mild (5') OGD while HSP70 expression levels increase robustly following lethal (90') OGD. Data are taken from representative experiments that were performed using at least four independent samples. D) Alterations in CHIP protein expression were quantified by performing high-resolution scans for densitometric quantification with Scion NIH IMAGE J. Values are expressed as means (± SEM) of 3 independent culturing sessions. * denotes statistical significance compared to control as determined by two-tailed *t*-test with $p < 0.05$.

In order to determine if protein degradation was altered, we evaluated the effects of mild (5'), moderate (15'), or lethal (90') OGD on neuronal proteasome activity. We observed that while mild OGD led to enhanced proteasome activity 3hr following the initial insult, it returned to baseline levels at 24hr. Moderate OGD did not affect proteasome activity at either time point we assessed, whereas lethal OGD and NMDA exposure resulted in a dramatic decrease in proteasome activity 24hr later (**FIGURE 2.4B**). These data support a model in which the proteasome is able to clear damaged and ubiquitin-tagged proteins following mild ischemic stress, but protein turnover is dramatically impaired by lethal injury.

As we observed an increase in CHIP and HSP70 expression following TIA and stroke in humans, we next sought to determine if these changes were recapitulated in our *in vitro* system. Twenty-four hours following mild, moderate or lethal OGD, CHIP levels were indeed significantly increased (**FIGURE 2.4C, D**). Moreover, HSP70 was not substantially induced until we moved beyond a 15min exposure which we have shown to be the maximal subtoxic period of OGD that these cells can withstand (Legos et al., 2002) (**FIGURE 2.4C**).

Chronic CHIP overexpression alters chaperone expression profiles following oxidative injury *in vitro*

In order to determine if cell viability was enhanced in neural systems exposed to acute oxidative stress when CHIP was chronically overexpressed, we moved into the HT-22 cells which are a neural hippocampal cell line, and a well-characterized model of neural oxidative injury (Maher, 2005, van Leyen et al., 2005). The HT-22 derived neural

cell line was generated by placing a CHIP myc construct into the HT-22 cell line. These cells are easy to transfect, reproducibly undergo glutamate induced toxicity and have many of the signaling systems essential for mediating ischemic injury (Maher, 2005, van Leyen et al., 2005, Wang et al., 2005).

Given CHIP's function as a modulator of HSP70 expression and turnover (Qian et al., 2006), we first evaluated the effects of stable CHIP overexpression on expression profiles of inducible HSPs following acute oxidative injury by exposing neural cell lines to glutamate (3mM) or the proteasome inhibitor MG132 (10μM) for 3hr. We observed that HSP40 and HSP90 expression levels remained constant in the presence of glutamate in both neural lines while HSP70 levels increased in the HT-22 derived neural line upon exposure to glutamate. Myc and CHIP expression were used as positive controls to confirm the presence of the myc-tagged CHIP construct in this cell line (**FIGURE 2.5**).

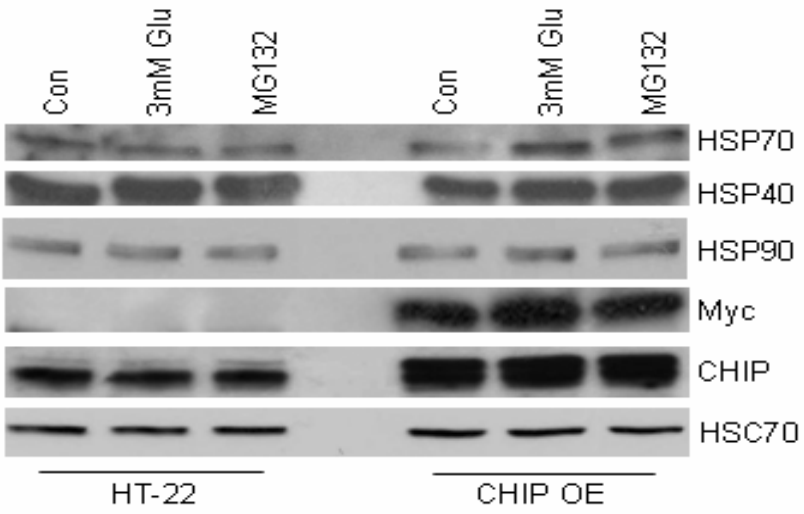

FIGURE 2.5: CHIP overexpression alters HSP expression profiles following oxidative injury. Both neural cell lines were treated with glutamate (3mM) or proteasome inhibitor for 3hr after which whole cell extracts were harvested and prepared for immunoblotting. Proteins were separated on SDS-PAGE gels and probed with antibodies specific to HSP70, HSP40, HSP90, Myc, CHIP or HSC70 as a loading control. Exposure to glutamate or the proteasome inhibitor MG132 increased HSP70 levels in the HT-22 derived neural lines cells while HSP40 and HSP90 expression levels remained constant in the presence of glutamate in these cells. Immunoblots represent results from five independent culturing sessions.

CHIP overexpression is associated with increased protein carbonyl formation following oxidative injury and enhanced baseline polyubiquitination

Given the extent of CHIP overexpression and HSP70 induction by stress, we next sought to determine if neural cells with chronically elevated CHIP levels experience alterations in the turnover of oxidized proteins. We exposed both neural cell lines to glutamate (3mM) for 3hr after which cells were harvested and total protein carbonyl formation was examined. Under control conditions, HT-22 derived neural lines exhibited an apparent decrease in total protein oxidization compared to control cells. The presence of oxidized proteins increased in both cell types following exposure to glutamate but to a greater extent in the CHIP overexpressing cultures (**FIGURE 2.6A**).

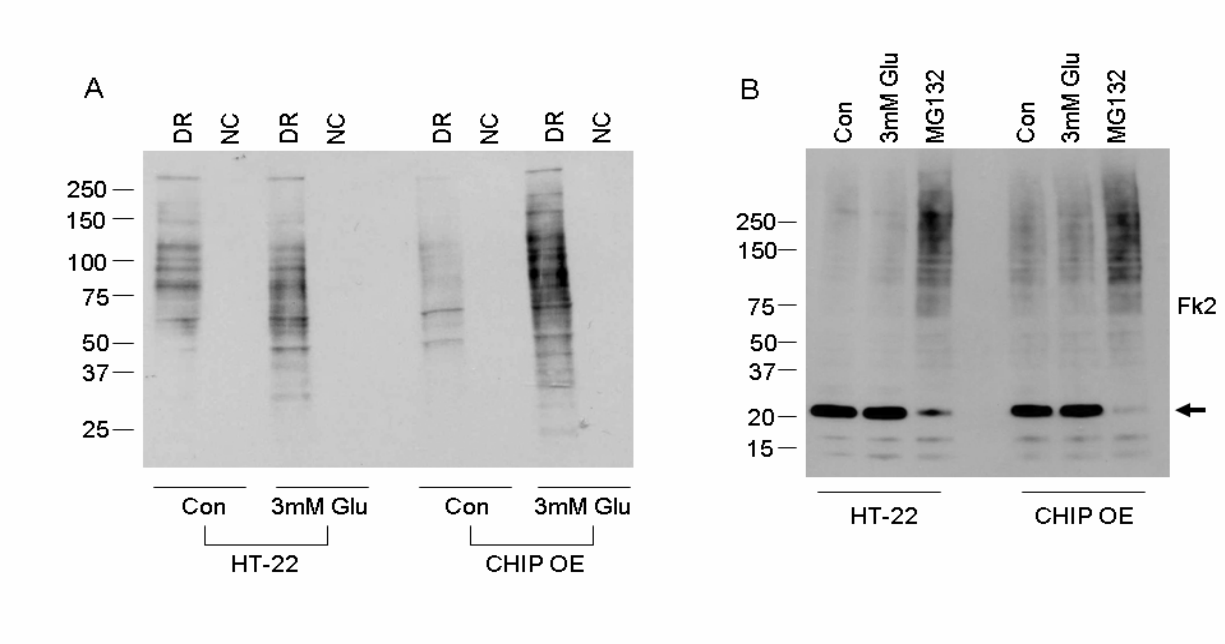

FIGURE 2.6: CHIP overexpression increases protein carbonyl formation following exposure to glutamate and baseline protein ubiquitination. A) Both neural cell lines were exposed to glutamate (3mM) for 3hr after which whole cell extracts were harvested and prepared for OxyBlotting. Exposure to glutamate results in higher levels of protein oxidation in HT-22 derived neural lines. DR, Derivatization Reaction; NC, Negative Control. B) Both neural cell lines were treated with glutamate (3mM) or proteasome inhibitor for 3hr after which whole cell lysates were prepared for immunoblotting. Equal amounts of proteins were separated by SDS-PAGE gels and probed for mono – and polyubiquitinated proteins using the Fk2 antibody. Results show increased levels of polyubiquitinated proteins in HT-22 derived lines cells at baseline. Proteasome inhibition results in a robust increase in polyubiquitinated protein levels along with a decrease in monoubiquitinated proteins (arrow) in both neural lines. Data represent results from five independent culturing sessions.

To determine if oxidized proteins were also being tagged for proteasomal degradation, we exposed both neural lines to glutamate (3mM) or the proteasome inhibitor MG132 (10μM) for 3hr after which cells were harvested and protein ubiquitination was analyzed by immunoblotting using the Fk2 antibody (**FIGURE 2.6B**). We observed increased baseline levels of polyubiquitinated proteins in CHIP overexpressing cells represented by a smear of higher molecular weight proteins. Exposure of both neural cell types to the proteasome inhibitor MG132 resulted in a robust increase in polyubiquitinated proteins along with a decrease in monoubiquitinated protein

levels (**FIGURE 2.6B**; arrow), suggesting that the ubiquitin conjugating machinery in both cell lines was highly efficient.

Exposure to oxidative injury results in an increase in ubiquitin inclusion bodies and a loss of proteasome activity in CHIP overexpressing cells

We next used immunofluorescence to evaluate the localization and morphology of ubiquitinated proteins in control and stressed cells. There was an appreciable increase in Fk2 staining following a 3hr exposure to either proteasome inhibition or oxidative challenge. Moreover, exposure to the proteasome inhibitor MG132 resulted in the formation of large, dense, cytosolic ubiquitin inclusion bodies which were predominantly localized in close proximity to the nucleus in the HT-22 derived neural lines (**FIGURE 2.7**, arrow, inset). This finding is consistent with the work by Dai et al. and Anderson et al. who demonstrate nuclear translocation of CHIP following exposure to stress (Anderson et al., 2009, Dai et al., 2003) thereby supporting CHIP's involvement in the stress response via its ability to interact with heat shock factor 1 (HSF1) and ultimately resulting in the induction of HSP expression (Dai et al., 2003, Qian et al., 2006). In contrast, small, disperse inclusion bodies were observed in the cytosol of HT-22 cells (**FIGURE 2.7A,** inset). This staining is consistent with our biochemical assessment of the chymotrypsin-like activity of the proteasome in which we observed a significant loss of baseline proteasome function in the HT-22 derived neural line (**FIGURE 2.7B**). A six hour exposure to glutamate reduced proteasome activity equally in both neural lines (**FIGURE 2.7B**). These data suggest that the chronic overexpression of CHIP decreases baseline proteasome activity, which is not toxic, but results in the accumulation of damaged proteins within cells.

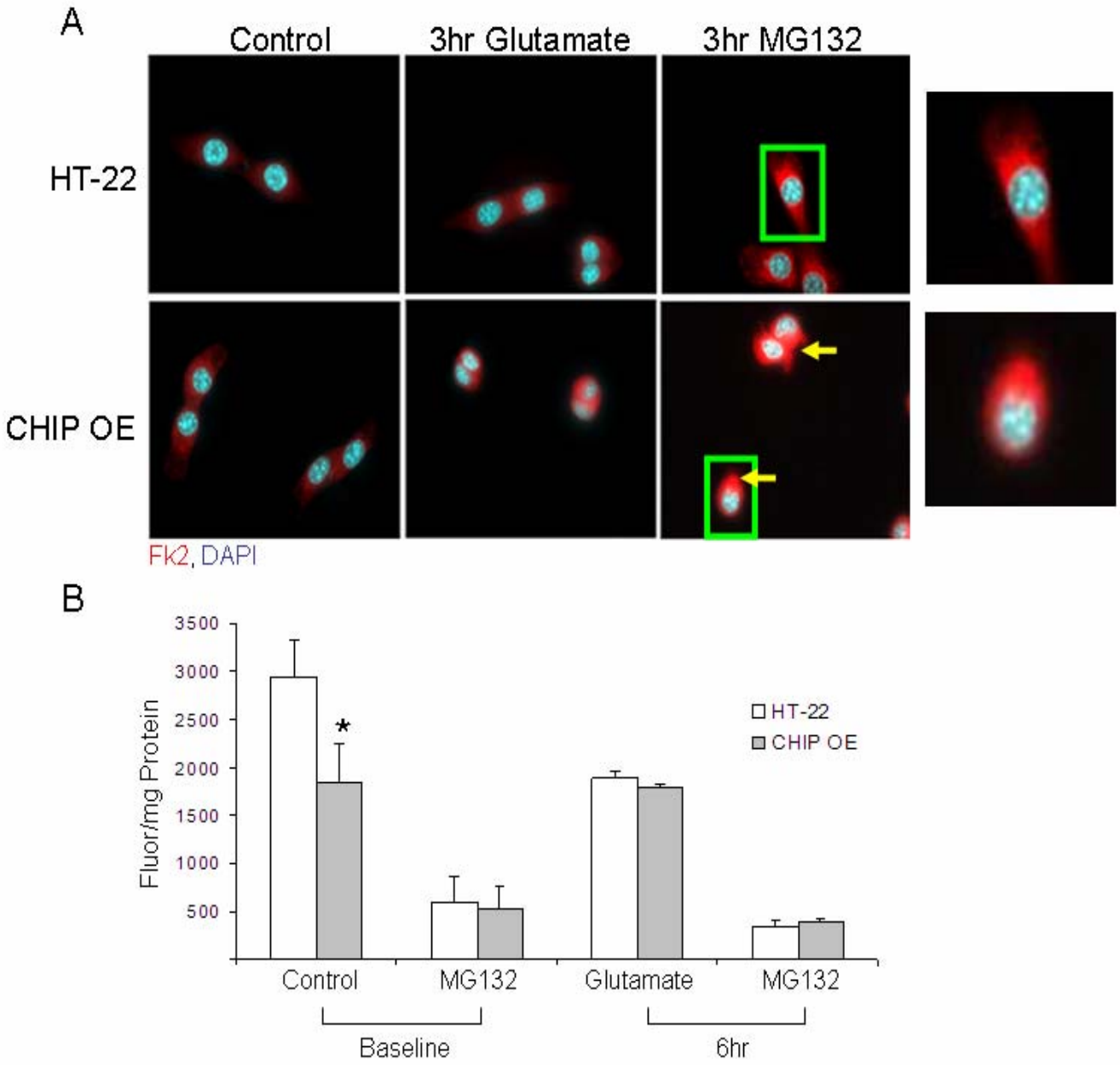

FIGURE 2.7: Exposure to oxidative injury leads to an increase in ubiquitin inclusion bodies and a loss of proteasome activity in CHIP overexpressing cells. Cells were exposed to glutamate (3mM) for 3hr in the presence or absence of the proteasome inhibitor MG132 (10μM). Immunofluorescence was performed using an Fk2 antibody (red) to evaluate ubiquitinated proteins alongside DAPI (blue) to stain cell nuclei. The increase in ubiquitin aggregates in stressed cells overexpressing CHIP is highlighted with arrows. B) Both cell lines were exposed to glutamate (3mM) for 6hr and the chymotrypsin-like activity of the proteasome was measured using the fluorescent substrate Suc-LLVY-AMC. CHIP overexpression results in decreased baseline proteasome activity. Data is expressed as fluorescence per mg protein and represent the (± SEM) of six independent experiments performed in quadruplicate. * denotes statistical significance as determined by two-tailed *t*-test with $p < 0.05$, $n = 6$.

Chronic CHIP overexpression increases vulnerability to oxidative injury *in vitro*

Taken together, these data suggest that neural cells which stably overexpress CHIP experience a baseline level of protein turnover inhibition or increased production of oxidatively damaged proteins which could alter cell fate in response to acute injury. To test this hypothesis, both cell lines were exposed to extracellular glutamate (1, 3, or 5mM) and incubated for 24hr. Cells were visually inspected and death was assessed by biochemical viability assays. Representative photomicrographs were taken 24hr later (**FIGURE 2.8A-D**). In both cell lines, similar numbers of steady state and mitotically active cells were found (Stankowski, Cohen and McLaughlin, unpublished observations), were adherent and showed healthy cellular morphology (**FIGURE 2.8A, C**). Exposure to 3mM glutamate for 24hr increased cell detachment, neural shrinkage and cell death, all of which were more pronounced in the HT-22 derived neural line (**FIGURE 2.8B, D**). CHIP overexpression was associated with a 50% decrease in cell viability following exposure to glutamate (3mM; **FIGURE 2.8E**).

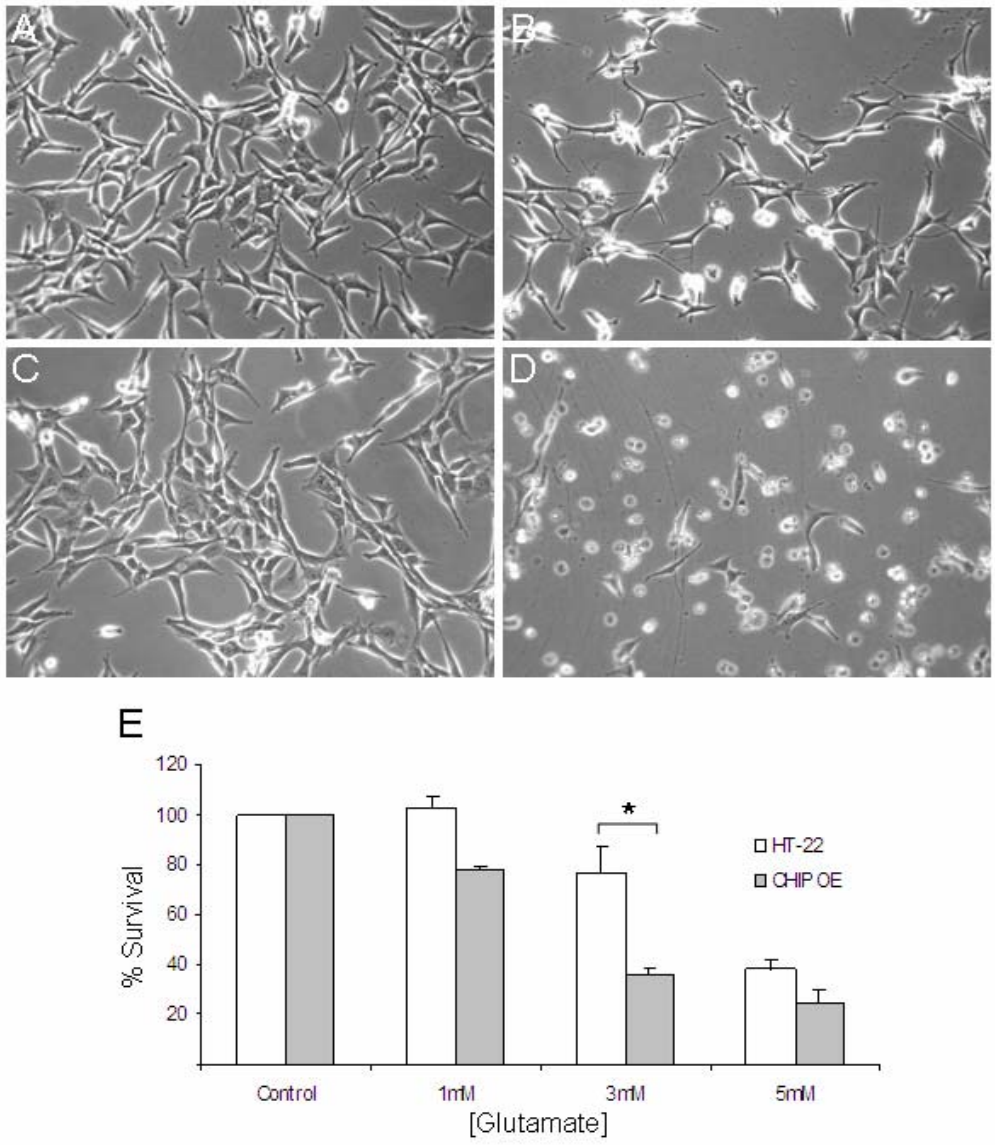

FIGURE 2.8: CHIP overexpression increases vulnerability to oxidative injury *in vitro*. Neural cell lines were treated with glutamate (3mM) for 24hr after which cell viability was determined by visually inspecting cells under phase-bright microscopy. A) Photomicrographs of control HT-22 cells B) HT-22 cells exposed to 3mM glutamate for 24hr, C) HT-22 derived neural control cultures and D) those exposed to 3mM glutamate for 24hr. Note the loss of adherent cells in panels B and D compared to respective controls and enhanced neural shrinkage and pyknosis in HT-22 derived cells compared to HT-22 cells exposed to glutamate. E) Both cell lines were treated with increasing concentrations of glutamate for 24hr and cell viability was assessed with MTT assays. Data are expressed as percent survival compared to the control and represent the mean ± SEM of five independent experiments performed in quadruplicate. * denotes statistical significance as determined by two-tailed *t*-test with $p < 0.05$, $n = 5$.

Neuronal tolerance to acute oxidative injury is enhanced when CHIP expression is silenced

As chronic CHIP overexpression was deleterious to neural survival following acute oxidative stress, we next sought to determine if blocking CHIP expression would increase neuronal tolerance in this paradigm. Primary neuronal cultures were transfected with CHIP siRNA and a green fluorescent protein (GFP) reporter followed by exposure to glutamate (3mM) 72hr later. The 72hr time point was chosen because pilot experiments using CHIP siRNA determined that optimal CHIP protein knock-down in primary neurons occurs at this time point (**FIGURE 2.1B**). The 30% transfection efficiency we achieved with this system made it amenable to immunofluorescence and cell counting to assess injury but not to biochemical analysis. Three days after CHIP silencing, neurons were exposed to mild oxidative stress for 9hr followed by incubation in propidium iodide to assess neuronal viability. We observed propidium iodide uptake predominately in cells that were not transfected with CHIP siRNA or GFP (**FIGURE 2.9A**, arrowheads). Cell counts revealed that 17% of the non-transfected cells were propidium iodide positive under control conditions, while only 1% of neurons in which CHIP expression levels were suppressed were positive for propidium iodide (**FIGURE 2.9B**). This suggests that decreasing CHIP expression increases survival following electroporation and transfection stress. Nine hours after exposure to acute oxidative injury, there was a significant increase in cells which took up propidium iodide. Thirty percent of non-transfected cells were positive for the cell death marker, whereas decreased CHIP levels dramatically improved survival with only 2% of green transfected cells also including the red staining of propidium iodide (**FIGURE 2.9A**). Taken

together, these data suggest that reducing CHIP expression levels renders neurons more resistant to acute oxidative injury.

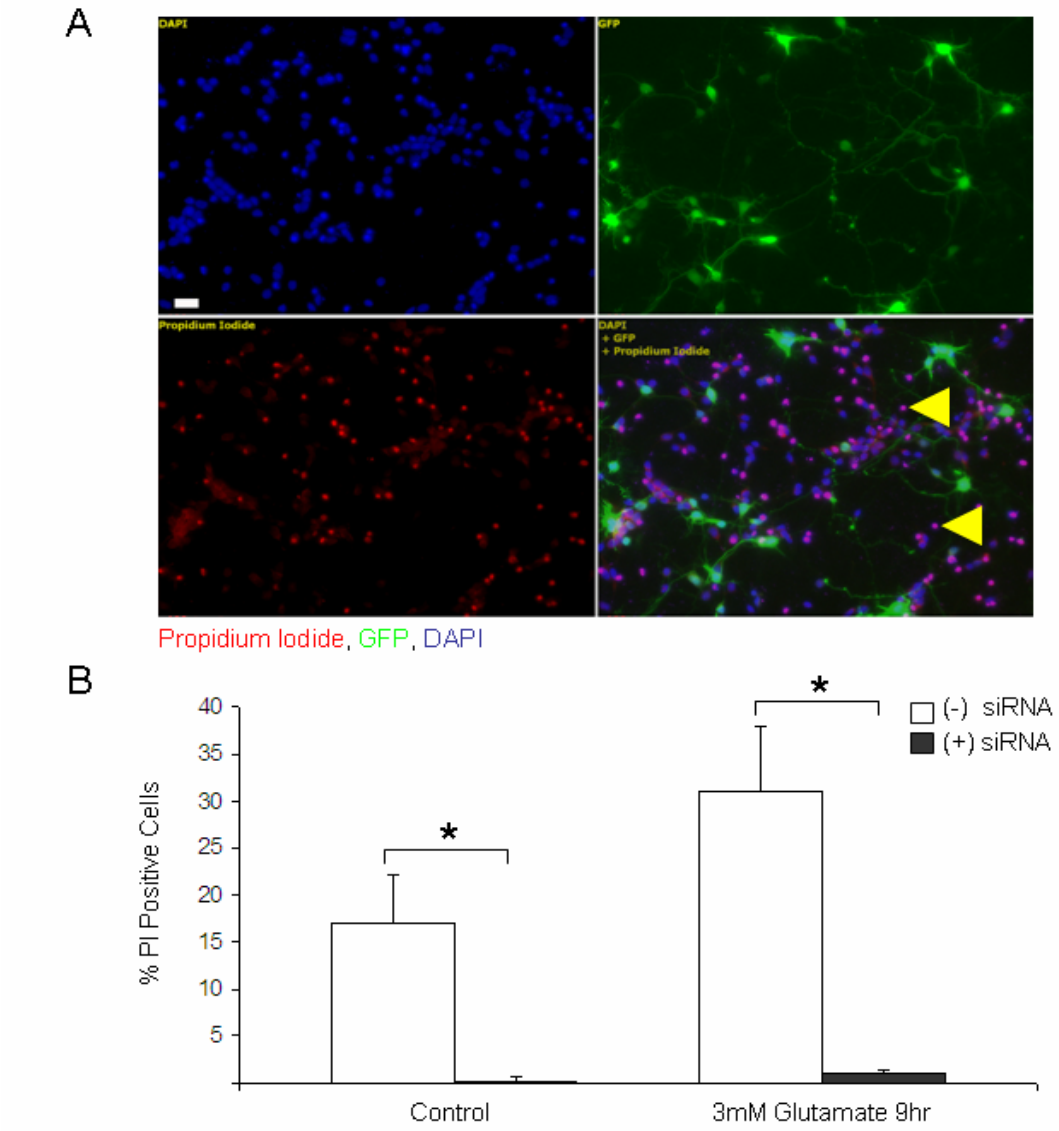

FIGURE 2.9: Decreasing CHIP expression enhances neuronal tolerance to oxidative stress. Primary cultures were transfected with CHIP siRNA upon dissociation and plated. After 72hr, cells were exposed to glutamate (3mM) for 9hr followed by incubation in propidium iodide (PI, 10μM) for 10min and fixed for immunofluorescent analysis of propidium iodide uptake (red) in cells that received CHIP siRNA (green). *See supplemental **FIGURE 2.1B** for verification of decreased CHIP expression in neurons induced by siRNA electroporation optimized to 72hr.* B) Quantification of the percent of non-transfected and CHIP transfected neurons positive for the cell death marker propidium iodide. Cell counts performed by three independent investigators of >1500 neurons revealed a significant decrease in propidium iodide uptake in neurons transfected with CHIP siRNA following exposure to acute oxidative stress. Results represent data from three independent experiments. Data was analyzed by two-tailed ANOVA and Bonferroni *post hoc* analysis performed on a group effect with * represents p <0.05. PI, Propidium iodide. Scale bar = 100μM.

Discussion

Stroke is the third leading cause of death in the US with 87% of all stroke cases being ischemic in nature (Lloyd-Jones et al., 2009, Rosamond et al., 2008). The cellular and molecular mechanisms associated with neuronal death following ischemic stroke have been extensively studied. Yet, we have failed to design effective neurotherapeutics that can increase neuronal survival following stroke (Ginsberg, 2008). While many preclinical studies have demonstrated the neuroprotective effects of molecular chaperones (Sharp et al., 1999, Yenari, 2002), we are only beginning to understand the mechanisms by which protection is afforded.

The major protective effects of the HSP70 chaperone complex are associated with sequestering activated proteases and enhancing protein refolding and degradation (Arndt et al., 2007, Beere et al., 2001, Hohfeld et al., 2001). The ability of cells to monitor the folding status of newly synthesized and preexisting polypeptides via the help of HSP70 and its associated co-chaperone complexes, assures the preservation of protein homeostasis and is essential for cellular survival (Arndt et al., 2007, Goldberg, 2003, Hohfeld et al., 2001).

The HSP70 co-chaperone of particular interest is the E3 ubiquitin ligase CHIP. This dual-function co-chaperone/E3 ligase has been predominantly studied in the context of chronic neurodegenerative diseases, with data supporting a model whereby CHIP overexpression provides neuroprotection by enhancing the degradation of damaged proteins and by substituting for the loss of other ubiquitin ligases (**FIGURE 2.10)** (Imai et al., 2002, Sahara et al., 2005). CHIP's role in governing cell fate in acute neurological

disorders as well as the ability of the brain to regulated CHIP expression following ischemic injury have, however, not been assessed up until now.

Our results are the first evidence that CHIP expression levels are increased in the human cerebral cortex following ischemic stroke. Yet, when moving into our neuronal *in vitro* model system, which provides a reproducible and accessible platform to mimic biological components seen in TIA and stroke, we found that the degree of CHIP upregulation was not as pronounced as in the human tissue samples. This observation may be due to the fact that we used neuron enriched cultures for our OGD experiments, which allow us to better detect neuronal CHIP expression levels as compared to the human tissue samples which include neurons and glia. Due to our concern that we would not be able to fully capture the molecular effects of CHIP upregulation on cell fate, we moved into the HT-22 neural cell line which allowed us to stably drive CHIP expression at high levels.

The HT-22 neural cells were chosen for our studies because they have been used extensively to model oxidative injury (Luo et al., 2006, van Leyen et al., 2005). The absence of functional NMDA receptors in these cells makes for a near pure oxidative insult versus a mixed oxidative and excitotoxic insult (Luo et al., 2006, Maher, 2005, van Leyen et al., 2005). In this model, the addition of extracellular glutamate blocks the glutamate-cystine anti-porter in the plasma membrane, subsequently leading to the loss of the intracellular antioxidant glutathione (Luo et al., 2006, Maher, 2005, van Leyen et al., 2005).

While we initially hypothesized that increasing CHIP would be neuroprotective, we observed quite the opposite. Although we did not observe significant alterations in

baseline GSH or GSSG levels in our cell lines (data not shown), we found that chronic CHIP overexpression was associated with decreased proteasome function, increased protein inclusion formation, increased levels of total oxidized proteins and poor survival following acute oxidative injury (**FIGURE 2.10**). Increased protein ubiquitination and a loss of proteasome activity have also been reported following ischemic stress in animal models, but they have never been linked to increases in expression levels of CHIP or other E3 ligases (Keller et al., 2000). We hypothesize that the increased accumulation of ubiquitinated and oxidized proteins observed in CHIP overexpressing cells is linked to either increased substrate generation or decreased substrate turnover. We favor a model in which CHIP overexpression leads to a physiological overload of polyubiquitinated proteins, thereby resulting in decreased substrate cleavage as CHIP-tagged substrates compete with the fluorogenic proteasome substrate Suc-LLVY-AMC for access to the proteasome. Our data furthermore support a model in which CHIP overexpression may fundamentally alter baseline proteasome activity. Moreover, by moving to primary neuronal cultures, we found that short-term silencing of CHIP significantly decreases vulnerability to oxidative stress.

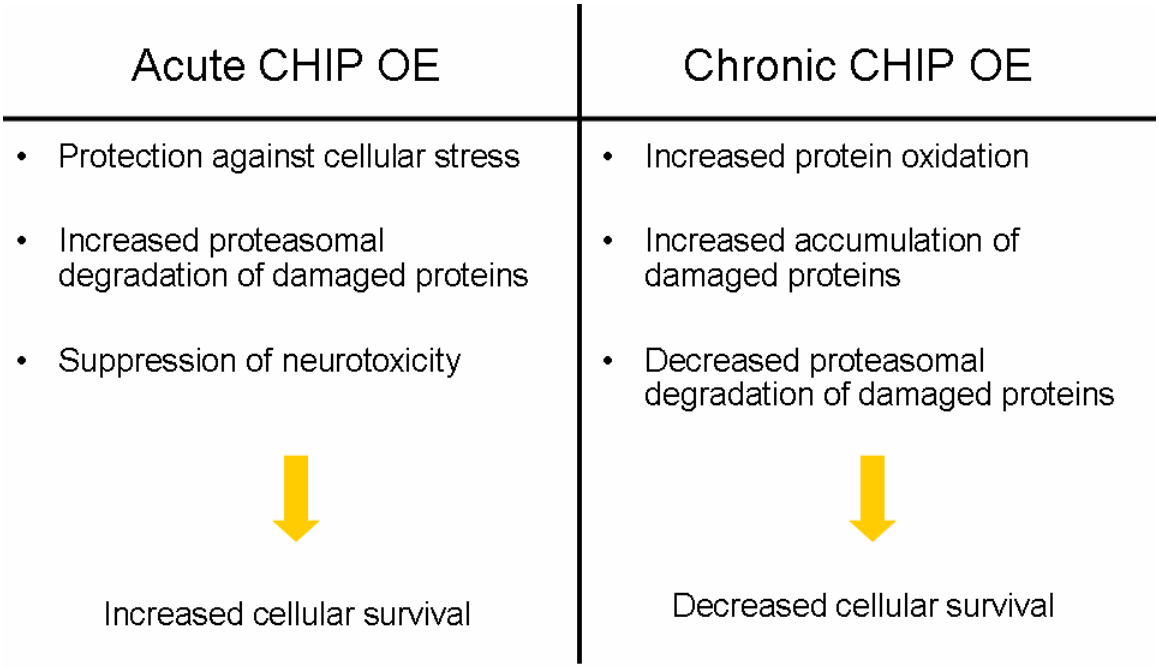

FIGURE 2.10: Effects of acute versus chronic CHIP overexpression on cell survival. Acute CHIP overexpression results in increased cellular survival due to CHIP's ability to remove damaged proteins from the cell, while chronic CHIP overexpression results in decreased cellular survival due to decreased protein turnover.

Taken together, this work is the first evidence that CHIP expression levels are elevated in the cerebral cortex of patients following ischemic stroke. While our post-mortem tissue samples are an excellent means to investigate the effects of ischemic stroke on the expression levels of CHIP, we do not know the exact time point at which CHIP expression is highest following a lethal ischemic insult, and we also do not know how the presence of other risk factors for stroke influence CHIP expression in humans. Moreover, we have a poor understanding of how CHIP expression levels change in patients who have suffered from either TIA or stroke and survived. Given the plethora of molecular events that are elicited in the days following the initial ischemic insult, it would be very intriguing to determine how long following a TIA or stroke CHIP levels

remain high and if CHIP levels are upregulated in individuals who are at high risk for stroke. Knowing if a correlation between increased CHIP expression levels and increased risk for stroke exists would allow scientists to determine if lowering CHIP expression levels would decrease the likelihood of high risk patients to suffer from the actual ischemic insult.

Given the lack of availability of not only methodologies that allow for the detection of CHIP expression levels in human CNS but also national stroke banks that would allow scientists to gather information about CHIP expression profiles from multiple post-mortem time points, scientists have to rely on model systems to study stroke. In our case, we relied on our neuronal *in vitro* model system of OGD and the HT-22 neural cell line to investigate the effects of elevated CHIP levels on neuronal survival following acute stress. Given that CHIP levels did not increase as robustly in our neuronal *in vitro* model as they did in the human tissue samples, we took advantage of the HT-22 neural cell line. The HT-22 model system allowed us to drive CHIP expression at high levels and to investigate the effects of chronic CHIP upregulation on neural survival following a pure oxidative insult. For the first time, this showed that chronic CHIP overexpression impairs neural survival following oxidative stress. While the HT-22 model system lacks several of the biological features of stroke as described in Chapter I, it provides us with a unique opportunity to identify early protein targets of oxidative stress in neural cells in order to not only establish if these proteins are potential CHIP clients, but also investigate if these oxdiatively modified proteins play a role in the pathology underlying stroke. In the work described in Chapter III, we present a novel

and powerful methodology that allows for the identification of these specific protein targets of oxidative stress.

CHAPTER III

ANALYSIS OF PROTEIN TARGETS BY OXIDATIVE STRESS USING THE OXYBLOT AND BIOTIN-AVIDIN-CAPTURE METHODOLOGY

Abstract

Carbonyl group formation on protein side chains is a common biochemical marker of oxidative stress and is frequently observed in acute and chronic neurological diseases including stroke, Parkinson's and Alzheimer's disease. We recently reported that the levels of total oxidized proteins are elevated in primary neurons following exposure to oxygen glucose deprivation, as well as in CHIP overexpressing cells following exposure to acute oxidative stress. Given the importance of proper protein function for cellular survival, it is critical to determine how oxidative stress can alter protein structure and function and how these damaged proteins contribute to disease pathology. In contrast to the traditional notion assuming that protein modification by reactive oxygen species is a random process, it has become increasingly clear that protein modifications by reactive oxygen species are specific and selective. In this work, we present two approaches that allow for the detection of protein carbonyl groups. The OxyBlot methodology allows for the evaluation of general oxidative stress, while the use of the novel and powerful biotin-avidin-capture methodology allows for the identification of specific proteins that have been targeted by oxidative stress.

Introduction

A common biochemical marker of protein oxidation is the formation of protein carbonyl groups (aldehydes and ketones) on protein side chains, particularly on prolines, arginines, lysines and threonines (Dalle-Donne et al., 2003, Levine et al., 1990, Liebler, 2008, Robinson et al., 1999, Stadtman, 2006). Protein adduction by reactive oxygen species (ROS) can not only irreversibly alter protein structure and function, but also result in polypeptide fragmentation and protein-protein cross linkage (Liebler, 2008, Stadtman, 2006).

Due to the damaging effects of ROS on protein structure and function as well as the fact that the accumulation of oxidatively modified proteins is a desirable means to evaluate cell stress, several techniques have been developed that allow investigators to determine both the levels of total oxidized proteins and the identity of adducted proteins. This is particularly salient given that until recently, protein adduction by ROS was thought to be a random process (Liebler, 2008). It has, however, become increasingly clear that protein adduction by free radicals is a selective and specific process and that approximately 80% of all proteins are modified at a single cysteine residue only (Liebler, 2008).

Using our primary neuronal *in vitro* model system of oxygen glucose deprivation (OGD) as a pliable platform to mimic the biological components seen in TIA and stroke in combination with the OxyBlot methodology to derivatize protein carbonyl groups, we demonstrated that the levels of total oxidized proteins are elevated following mild or moderate OGD. While this model system captures the many biological features of ischemic stroke, we were interested in investigating the effects of a pure oxidative insult

on protein oxidation status. For this, we moved into the HT-22 neural cell line, as exposure of these cells to extracellular glutamate results in pure oxidative stress (Maher, 2005, Stankowski & Zeiger et al., 2010, van Leyen et al., 2005).

Using the OxyBlot methodology, we reported in Chapter II that HT-22 cells which chronically overexpress the E3 ligase CHIP accumulate higher levels of total oxidized proteins following acute injury. While valuable, this technique does not allow for the identification of the specific protein targets of oxidative stress. Using the biotin-avidin-capture methodology as a means to identify specific protein targets of oxidative stress, we found that tau, a highly abundant and well known protein target of oxidative stress (Dias-Santagata et al., 2007, Egana et al., 2003, Goldbaum et al., 2002, Melov et al., 2007, Poppek et al., 2006, Vanhelmont et al., 2010, Zhu et al., 2000), was heavily oxidized in CHIP overexpressing cells upon exposure to glutamate. The detection of tau was used as a proof-of-principle showing that this novel technique is applicable to our *in vitro* model system as it has predominantly been used to test protein damage triggered by exogenous applications of toxic chemicals, including 4-hydroxy-2-nonenal (4-HNE) (Codreanu et al., 2009, Liebler, 2008). Ultimately, the biotin-avidin-capture methodology offers the potential to determine which specific proteins are oxidatively modified. This in turn will allow investigating if these proteins are potential CHIP clients and if proteins that are modified by oxidative stress play a role in the pathology underlying stroke.

Principles of the OxyBlot methodology

The chemical reaction underlying the OxyBlot methodology was initially described by Shacter's group in 1994 (Levine et al., 1994) and has been extensively employed thereafter (Dalle-Donne et al., 2003, Robinson et al., 1999, Shacter et al., 1994). Carbonylated proteins are relatively stable, which allows the derivatization of carbonyl groups with 2,4-dinitrophenylhydrazine (DNPH) resulting in the formation of a stable dinitrophenyl (DNP) hydrazone product (**FIGURE 3.1**). The subsequent separation of oxidatively modified proteins by electrophoresis followed by the identification of the DNP moiety of the protein (**FIGURE 3.1**) using the Western blot technology and anti-DNP antibodies allows for the rapid and highly sensitive determination of total protein carbonyl formation (Dalle-Donne et al., 2003, Levine et al., 1994, Robinson et al., 1999, Shacter et al., 1994).

The use of the derivatization control solution (negative control) allows for a side-by-side comparison of proteins that have and have not been oxidatively modified. Specifically, bands that are present in the derivatization reaction, but are absent in the negative control reaction, have undergone modifications. Moreover, with the use of proper controls, the overall intensity of the bands correlates to the overall degree of protein oxidation. That is, the more intense the bands are, the more oxidized proteins are present in a given sample.

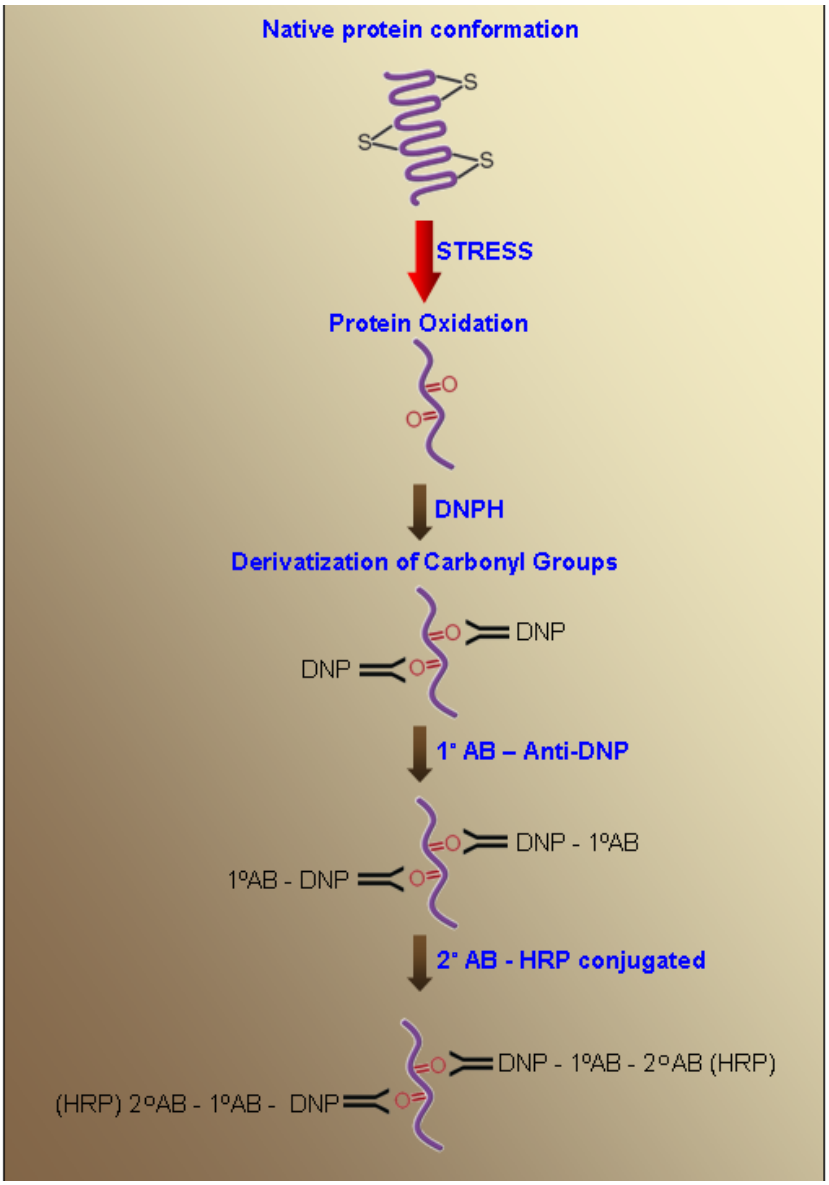

FIGURE 3.1: Schematic of the derivatization of protein carbonyl groups. Cellular exposure to stress results in protein damage characterized by the formation of protein carbonyl groups (red side chains). The OxyBlot methodology uses 2,4-dinitrophenylhydrazine (DNPH) to derivatize protein carbonyl groups leading to the formation of a stable dinitrophenyl (DNP) hydrazone product. The primary antibody is directed against the DNP moiety of the protein. The secondary, HRP-conjugated antibody, allows for the use of chemiluminescent reagents to visualize bands of oxidized proteins upon exposure to film.

Materials for OxyBlot procedure

All materials required for the OxyBlot procedure are listed below. It should be noted that similar products and equipments may be used from alternate vendors at the user's discretion.

1. The OxyBlot Protein Oxidation Detection Kit (S7150) was purchased from Chemicon International (Temecula, CA). The mixture of standard proteins with attached DNP residues should be stored at -20ºC after the first use. All other reagents can be stored at 4ºC.
2. 6-well tissue culture plates.
3. 1.5ml Eppendorf tubes. For each condition, the following pre-labeled Eppendorf tubes are needed:
   a. Sample for protein assay
   b. Sample for Western blotting
   c. Sample for OxyBlot
   d. Derivatization reaction for OxyBlot
   e. Negative control for OxyBlot
4. Ice cold 1xPBS (100ml 10xPBS; 900ml milliQ H_2O)
5. TNEB (50mM Tris-HCl, 2mM EDTA, 100mM NaCl and 1%NP-40; pH 7.8) with added protease inhibitor cocktail (P8340, Sigma-Aldrich, St. Louis, MO).
6. Dithiothreitol (DTT; D9779, Sigma-Aldrich, St-Louis, MO). Prepare a 1M stock solution in milliQ H_2O and store at -20ºC. The working concentration of DTT is 50mM and should not be stored for more than 6hr.

7. Laemmeli Buffer (Cat # 161-0737, Bio-Rad Laboratories, Hercules, CA) with ß-mercaptoethanol (M7154, Sigma-Aldrich, St. Louis, MO) at a ratio of 1:19.
8. 12% sodium dodecyl sulfate made in milliQ H_2O (SDS; L3771, Sigma-Aldrich, St. Louis, MO).
9. Bio-Rad D_c Protein Assay kit (Bio-Rad Laboratories, Hercules, CA).

Materials for the Western blot procedure

1. 4-12% Criterion Bis-Tris gels (Cat # 345-0123, Bio-Rad Laboratories, Hercules, CA).
2. Precision Plus Protein Standard All Blue Molecular Weight Marker (Cat # 161-0373, Bio-Rad Laboratories, Hercules, CA).
3. XT-MOPS running buffer (Cat # 161-0788, Bio-Rad Laboratories, Hercules, CA).
4. 1xTris/Glycine transfer buffer (Cat # 161-0772, Bio-Rad Laboratories, Hercules, CA).
5. Hybond P polyvinylidene difluoride (PVDF) membrane (Cat # RPN303F, GE Healthcare, Piscataway, NJ).
6. Western Lightning Chemiluminescence Reagent Plus (Cat # NEL105, Perkin Elmer Life Sciences, Inc., Boston, MA).
7. Gel Code Blue Stain Reagent (Cat # 24592, Thermo Scientific, Rockford, IL).
8. Methanol (439193, Sigma-Aldrich, St. Louis, MO).
9. Tween 20 (P7949, Sigma-Aldrich, St. Louis, MO).
10. 1xPBS-Tween 20 (0.05% Tween 20).
11. Blocking/Dilution buffer (1%BSA/PBS-Tween 20).

12. Primary Antibody: Rabbit Anti-DNP antibody (provided in OxyBlot kit).
13. Secondary Antibody: Goat Anti-Rabbit IgG (HRP-conjugated) antibody (provided in OxyBlot kit).

Methods

OxyBlot procedure using 5µl of each sample

1. Start by scraping cells from the dish using a rubber policeman in 350µl TNEB with added protease inhibitor cocktail. For each condition, cells grown in two wells of a 6-well plate are combined. A protein concentration of 1mg/ml is recommended for the OxyBlot methodology.
2. Of this cell suspension, save 50µl for the determination of protein concentrations and resuspend 150µl in an equal volume of Laemmeli Buffer with ß-mercaptoethanol. Heat sample to 95ºC for 10min and store at -20ºC. During preliminary experiments, it was noted that the concentration of DTT used for the OxyBlot procedure was not compatible with most standard protein assays. As a result, we decided to remove a 50µl aliquot from the cell suspension for the determination of protein concentrations.
3. Add the remaining 150µl of the cell suspension into a new Eppendorf tube containing dithiothreitol (DTT, 50mM) and vortex sample briefly. Ideally, it is best to perform the OxyBlot reaction (**FIGURE 3.2**) directly after lysing the cells. However, samples containing 50mM DTT may be frozen at -20ºC. For best results, do not store samples for more than one month.

4. For the OxyBlot procedure, follow the flow chart outlined in **FIGURE 3.2**. In brief, 5µl of the cell lysate designated for the OxyBlot procedure as well as 5µl 12% SDS should be added into two new Eppendorf tubes, of which one is designated for the derivatization reaction (DR) and the other one for the negative control (NC). Next, add 10µl of 1x 2,4-dinitrophenylhydrazine (DNPH) or 1x derivatization control solution into the 1.5ml Eppendorf tubes designated for the derivatization reaction or negative control, respectively. The sample for the derivatization reaction takes on an orange color following the addition of 2,4-dinitrophenylhydrazine. For the OxyBlot procedure more than 5µl of cell lysates per reaction tube may be treated, but the volumes of the other reagents have to be adjusted accordingly. For instance, if 10µl of cell lysate are used, double all reagent volumes (i.e., 10µl 12% SDS, 20µl 1xDNPH solution, 20µl 1x derivatization solution, 15µl neutralization solution). This allows for running two Western blots probing for oxidized proteins from the same sample. Moreover, in order to prevent an artificial increase in protein carbonyl content in the samples, do not allow samples to stand in the derivatization solution for more than 15-20min (Levine et al., 1994).
5. Allow samples to incubate at room temperature for 15min after which 7.5µl of the neutralization solution should be added to each sample.
6. Store samples at 4ºC and run samples on a gel within seven days of protein derivatization. Alternatively, samples can be aliquoted and stored at -20ºC. Samples should be allowed to reach room temperature prior to immunoblotting.

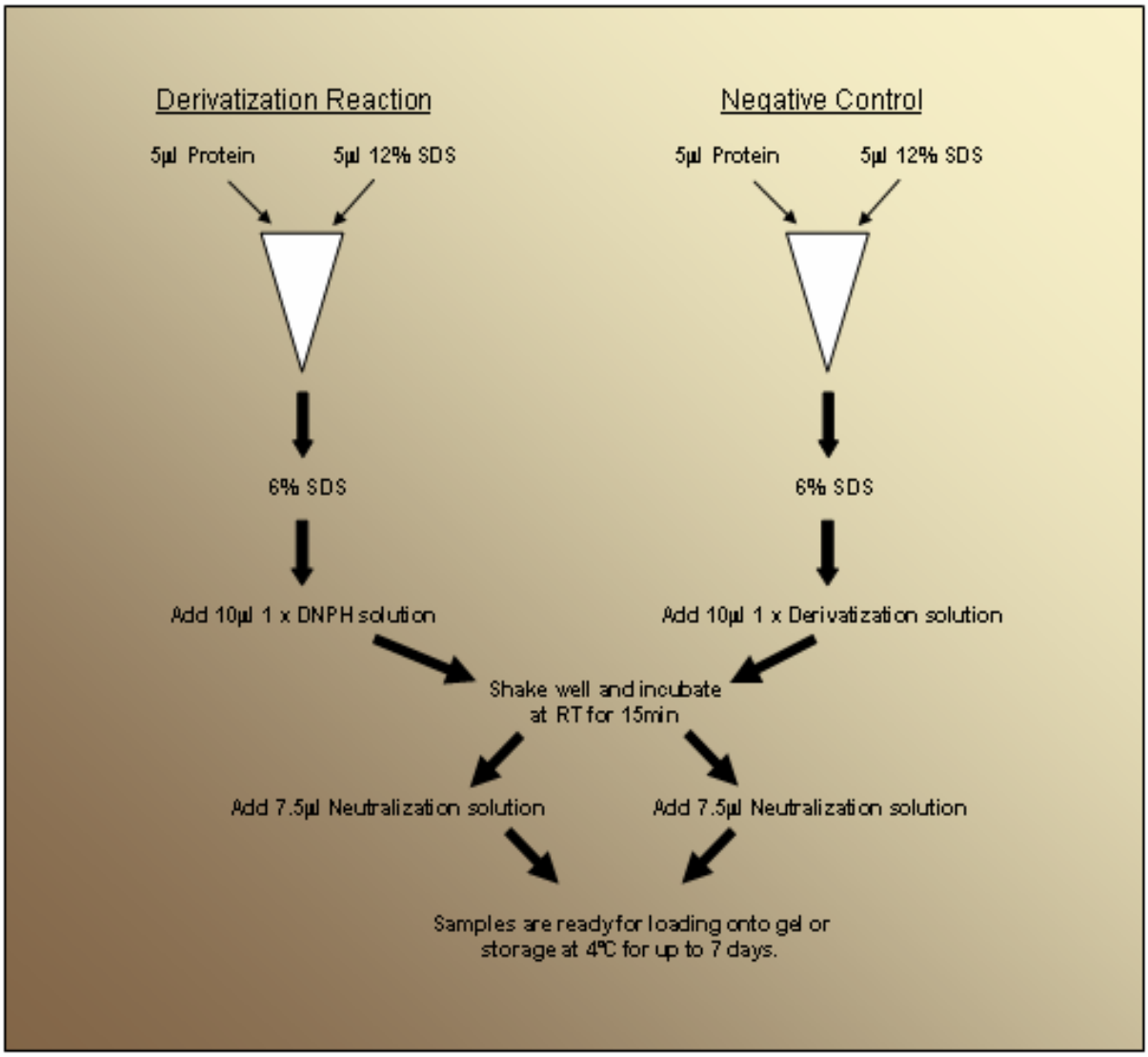

FIGURE 3.2: OxyBlot methodology flow-chart. Five µl sample are added to two pre-labeled 1.5ml Eppendorf tubes, of which one is designated for the derivatization reaction (DR) and the second one for the negative control (NC). Five µl of 12% SDS are added to each sample to obtain a final concentration of 6% SDS. Ten µl of 1xDNPH or 1x derivatization control solution should be added to samples designated for the derivatization reaction or negative control, respectively. Samples are allowed to incubate for 15min at room temperature, after which 7.5µl neutralization solution should be added to each sample. Samples are ready to be processed using gel electrophoresis.

Western blotting

1. Allow OxyBlot samples to reach room temperature prior to loading samples on a gel. Do not heat samples.
2. For best results, use a gradient gel (e.g., 4-12%).
3. Start loading the gel by adding 10µl of the Precision Plus Protein Standard All Blue Molecular Weight Marker.
4. Assuring equal protein concentrations of all samples, load the appropriate volume of the OxyBlot samples so that the sample of the derivatization reaction is next to the sample of the negative control. This allows for a more efficient comparison of bands during analysis. To assure equal protein loading, use samples prepared for Western blot analysis and run gels probing for HSC70, GAPDH or any other commonly used loading control.
5. Follow manufacturer's directions to run the gel.
6. Transfer proteins onto a PVDF membrane by following manufacturer's directions for the used transfer apparatus.
7. Block non-specific primary antibody binding by placing the membrane into methanol for 5min.
8. Allow membrane to dry for 15-20min before placing it into primary antibody.
9. Prepare 15ml of a 1:150 dilution of the primary antibody provided in the OxyBlot kit in blocking/dilution buffer. Preliminary experiments determined that the primary antibody provided in the OxyBlot kit cannot be reused. For best results, prepare new primary antibody for each Western blot.

10. Incubate the membrane in the primary antibody over night at 4ºC while shaking on an orbital shaker.
11. Using multiple changes of 1xPBS-Tween 20, wash membrane for a total of 30min before adding the secondary antibody.
12. Prepare 15ml of a 1:300 dilution of the secondary antibody provided in the OxyBlot kit in blocking/dilution buffer.
13. Incubate membrane for 1hr at room temperature while shaking on an orbital shaker.
14. Using multiple changes of 1xPBS-Tween 20, wash membrane for a total of 30min before adding the chemiluminescent reagent according to manufacturer's specifications and exposing the membrane to film.

Interpretation of data

1. All biological samples have oxidized proteins with higher levels of total protein oxidation in samples following biological stress.
2. The final result of the OxyBlot procedure shows several bands in the derivatization reaction sample of each condition (**FIGURE 3.3**). Bands that are present in the derivatization reaction but not in the negative control have undergone oxidative modifications. It has been determined that longer exposure times of the membrane are required in order for bands in the negative control reaction to appear. Exposure times of up to 15min have been required in order to see bands in the negative control reactions.

3. The degree of protein oxidation can be identified by the intensity of the bands. That is, the more intense the bands are, the higher the degree of stress specific protein oxidation.

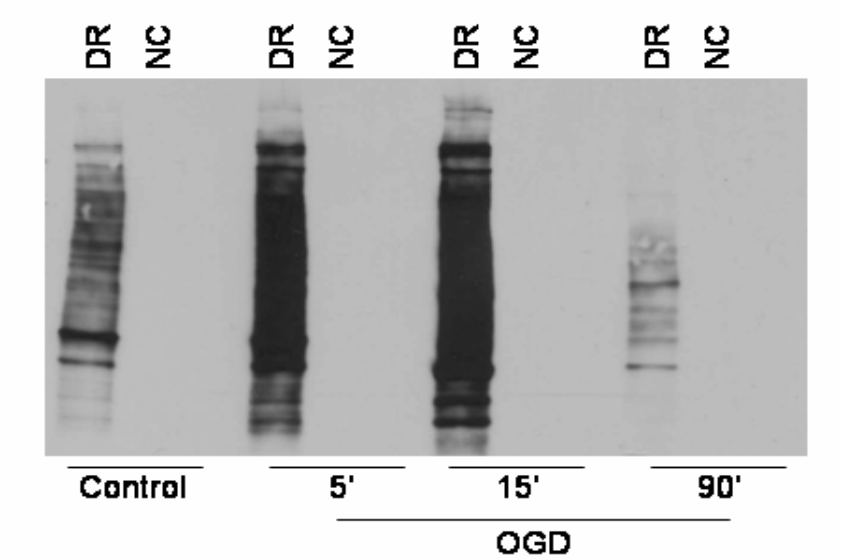

FIGURE 3.3: Neuronal exposure to OGD results in protein oxidation. Mature neuron enriched primary forebrain cultures were exposed to oxygen glucose deprivation (OGD) for various durations of time (5', 15' or 90') and protein oxidation was determined using the OxyBlot methodology 24hr following termination of OGD. Levels of total oxidized proteins increased robustly following mild (5') or moderate (15') OGD, but decreased strongly following exposure to lethal (90') OGD. DR, Derivatization Reaction; NC, Negative Control.

Principles of the biotin-avidin-capture methodology

The biotin-avidin-capture methodology combined with immunoblotting is a powerful new technology that allows for the detection of *specific* proteins that have been modified by oxidative stress. This methodology uses biotin hydrazide to covalently label carbonyl groups that have formed on protein side chains upon exposure to oxidative stress (**FIGURE 3.4**). Using immunoprecipitation, adducted proteins bound to biotin hydrazide are pulled down allowing for the elution of oxidatively modified proteins. The

subsequent immunoblotting analysis allows for a rapid screening of proteins of interest to determine if these proteins have been oxidized (**FIGURE 3.5**) (Codreanu et al., 2009).

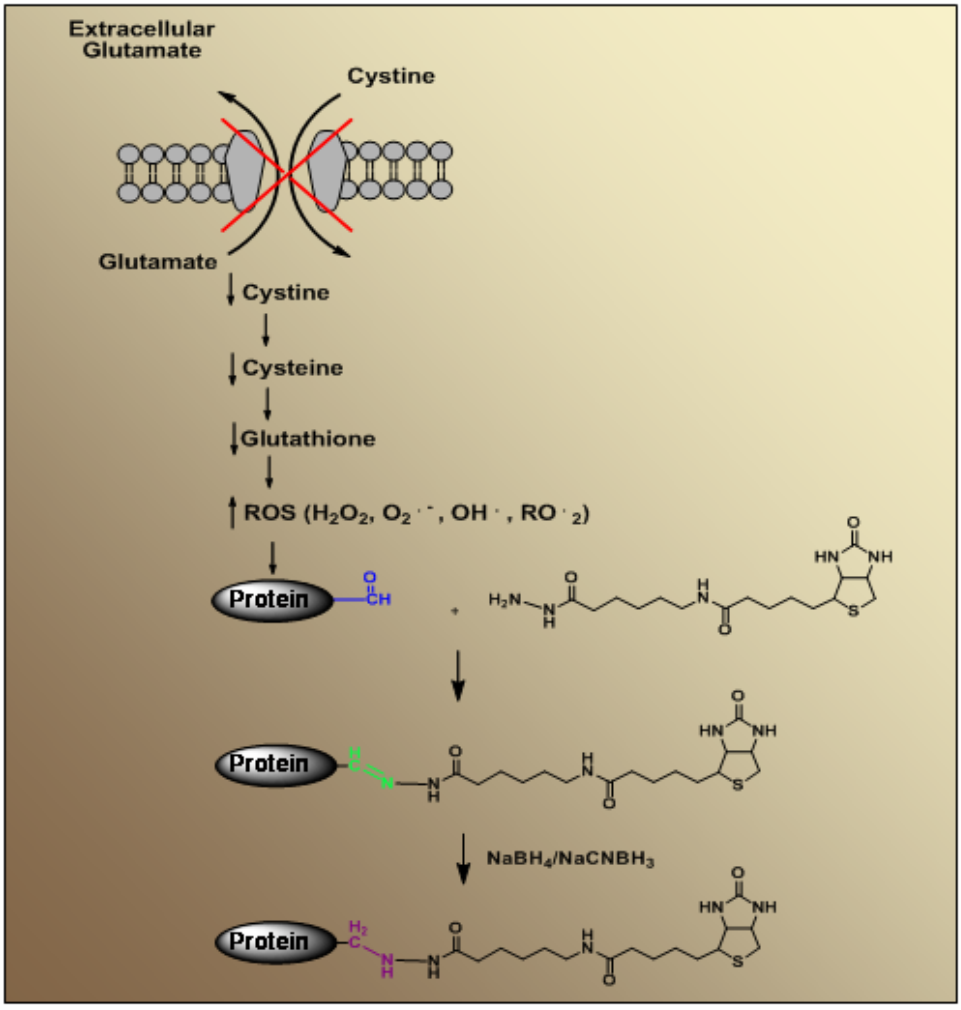

FIGURE 3.4: Schematic of the biotin-avidin-capture methodology. Exposure of HT-22 cells to extracellular glutamate results in the depletion of the main intracellular antioxidant glutathione and the elevation of ROS levels. Protein damage by ROS results in the formation of carbonyl groups on protein side chains (blue side chain) which are derivatized with biotin hydrazide (formation of green double bond). The addition of sodium borohydride reduces the initial Schiff base formed between the carbonyl and biotin hydrazide (formation of purple single bond), thus preventing the reversion of the adduct. The oxidative status of proteins of interest can then be analyzed by using the Western blot methodology. Although the addition of extracellular glutamate is used to induce oxidative stress in the HT-22 model system, interfering with glutathione synthesis at any other step or directly adding reactive oxygen species to the cells are equally effective means to induce oxidative stress.

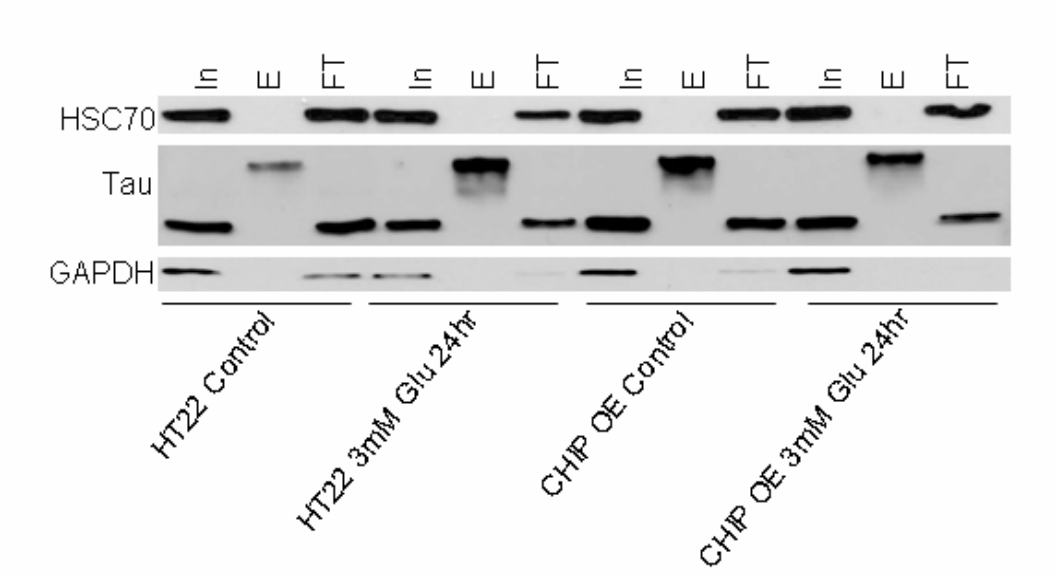

FIGURE 3.5: Tau is oxidized in HT-22 cells. To induce oxidative stress, HT-22 and CHIP OE cells were exposed to glutamate (3mM) for 24hr after which cells were harvested, protein concentrations were determined and oxidized proteins were immunoprecipitated using the biotin-avidin-capture methodology. Neither HSC70 nor GAPDH are oxidized in this cell line even after prolonged exposure to glutamate. The microtubule-associated protein tau and CHIP substrate is highly oxidized in CHIP OE cells (Band in 'eluate' lane). In, Input; E, Eluate; FT, Flow through.

Materials for the biotin-avidin-capture methodology

1. 1.5ml clear Eppendorf tubes.
2. Ice cold 1xPBS (100ml 10xPBS; 900ml milliQ H_2O).
3. TNEB (50mM Tris-HCl, 2mM EDTA, 100mM NaCl and 1%NP-40; pH 7.8) with added protease inhibitor cocktail (P8340, Sigma-Aldrich, St. Louis, MO).
4. Bio-Rad D_c Protein Assay kit (Bio-Rad Laboratories, Hercules, CA).
5. MilliQ H_2O.
6. Dimethyl sulfoxide (DMSO; D8418, Sigma-Aldrich, St. Louis, MO).

7. Biotin hydrazide (B3770, Sigma-Aldrich, St. Louis, MO). Prepare a 50mM stock solution in DMSO and prepare freshly before every experiment. The final concentration of biotin hydrazide per sample is 5mM.
8. Sodium borohydride (213462, Sigma-Aldrich, St. Louis, MO). Prepare a 500mM stock solution in milliQ H_2O and prepare freshly before every experiment. The final concentration of sodium borohydride is 50mM.
9. NuPAGE LDS Sample Buffer (4x) (NP0007, Invitrogen, Carlsbad, CA).
10. Amicon Ultra Centrifugal Filter Devices (UFC801024, Millipore, Billerica, MA).
11. Streptavidin Sepharose High Performance Beads (17-5113-01, GE Healthcare, Uppsala, Sweden).
12. 1% sodium dodecyl sulfate (SDS; L3771, Sigma-Aldrich, St. Louis, MO).
13. 1M sodium chloride (NaCl; S9525, Sigma-Aldrich, St. Louis, MO).
14. Dithiothreitol (DTT; D9779, Sigma-Aldrich, St-Louis, MO). Prepare a 1M stock solution and store at -20ºC. The working concentration of DTT is 50mM and should not be stored for more than 6hr.
15. 4M urea (U6504, Sigma-Aldrich, St. Louis, MO). Urea has to be freshly prepared before every experiment.

Materials for the Western blot procedure

1. 4-12% Criterion Bis-Tris gels (Cat # 343-0123, Bio-Rad Laboratories, Hercules, CA).
2. Precision Plus Protein Standard All Blue Molecular Weight Markers (Cat # 161-0373, Bio-Rad Laboratories, Hercules, CA).

3. XT-MOPS running buffer (Cat # 161-0788, Bio-Rad Laboratories, Hercules, CA).
4. 1xTris/Glycine transfer buffer (Cat # 161-0772, Bio-Rad Laboratories, Hercules, CA).
5. Hybond P polyvinylidene difluoride (PVDF) membrane (Cat # RPN303F, GE Healthcare, Piscataway, NJ).
6. Western Lightning Chemiluminescence Reagent Plus (Cat # NEL105, Perkin Elmer Life Sciences, Inc., Boston, MA).
7. Gel Code Blue Stain Reagent (Cat # 24592, Thermo Scientific, Rockford, IL).
8. Methanol (439193, Sigma-Aldrich, St. Louis, MO).
9. Tween 20 (P7949, Sigma-Aldrich, St. Louis, MO).
10. 1xTBS-Tween 20 (100ml 10 x TBS, 900ml milliQ H_2O, 0.05% Tween 20).
11. Carnation Instant Non-Fat Dry Milk Powder (Nestlé, Vevey, Switzerland).
12. Primary antibodies: Rabbit Anti-HSC70 (SPA-816; Stressgen, Ann Arbor, MI); Rabbit Anti-Tau (A0024; DaykoCytomation, Glostrup, Denmark); Mouse Anti-GAPDH (AM4300; Ambion, Inc., Austin, TX).
13. Secondary antibodies: Anti-rabbit IgG HRP-linked antibody (7074; Cell Signaling, Danvers, MA); Anti-mouse IgG HRP-linked antibody (7076; Cell Signaling, Danvers, MA).

Methods

Biotin-avidin-capture methodology

1. Start by harvesting cells and determining protein concentrations by using the Bio-Rad D_c Protein Assay kit.

2. Adjust protein concentrations to 2mg/ml for each sample. The final volume of each sample should be 1ml.
3. Remove 50µl sample from each tube and transfer into a new pre-labeled 1.5ml Eppendorf tube. Add DTT (50mM) and NuPage Sample buffer (4x) to each sample, heat samples for 10min at 95ºC, and store at -20ºC. This sample is referred to as the *whole cell lysate*.
4. Add biotin hydrazide (5mM) into the remainder of each sample and incubate samples for 2hr in the dark while rotating on a tube rotator.
5. Following the termination of the incubation time, add sodium borohydride (50mM) to each sample and allow samples to incubate for 30min at room temperature. The formation of bubbles indicates the reduction of double bonds into single bonds. Do not close Eppendorf tubes during this process.
6. During the 30min incubation time, prepare Amicon Ultra Centrifugal Filter Devices. One filter device per sample is needed. Add 1ml 1xPBS into the filter device followed by a 20min centrifugation at 2,472 x *g*.
7. Upon termination of the 30min incubation, add the entire sample and 2.5ml cold 1xPBS into the filter device. Spin samples at 2,472 x *g* for 20min. Remove the flow through upon termination of centrifugation. Add another 2.5ml 1xPBS into the filter device and centrifuge the sample at 2,472 x *g* for 20min. Remove the flow through upon termination of centrifugation and repeat washes for a total of three times.
8. During the last spin, start to prepare a bead slurry composed of 250µl Streptavidin Sepharose High Performance Beads and 250µl 1xPBS.

9. Wash the beads for a total of three times by following the subsequent steps:
   a. Vortex bead slurry.
   b. Centrifuge bead slurry on bench top centrifuge at 2,282 x *g* for approximately one minute.
   c. Carefully discard supernatant.
   d. Add 1ml 1xPBS.
   e. Repeat steps a-d.
10. Upon termination of the three washes of the beads, add 500µl 1xPBS to prevent the drying out of the beads until samples are ready to be added.
11. After termination of the final centrifugation, the approximate volumes of each sample have to be estimated. Prepare a new 1.5ml Eppendorf tube for each sample and estimate the approximate amount of the sample that did not flow through the filter by pipetting this volume into the designated pre-labeled 1.5ml Eppendorf tube, thereby paying attention to the volumes that are transferred.
12. Adjust all samples to an equal volume by adding the appropriate amount of 1xPBS to the samples. Volumes of samples have to be adjusted in order to facilitate the balancing of the samples on the tube rotator over night. Transfer 100µl of each sample into a new pre-labeled 1.5ml Eppendorf tube, followed by the addition of DTT (50mM) and NuPage Sample buffer (4x). Heat the samples for 10min at 95ºC and store at -20ºC. This sample is referred to as the *input*.
13. Centrifuge bead slurry on bench top centrifuge at 2,282 x *g* for approximately one minute and carefully remove the entire supernatant.

14. Add the remainder of each sample to the appropriate pre-labeled 1.5ml Eppendorf tube containing washed Streptavidin Sepharose High Performance Beads and carefully mix the beads with the sample.
15. Allow samples to incubate at 4ºC over night while rotating on a tube rotator.
16. The following day, prepare 1% SDS, 1M NaCl and 4M urea. Note that the urea has to be freshly prepared before every experiment.
17. Centrifuge samples on bench top centrifuge at 2,282 x *g* for approximately one minute.
18. Transfer 100µl of the supernatant into a new pre-labeled 1.5ml Eppendorf tube. Add DTT (50mM) and NuPage Sample buffer (4x) to each sample. Heat samples for 10min at 95ºC and store at -20ºC. This sample is referred to as the *flow through*. Transfer the remainder of the supernatant into another 1.5ml Eppendorf tube and store at -20ºC.
19. Follow steps a-e listed below for the following washes. Wash the beads twice with 1% SDS. Then wash beads with 4M urea. Next, beads should be washed 1M NaCl and finally with 1xPBS. (Example uses 1% SDS, which is the solution used for the first 2 washes. Save the supernatant after the first wash only. All other supernatants may be discarded):
    a. Add 1ml of 1% SDS to the beads.
    b. Vortex.
    c. Manually invert tubes approximately 20 times.
    d. Centrifuge samples on bench top centrifuge at 2,282 x *g* for approximately one minute.

e. Discard supernatant.

20. Elute beads in 90µl NuPage Sample buffer (4x) and DTT (50mM). This sample is referred to as the *eluate*.
21. Vortex all samples and heat for 10min at 95ºC. Store at -20ºC.

Western blotting

1. Heat input, eluate and flow through samples of each experimental condition for 10min at 95ºC.
2. Dedicate one lane of your gel to the protein standard by adding 10µl of the Precision Plus Protein Standard All Blue Molecular Weight Marker.
3. Load 10µl of the samples to the gel. Add samples in the following order: input, eluate, flow through. This allows for a more efficient comparison of bands during analysis. Given that the exact protein concentrations cannot be determined following the elution of oxidized proteins from the beads, we run Western blots assuming equal protein concentrations in the samples. These results should not be used for quantification purposes, but instead for the determination of the oxidative status of a protein only. Moreover, when using 10µl of each, input, eluate and flow through from each sample, a total of 10 gels can be run. However, stripping the membrane and incubating it with another antibody allows for the probing of one membrane with several different antibodies against proteins of varying molecular weights, thereby increasing the number of proteins that can be analyzed.
4. Follow manufacturer's directions to run the gel.

5. Transfer proteins onto a PVDF membrane by following manufacturer's directions for the used transfer apparatus.
6. Block non-specific primary antibody binding by placing the membrane into methanol for 5min.
7. Allow membrane to dry for 15-20min before placing the membrane into the primary antibody.
8. Prepare primary antibodies of interest in dilution buffer (5% non-fat dry milk, 1xTBS-Tween 20).
9. Incubate the membrane in primary antibody over night at 4ºC while shaking on an orbital shaker.
10. Using multiple changes of 1xTBS-Tween 20, wash membrane for a total of 30min before adding the secondary antibody.
11. Prepare appropriate secondary antibodies in dilution buffer (5% non-fat dry milk, 1xTBS-Tween 20).
12. Incubate membrane for 1hr at room temperature while shaking on an orbital shaker.
13. Using multiple changes of 1xTBS-Tween 20, wash the membrane for a total of 30min before adding the chemiluminescent reagent according to manufacturer's specifications and exposing the membrane to film.

Interpretation of data

1. Proteins that have undergone modifications following exposure to oxidative stress are identified as a band in the eluate lane (*see* **FIGURE 3.5**, Tau). The absence of

bands in the lane designated for the eluate sample indicates the absence of oxidative modifications of the protein of interest.

Discussion

The generation of ROS is part of normal human metabolism. When present at low levels and when pro- and antioxidants are balanced, ROS are indeed beneficial for proper cellular function (Droge, 2002, Halliwell et al., 2007, Hancock et al., 2001, Lambert et al., 2009, Sykes et al., 2007, Ying et al., 2007). When produced in excess and when antioxidants can no longer scavenge and detoxify ROS, tissue injury occurs via the ability of ROS to damage macromolecular structures including proteins, lipids and nucleic acids (Farmer et al., 2007, Halliwell, 1992, Halliwell et al., 2007).

In order to identify protein targets of oxidative stress, we used two well defined *in vitro* model systems, namely mature primary neurons which have been exposed to OGD, and HT-22 neural cell lines which have been exposed to extracellular glutamate. As described in Chapter II, exposure of neurons to mild (5') or moderate (15') OGD did not result in cell death. Neuronal exposure to lethal (90') OGD, however, significantly increased neuronal death (Stankowski & Zeiger et al., 2010). Using the OxyBlot methodology on our primary neuronal model system, we found that levels of total oxidized proteins were increased following mild or moderate OGD and decreased following lethal OGD (**FIGURE 3.3**). These results suggest that even brief exposures of neurons to OGD can cause damage to protein structure and function. The drastic decrease in total protein oxidation following lethal OGD may be a reflection of the severity of the insult, suggesting that extensive and unrecoverable neuronal death may have occurred at this time point.

Exposure of neurons to OGD results in the activation of a variety of cellular signaling cascades, thereby replicating the molecular events triggered in the human brain

following TIA or stroke (Gonzalez-Zulueta et al., 2000, Irving et al., 2002, Jarvis et al., 2001, Joshi et al., 2001, Liu et al., 2006, McLaughlin et al., 2003, Mehta et al., 2007, Onteniente et al., 2003, Zeiger et al., 2009). To investigate the effects of only one of the many events triggered by OGD on protein function, namely oxidative stress, we moved into the HT-22 neural cell line, which is an excellent and well characterized model of pure oxidative stress (Maher, 2005, van Leyen et al., 2005, Wang et al., 2005). Moreover, while the OxyBlot methodology used in our *in vitro* neuronal model system is a rapid technique that allows scientists to obtain a general overview of the degree of protein damage in a given model system, it does not allow for the identification of specific targets of oxidative stress.

For the identification of specific protein targets of oxidative stress, we used the biotin-avidin-capture methodology on our HT-22 model system. Using HT-22 and CHIP overexpressing cells to confirm that this novel methodology is applicable to our *in vitro* model system, we first investigated the effects of oxidative stress on the oxidation status of the microtubule-associated protein and CHIP substrate tau. The tau protein plays a major role in regulating neuronal microtubule assembly and stability, is highly abundant and has also been extensively demonstrated to be a target of oxidative stress (Avila et al., 2004, Dias-Santagata et al., 2007, Egana et al., 2003, Goldbaum et al., 2002, Melov et al., 2007, Poppek et al., 2006, Vanhelmont et al., 2010, Zhu et al., 2000). Our results demonstrated that tau is indeed oxidized in the HT-22 cells, and its degree of oxidation is further increased in CHIP overexpressing cells following exposure to acute oxidative injury (**FIGURE 3.5**). Moreover, the observed molecular weight shift of tau in the eluate suggests that phosphorylated tau species are predominant targets of oxidative stress in our

model system (**FIGURE 3.5**). Of all post-translational modifications that have been described for tau, phosphorylation of the tau protein remains the most extensively studied one (Avila et al., 2004). While studies have demonstrated that tau phosphorylation mediates the protein's cellular distribution under physiological conditions, no correlations between the phosphorylation of specific tau residues and oxidative stress have been made. Using the HT-22 cell line and the immunblotting methodology to probe for different phospho-tau species, Poppek and colleagues demonstrate that the induction of oxidative stress by means of hydrogen peroxide results in a subtle change in the pattern of tau phosphorylation (Poppek et al., 2006). The difference in both the nature and duration of our insult and that used by Poppek and co-workers is proposed to be sufficient to trigger unique and insult-specific phosphorylation patterns of tau (Poppek et al., 2006), further underlining the complexity of tau phosphorylation in the context of oxidative stress.

Taken together, the use of the biotin-avidin-capture methodology will not only allow for the identification of specific protein targets of oxidative stress, but it will subsequently also allow us to elucidate if any of these oxidized proteins are potential CHIP substrates and how oxidative modifications of these proteins influence the progression of the pathology underlying ischemic stroke. Moreover, when moving into our neuronal *in vitro* model system of OGD as well as our CHIP knockout mice, we will be able to investigate if the targets of oxidative stress differ when a variety of molecular events are elicited by the insult and when different levels of CHIP are present. Ultimately, understanding and defining the relationship between specific protein modifications and subsequent changes in protein function will allow scientists to not only

improve their understanding of pathways involved in stress signaling and the pathology underlying a multitude of human diseases, but it will also aid in the development of novel, safe and effective therapeutics for several human diseases.

CHAPTER IV

C-TERMINUS OF HSC70 INTERACTING PROTEIN IS AN ESSENTIAL DETERMINANT OF MITOCHONDRIAL STRESS SIGNALING IN NEURONS

Abstract

Overexpression of the E3 ubiquitin ligase C-terminus of HSC70 interacting protein (CHIP) blocks neural cell dysfunction in models of Parkinson's, Alzheimer's and other neurodegenerative diseases. We recently reported that CHIP expression is acutely increased in post-mortem tissue samples from individuals who suffered ischemic attacks, but we also found that chronically elevated CHIP was associated with increased levels of ubiquitinated and oxidized proteins as well as decreased proteasome activity. In this work, we report that CHIP knockout animals have high baseline levels of oxidized proteins as well as increased expression of the mitochondrial stress associated kinase PINK1 and the autophagic marker LC3. Following neuronal oxygen glucose deprivation, CHIP expression increased and relocalized to mitochondria. Using immunoblotting and the biotin-avidin-capture methodology on tissue samples from CHIP deficient animals, we found that expression levels of markers of mitochondrial maintenance and dynamics, including VDAC, COX IV and mitofusin, remained unchanged compared to wild type and heterozygous littermates and that these proteins were also not oxidatively modified. However, when mitochondria isolated from these animals were exposed to calcium challenge, they underwent significantly accelerated mitochondrial permeability transition activities. These data suggest that CHIP plays an essential role in mitochondrial

homeostasis as well as protein turnover, and that under conditions of protein stress, CHIP is a crucial regulator of protein and mitochondrial turnover.

Introduction

Mutations in the *PARK2* gene, which encodes the RING domain-containing E3 ubiquitin ligase Parkin, are associated with an autosomal-recessive form of juvenile-onset Parkinson's disease (Helton et al., 2008, Imai et al., 2002). E3 ubiquitin ligases function as part of the ubiquitin proteasome pathway (UPP) mediating the transfer of ubiquitin to damaged client proteins, thereby tagging them for proteasomal degradation (McLaughlin et al., 2005). The specificity of the UPP lies at the level of the E3 ligases (McLaughlin et al., 2005), yet there is redundancy in the substrates that E3 ligases can tag (Morishima et al., 2008). Specifically, the U-box domain containing E3 ubiquitin ligase CHIP has come to the forefront when its acute overexpression has been shown to compensate for loss of Parkin function, thereby promoting the removal of damaged proteins from the cell and increasing cellular survival (Imai et al., 2002).

CHIP has predominately been associated with protection from chronic neurodegenerative diseases including Parkinson's and Alzheimer's diseases (Adachi et al., 2007, Dickey & Patterson et al., 2007, Jana et al., 2005, Sahara et al., 2005, Shimura et al., 2004). These studies support a model whereby the acute overexpression of CHIP proves to be beneficial for cellular survival, aiding in the removal of damaged proteins from the cell (Arndt et al., 2007, Dickey & Patterson et al., 2007). We recently showed that CHIP levels are increased in human tissue following acute ischemic injury, yet we found that chronic CHIP overexpression worsens cellular outcome in an acute neurological injury setting. Specifically, CHIP overexpression was associated with decreased baseline proteasome activity as well as increased protein ubiquitination and oxidation following acute oxidative injury, suggesting either a failure of the cells' ability

to turnover damaged proteins or an increase in the production of damaged proteins. In contrast, decreasing CHIP expression levels enhanced neuronal survival following acute oxidative injury, implying that an exquisite balance of CHIP expression is required to improve cellular survival (Stankowski & Zeiger et al., 2010).

While the association of E3 ubiquitin ligases with the clearance of damaged proteins via the ubiquitin proteasome pathway is apparent, a previously unknown role of E3 ubiquitin ligases, and Parkin in particular, has recently been identified, namely their association with mediating autophagy-dependent clearance of damaged mitochondria, or mitophagy (Rakovic et al., 2010). A multitude of studies suggests that Parkin's ability to influence mitochondrial integrity depends on its interaction with the serine-threonine kinase, PTEN-induced putative kinase 1 (PINK1). Although the precise mechanism by which PINK1 and Parkin modulate mitochondrial dynamics remains unknown, mounting evidence suggests that both proteins function in a common pathway, with PINK1 acting upstream of Parkin (Poole et al., 2008, Ziviani et al., 2010).

In the current study, we focus on the potential role of CHIP in governing mitochondrial integrity and mitophagy, as we found that CHIP deficient animals have high levels of total oxidized proteins suggesting that excessive levels of ROS may be generated in CHIP deficient animals. Moreover, the lack of CHIP also resulted in increased expression of the mitochondrial stress sensor PINK1 and the autophagic marker LC3 as well as accelerated stress-induced mitochondrial permeability transition activities. Using the biotin-avidin-capture methodology to determine if CHIP deficiency results in oxidation of proteins associated with mitochondrial homeostasis and integrity, we found that known markers of these processes were not oxidatively modified. In our

pathophysiologically relevant model of neuronal oxygen glucose deprivation, CHIP expression is not only elevated, but CHIP is also associated with mitochondria suggesting a potential role for CHIP in regulating redox tone, mitochondrial integrity and mitophagy.

Materials and Methods

User-friendly versions of all protocols and procedures in this work can be found on our website at

http://www.mc.vanderbilt.edu/root/vumc.php?site=mclaughlinlab&doc=17838.

Reagents

Commercial vendors of our chaperone antibodies as well as reagents and supplies used for our immunoblotting, immunofluorescence and cell culture experiments are the same as we previously described in Brown et al. (Brown et al., 2010) and Stankowski, Zeiger et al. (Stankowski & Zeiger et al., 2010). Additional primary antibodies used for immublotting in this study include $p66^{shc}$ (566807, EMD), VDAC, COX IV and Parkin (4866, 4850 and 2132, respectively; Cell Signaling), PINK1 and mitofusin (MFN1) (BC 100-494 and NB 110-58853, respectively; Novus Biologicals) and cytochrome c (556433, BD Pharmingen). Commercially available kits utilized were the D_C Protein Assay kit (500-0112, Bio-Rad) and the OxyBlot Protein Oxidation Detection Kit (Millipore, S7150). Reagents and materials required for the biotin-avidin-capture methodology were obtained from the same companies as previously described (Stankowski & Codreanu et al., 2010). Unless otherwise stated, all other chemicals were purchased from Sigma-Aldrich.

Animals

The generation of CHIP deficient mice used in this study has previously been described (Dai et al., 2003). All animals were maintained on a mixed background of

C57BL/6 and 129SvEv. The Institutional Animal Care and Use Committee at Vanderbilt University approved all animal husbandry and experiments. Genotyping was performed by PCR using DNA obtained from tail clippings with primers for the CHIP allele. The primers were purchased from XXIDT and the sequences of the reverse and forward CHIP primers used for genotypic analyses were 5' TGA CAG TCC TCC AGT TCC CTG AG 3' and 5' AAT CCA CGA GGC TCC GCC TTT 3', respectively.

Determination of total oxidized proteins using the OxyBlot methodology

Derivatization of oxidized proteins was performed as previously described (Stankowski & Codreanu et al., 2010, Stankowski & Zeiger et al., 2010). Briefly, following addition of 50mM DTT to whole brain lysates, samples were divided into the derivatization reaction (DR) containing 2,4-dinitrophenylhydrazine and the negative control (NC) solution. Samples were stored at 4ºC and run within seven days. Equal protein concentrations were separated using 4-12% Criterion Bis-Tris gels and processed as described in the *Immunoblotting* section below. Antibodies specific for the detection of oxidized proteins were provided by the manufacturer.

Immunoblotting

Immunoblotting was performed as previously described (Brown et al., 2010, McLaughlin et al., 2001, Stankowski & Zeiger et al., 2010). Semi quantitative analyses of immunoblot results were generated by performing high resolution scans for densitometric quantification using the Scion NIH Image J analysis program as previously described (McLaughlin et al., 2003).

Biotin-avidin-capture methodology

Derivatization of specific protein targets of oxidative stress was performed using the biotin-avidin-capture methodology as previously described (Stankowski & Codreanu et al., 2010). Briefly, liver mitochondrial extracts from P41 CHIP animals were prepared as described in the *mitochondrial preparation* section described below. Equal protein concentrations (2mg/ml) were incubated with biotin hydrazide (5mM) while rotating in the dark for 2hr at RT, after which samples were incubated with sodium borohydride (50mM) for 30min at RT. Samples were then transferred into Amicon Ultra Centrifuge Filter Devices (UFC 801024, Millipore), and washed three times via addition of cold 1xPBS followed by centrifugation for 30min at 2,472 x *g*. Following the last wash, a 100µl aliquot was removed to prepare the input via addition of DTT (50mM) and NuPage Sample buffer (4x; NP0007, Invitrogen). The remainder of the sample was added onto Streptavidin Sepharose High Performance Beads (17-5113-01, GE Healthcare) and incubated while rotating overnight at 4ºC. The next day, samples were centrifuged briefly at 2,282 x *g*. The supernatant of the first spin was saved and a 100µl aliquot of this sample was used to prepare the flow through via addition of DTT (50mM) and NuPage Sample buffer (4x). Samples were eluted from the beads by treating twice with each of the following reagents: SDS (1%), urea (4M), NaCl (1M) and 1x PBS. Beads were then eluted in 90µl NuPage Sample buffer and DTT (50mM), heated for 10min at 95ºC and stored at -20ºC. Proteins were separated by SDS-PAGE gels as described in the *immunoblotting* section above and probed with antibodies specific for mitofusin, VDAC, cytochrome c and COX IV.

Primary cell culture

Cortical cultures were prepared from embryonic day 18 Sprague-Dawley rats as previously described (McLaughlin & Nelson & Erecinska et al., 1998, Stankowski & Zeiger et al., 2010). Briefly, cortices were digested in trypsin and dissociated. Resultant cell suspensions were adjusted to 335,000cells/ml. Cells were plated 2ml/well in 6-well tissue culture plates containing five 12mm or one 25mm poly-L-ornithine-coated coverslip(s) and maintained at 37^{o}C, 5% CO_2 in growth media composed of a volume to volume mixture of 84% DMEM (11960, Invitrogen), 8% Ham's F12-nutrients, 8% fetal bovine serum, 24U/ml penicillin, 24μg/ml streptomycin, and 80μM L-glutamine. Glial proliferation was inhibited after two days in culture with 1-2μM cytosine arabinoside, after which cultures were maintained in Neurobasal medium (Invitrogen) containing 2% B27, 2xN2 and 4% NS21 supplements (Chen et al., 2008) with antibiotics. All experiments were conducted 21-25 days following dissociation.

Oxygen glucose deprivation (OGD)

OGD experiments were preformed between DIV21-25, at which time neurons represent at least 95% of the population as assessed by NeuN and GFAP staining (McLaughlin & Nelson & Silver et al., 1998). OGD was performed as previously described (Stankowski & Zeiger et al., 2010) by complete exchange of media with deoxygenated, glucose-free Earle's balanced salt solution (150mM NaCl, 2.8mM KCl, 1mM $CaCl_2$ and 10mM HEPES; pH 7.3), bubbled with 10% H_2/85% N_2/5% CO_2. Cultures were exposed to OGD in an anaerobic chamber (Billups-Rothberg) for 90min at 37ºC. Upon OGD termination, cells were washed with MEM/BSA/HEPES (0.01% BSA

and 25mM HEPES) and maintained in MEM/BSA/HEPES/2xN2 for various recovery times at the completion of which protein extracts were prepared for immunblotting as previously described (McLaughlin et al., 2003), or cells were fixed for immunofluorescence as described below.

MitoTracker labeling and immunofluoresence

MitoTracker Orange is a highly charged positive stain that accumulates in mitochondria based on the mitochondrial membrane potential. A working concentration of 790nM MitoTracker Orange was added to MEM/BSA/HEPES/2xN2 45min before termination of the recovery time points following OGD. After termination of the recovery period, media was removed, the coverslips were washed with 1xPBS, and fixed with 4% formaldehyde. Cells were then permeabilized with 0.1% Triton X-100, washed with 1xPBS, and blocked with 8% BSA diluted in 1xPBS. After 25min of blocking, coverslips were incubated in rabbit anti-CHIP (1:500) or rabbit anti-PINK1 (1:500) primary antibodies diluted in 1% BSA overnight at 4°C. Cells were then washed in 1xPBS for a total of 30min and incubated in goat anti-rabbit Cy2 secondary antibody diluted in 1xPBS for 1hr. Cells were then washed for a total of 30min in 1xPBS and incubated in 1.4μM DAPI for 10min. After 30min of additional washing, coverslips were mounted via Prolong Gold, and fluorescence was visualized with a Zeiss Axioplan microscope equipped with an Apotome optical sectioning slider.

Mitochondrial preparation

Mitochondrial homogenates were generated from P41 CHIP WT, Het and KO animals as previously described (Zeiger et al., 2009). Briefly, the liver was removed, washed in ice-cold 1xPBS and weighed. The liver was then homogenized in ice-cold isolation media (250mM sucrose, 10mM Tris and 2mM EGTA at pH 7.4) using a 7mL glass dounce homogenizer at 10mL/g of tissue. Homogenates were spun at 500 x *g* for 10min at 4°C and the supernatant was removed and placed in a new tube. Supernatants were spun at 9,400 x *g* for 10min. The pellet was then washed with 10mL of isolation media (without EGTA) and spun again at 9,400 x *g* for 10min. The remaining pellets were resuspended in 1mL of TNEB lysis buffer with protease inhibitors, subject to protein assay and either processed for immunoblotting or resuspended in 1mL of EGTA free isolation media, subjected to protein assay and processed for the mitochondrial permeability transition assay as described below.

Mitochondrial permeability transition assay

The mitochondrial permeability transition assay was performed as previously described (Zeiger et al., 2009). Briefly, isolated mitochondria (1mg) were suspended in 1mL of assay buffer (40mM HEPES, 195mM mannitol, 25mM sucrose, 5mM succinate and 1μM rotenone at pH 7.2). Following a 2min equilibration period, either 50μM or 100μM Ca^{2+} was added and the absorbance was measured at 535nm over a 20min period at 37^{o}C. Lag time before the onset of cell swelling was measured by determining the time when the maximal rate of change in absorbance was evident following Ca^{2+} addition. Lag time was normalized to that of the WT CHIP animals. Data represent the

means from four independent experiments ± SEM. Statistical significance was determined by two-tailed *t* test assuming unequal variances with $p < 0.05$.

Analysis and statistics

Except where otherwise noted data were summarized and are represented as mean ± SEM. The statistical significance of differences between means was assessed using one-way analysis of variance (ANOVA) at the 95% level ($p < 0.05$), followed by the Tukey multiple comparison tests using GraphPad Prism software.

Results

CHIP deficient animals have increased CNS protein oxidation

We have previously demonstrated that CHIP expression levels are increased in post-mortem human tissue from patients who suffered an ischemic stroke as well as in our neuronal *in vitro* model of stroke (Stankowski & Zeiger et al., 2010). In contrast to the benefits associated with transiently increased CHIP expression in blocking cell death in the context of chronic neurological diseases, we found that chronic overexpression of CHIP actually worsens cellular outcome following acute ischemic injury. Decreasing CHIP levels, however, increased neuronal tolerance to acute injury, implying that chronically increased CHIP expression levels may have previously unappreciated deleterious effects (Stankowski & Zeiger et al., 2010). To further evaluate the effects of CHIP deficiency on cell fate in the context of acute injury, we first investigated oxidative protein injury by comparing the levels of total oxidized proteins in CNS samples obtained from CHIP wild type (WT), heterozygous (Het) and knockout (KO) animals (**FIGURE 4.1**), and observed a robust increase, in total protein oxidation in CHIP knockout animals (**FIGURE 4.1**).

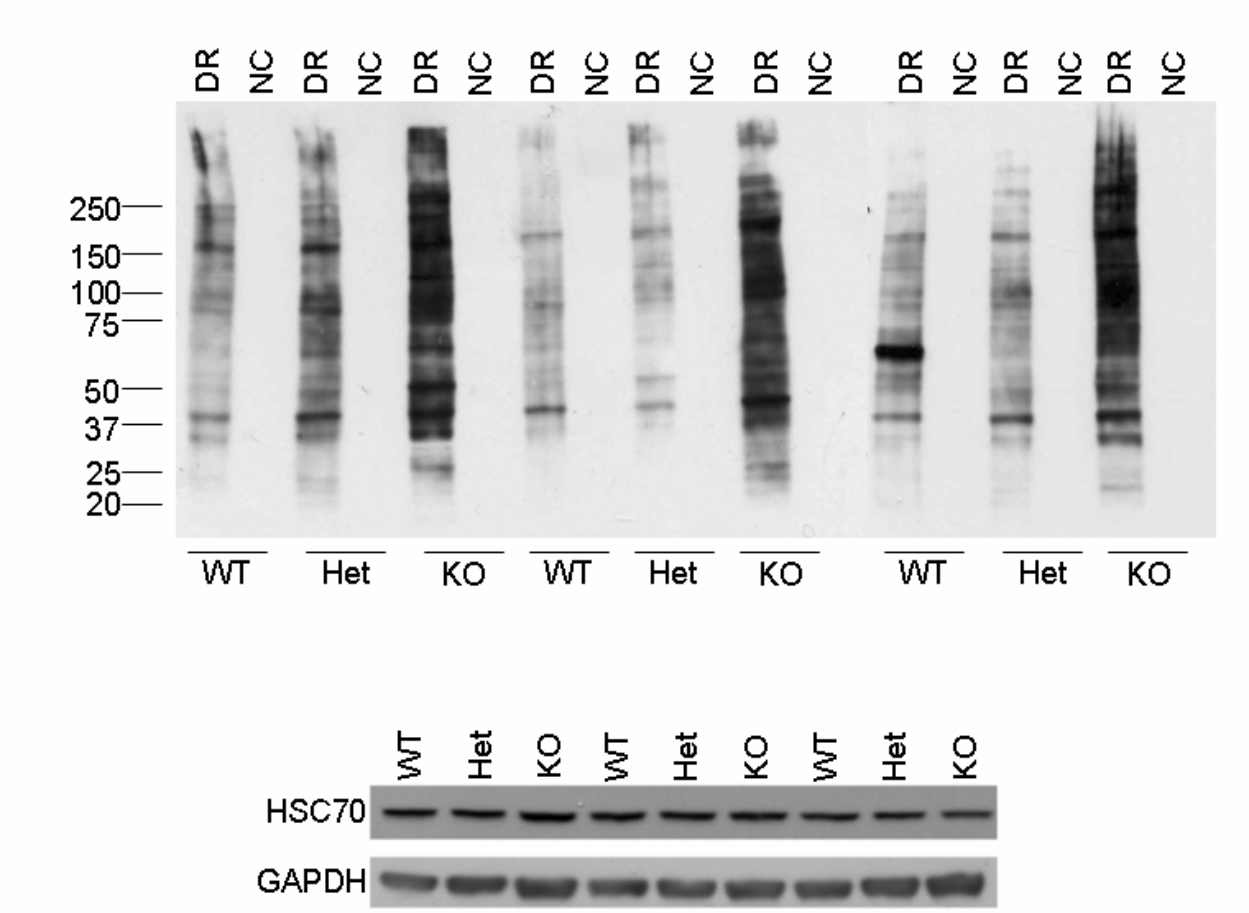

FIGURE 4.1: CHIP deficient animals have increased CNS protein oxidation. Whole brain lysates from P35 wild type (WT), heterozygous (Het) or knockout (KO) CHIP animals were prepared and oxidative protein damage was assessed using the OxyBlot methodology. CHIP KO animals show high levels of total oxidized proteins as compared to their WT and Het littermates. HSC70 and GAPDH serve as loading controls. Immunoblots represent results from three independent experiments. DN, Derivatization Reaction; NC, Negative Control.

CHIP deficiency results in increased markers of stress but no change in oxidation of essential mitochondrial proteins

The increase in total oxidized proteins in unstressed CHIP KO animals suggested that an endogenous source of reactive oxygen species (ROS) may increase protein damage in the absence of CHIP (Halliwell et al., 2007). Given that the electron transport

chain of the mitochondria has been recognized as the major source of cellular ROS (Liu et al., 2002), we next wanted to determine if proteins associated with mitochondrial function and cellular stress were altered in CHIP deficient animals. Expression levels of VDAC, mitofusin and COX IV, which are proteins associated with mitochondrial dynamics, integrity and function, remained unchanged in CHIP KO animals (**FIGURE 4.2A**). In contrast, expression levels of PINK1 and LC3, which are associated with autophagy-dependent clearance of damaged mitochondria, or mitophagy, were elevated in CHIP KO animals (**FIGURE 4.2A**).

To determine if the redox stress in CHIP deficient animals causes specific modifications of proteins involved in mitochondrial homeostasis, we used the biotin-avidin-capture methodology on freshly isolated liver mitochondria from CHIP WT, Het and KO animals yet found that none of these proteins were subject to carbonyl adduction (**FIGURE 4.2B**).

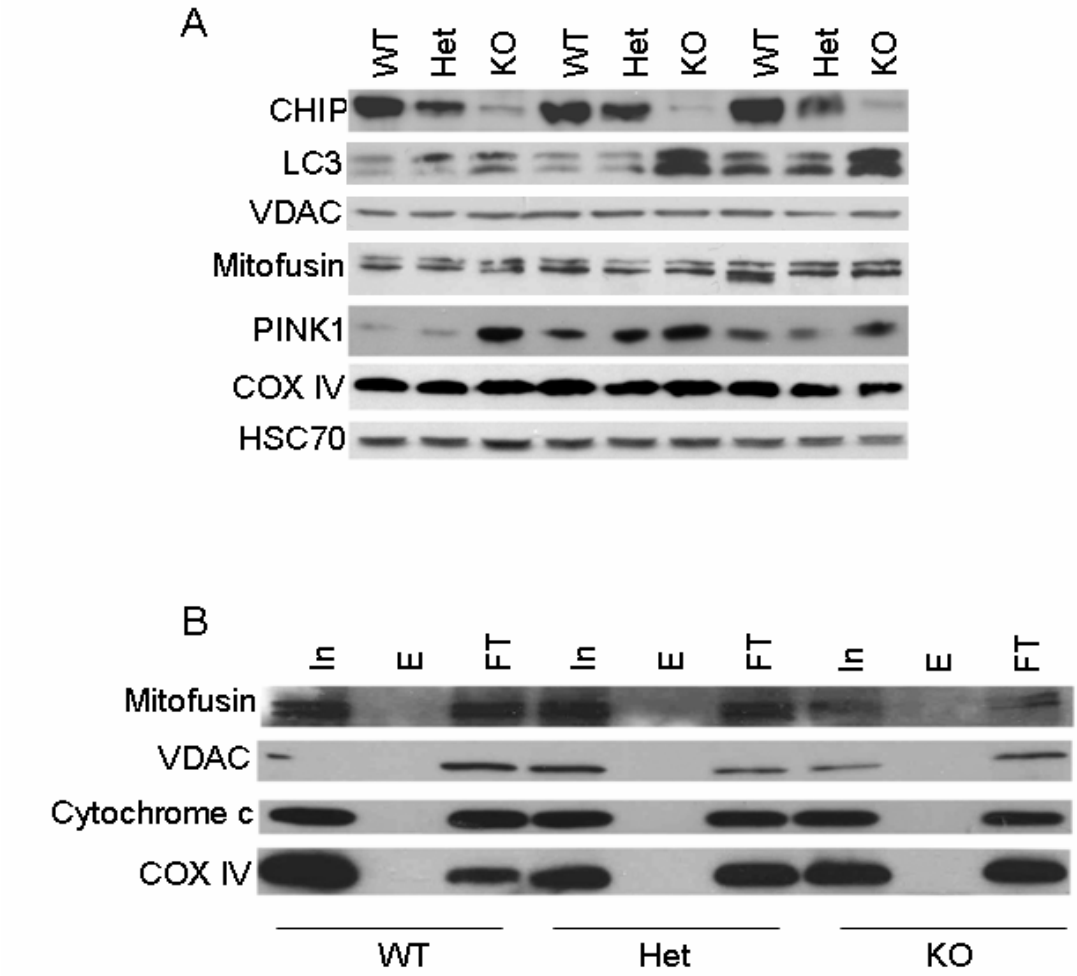

FIGURE 4.2: CHIP deficiency results in increased markers of stress but no change in oxidation of essential mitochondrial proteins. A) Whole brain lysates from P35 wild type (WT), heterozygous (Het) or knockout (KO) CHIP animals were prepared. Proteins were separated on SDS-PAGE gels and probed with antibodies specific to CHIP, LC3, VDAC, mitofusin, PINK1, COX IV and HSC70. CHIP KO animals show increased expression of the autophagic marker LC3 as well as the mitochondrial stress associated kinase PINK1. Data are from a representative experiment (n=3). B) Liver mitochondrial extracts were prepared from P41 WT, Het or KO CHIP animals. Specific protein targets of oxidative stress were detected using biotin-avidin-capture methodology. Protein extracts were separated on SDS-PAGE gels and probed with antibodies specific to mitofusin, VDAC, cytochrome c and COX IV. Proteins of interest were not subject to oxidative modification. Immunoblots represent results from three independent experiments. In, Input; E, Eluate; FT, Flow through.

Oxygen glucose deprivation increases perimitochondrial CHIP association

Given that PINK1 and LC3 were subsequently upregulated in CHIP deficient animals, we next sought to determine the mechanisms associated with mitochondrial stress in CHIP knockout animals using our neuron enriched *in vitro* model system in which cultures were exposed to oxygen glucose deprivation (OGD) for 90min. We observed that while CHIP and PINK1 expression levels were upregulated 1hr following the insult, the redox-sensitive adaptor protein $p66^{shc}$ as well as the autophagic marker LC3 were robustly increased immediately following termination of OGD (**FIGURE 4.3A**). We next sought to determine if CHIP associates with mitochondria. Six hours following exposure of mature neurons to OGD, we detected mitochondrial co-localization of CHIP, indicating that CHIP may directly regulate mitochondrial tone (**FIGURE 4.3B,** arrows). Moreover, a stabilization of PINK1 at the mitochondria was also detected at 6hr following OGD (**FIGURE 4.3C,** arrows).

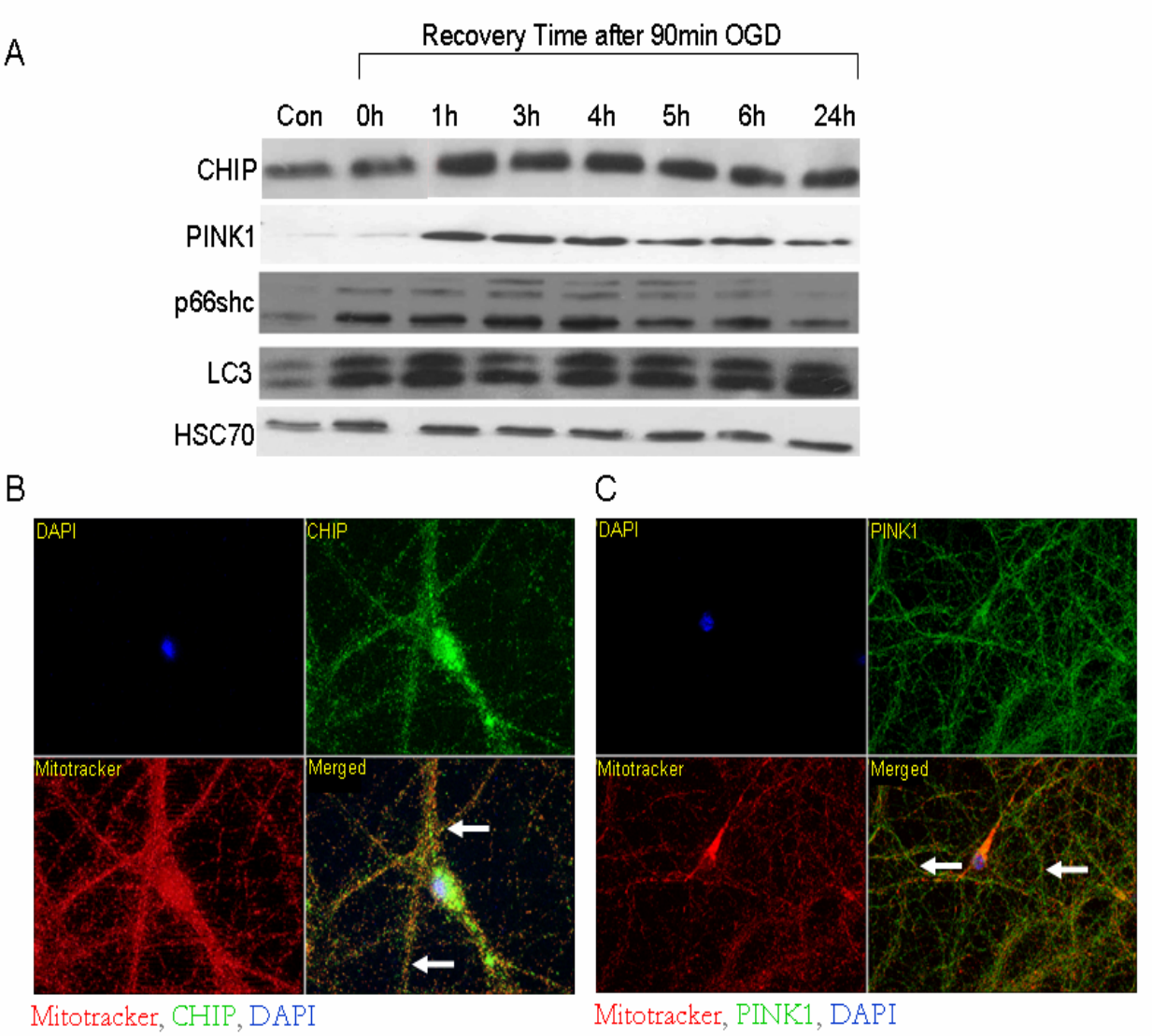

FIGURE 4.3: Oxygen glucose deprivation increases perimitochondrial association of CHIP. Neuron enriched primary cultures were exposed to oxygen glucose deprivation (OGD) for 90min after which expression profiles as well as intracellular localization of proteins associated with mitochondria were analyzed at varying time points. A) Whole cell extracts of neuronal cultures were harvested immediately (0hr), 1hr, 3hr, 4hr, 5hr, 6hr or 24hr following exposure to OGD. Proteins were separated on SDS-PAGE gels and probed for CHIP, PINK1, $p66^{shc}$, LC3 and HSC70. While $p66^{shc}$ and LC3 expressions levels are increased immediately following the insult, CHIP and PINK1 expression levels increased robustly at 1hr. Immunoblots represent results from three independent experiments. Six hours following neuronal exposure to OGD, neurons were loaded with MitoTracker Orange and co-stained with B) CHIP or C) PINK1. Both proteins associate with mitochondria at this time point (arrows).

CHIP deficiency increases stress-induced mitochondrial transition activities

Given the association of CHIP with mitochondria, we next sought to determine if CHIP regulated mitochondrial stress signaling. Using intact mitochondria from liver of WT, Het and KO CHIP animals, we found a significant increase in Ca^{2+}- induced mitochondrial permeability transition activities in CHIP KO animals as compared to WT or Het littermates. Notably, CHIP Het mice showed more rapid stress induced mitochondrial permeability transition activities than WT animals, yet this response was not as robust as that observed in the CHIP KO animals (**FIGURE 4.4A, B**). Taken together, these data suggest that CHIP is an essential regulator of mitochondrial health and degradation of injured mitochondria.

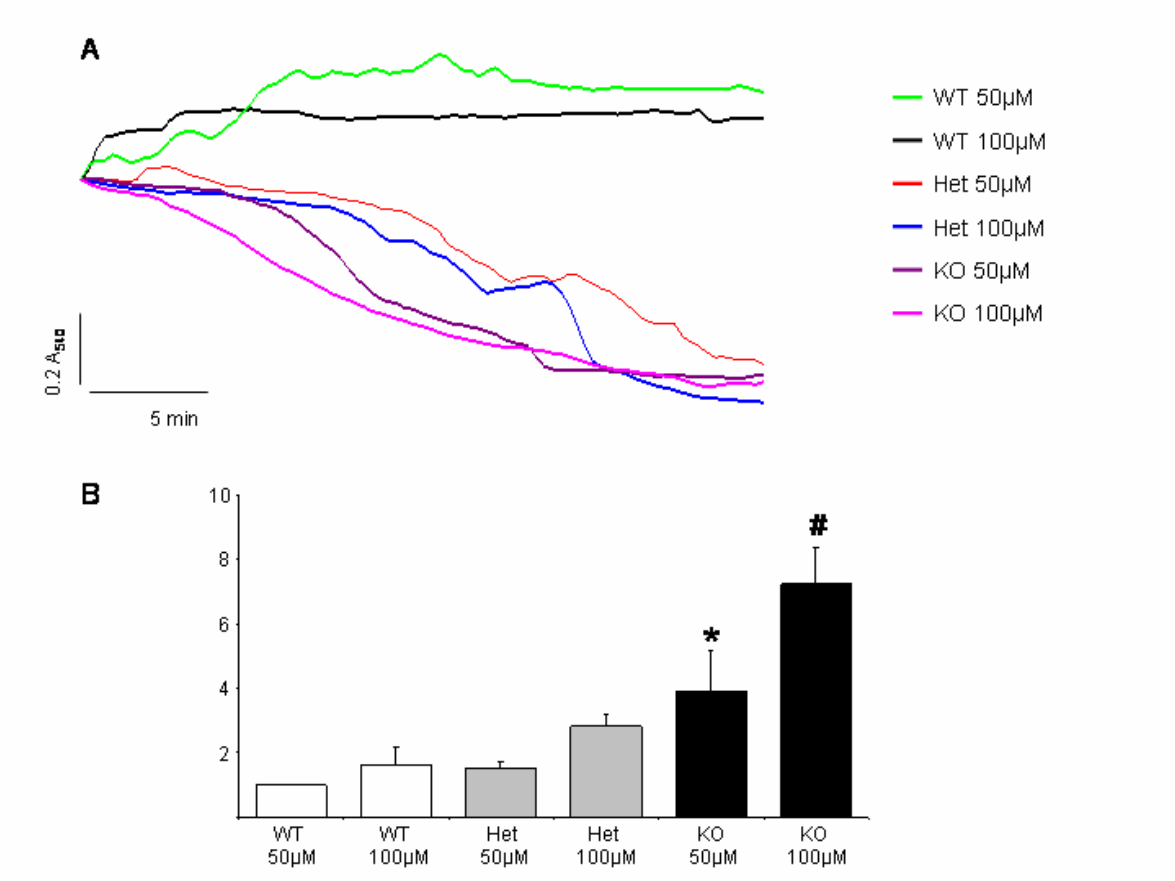

FIGURE 4.4: CHIP deficiency increases mitochondrial transition activities induced by stress. A) Purified mitochondria from P35 wildtype (WT), heterozygous (Het) or CHIP knockout (KO) mice were incubated in the absence or presence of increasing amounts of Ca^{2+}, and mitochondrial permeability transition was assessed by measuring alterations in absorbance over time. Data are from a representative experiment (n=4). B) The average lag time to mitochondrial permeability transition was measured by determining the maximal rate of change and normalized to the corresponding WT mitochondria. Data represent the normalized lag time ± SEM from four independent experiments. Statistical significance was determined by two-tailed *t* test with $p < 0.05$ compared to WT mitochondria incubated with 50μM (*) or 100μM (#) Ca^{2+}.

Discussion

The presence of biochemically and energetically intact mitochondria is essential for neuronal survival. Mitochondria govern important cellular functions including energy production, apoptosis, calcium homeostasis and oxidative stress response (Erecinska et al., 1994, Liu et al., 2009). It has become increasingly evident that mitochondrial dysfunction is associated with the onset of a multitude of human diseases, including stroke, Parkinson's and Alzheimer's disease (Bolanos et al., 2009). As the accumulation of damaged mitochondria is particularly neurotoxic, neurons have evolved powerful means to remove injured organelles from the cell (Michiorri et al., 2010). The molecular mechanisms associated with autophagy-based clearance systems are thought to involve mitochondrial fission and fusion events as well as the recruitment of stress sensitive kinases and ubiquitin ligases (Brown et al., 2010, Kleman et al., 2010). The process by which damaged mitochondria are removed from cells is commonly referred to as mitophagy and it is now widely accepted that this process plays a critical role in mitochondrial quality control (Krebiehl et al., 2010).

In the past 5 years, a plethora of studies has focused on the role of mitochondrial dysfunction in Parkinson's disease. Mutations in both the serine-threonine kinase PINK1 and the E3 ubiquitin ligase Parkin have been associated with the onset of autosomal recessive forms or Parkinson's disease (Poole et al., 2008, Ziviani et al., 2010). PINK1 is constitutively expressed and targeted to mitochondria where it is rapidly removed under normal conditions. In contrast, under conditions of stress, such as mitochondrial depolarization, PINK1 associates with damaged mitochondria where it has been associated with mitophagy (Matsuda et al., 2010). Our work is the first study

documenting an increase in PINK1 expression levels following exposure of primary neurons to OGD suggesting that signaling pathways similar to those observed in Parkinson's disease may mediate ischemic cell death. Moreover, the discovery that the E3 ubiquitin ligase Parkin is involved in governing mitophagy revealed a previously unknown function of E3 ubiquitin ligases. The finding that CHIP can compensate for the loss of function of Parkin suggests that there is redundancy with regard to the protein substrates E3 ligases can interact with (Imai et al., 2002). We therefore investigated CHIP's possible role in governing mitochondrial homeostasis.

In this work, we sought to identify the mechanism associated with increased protein oxidation observed as a consequence of CHIP deficiency. CHIP has been shown to be neuroprotective when transiently overexpressed *in vitro* (Adachi et al., 2007, Dickey & Kamal et al., 2007, Dickey & Patterson et al., 2007, Dikshit et al., 2007, Jana et al., 2005, McDonough et al., 2003), yet chronic CHIP overexpression is associated with proteasome dysfunction and increased vulnerability to oxidative stress (Stankowski & Zeiger et al., 2010). In addition to previous studies demonstrating increased levels of lipid peroxidation in various tissues from CHIP knockout animals as determined by measuring levels of 8-isoprostanes (Min et al., 2008), our data demonstrate a dramatic increase in protein carbonyl group formation in these mice. Moreover, loss of CHIP was associated with increased expression of the mitochondrial redox sensor PINK1 and the autophagic clearance protein LC3. Expression levels of proteins involved in mitochondrial integrity and function, however, including VDAC, mitofusin and COX IV remained unchanged. To identify specific protein targets of oxidative stress, we used the

biotin-avidin-capture methodology and found that these proteins were not directly modified by oxidation.

Due to the increased expression levels of PINK1 and LC3 in CHIP deficient animals, we next sought to investigate the relationship between CHIP and the mitochondria. Using our neuronal *in vitro* model system of OGD, we showed that in the presence of a pathophysiologically relevant stressor, expression levels of the redox-sensitive adaptor protein $p66^{shc}$ are immediately upregulated. We have previously shown that $p66^{shc}$ rapidly translocates to damaged mitochondria in the presence of oxidative stress in order to evoke signaling cascades associated with governing autophagy (Brown et al., 2010, Kleman et al., 2010). Interestingly, the expression levels of the autophagic marker LC3 also increase rapidly following OGD, suggesting that $p66^{shc}$-activated signaling pathways lead to the recruitment of the autophagic machinery in an attempt to remove damaged mitochondria from the cellular environment.

Similarly, our data also demonstrate that PINK1 expression levels start to increase 1hr following the initial insult. Given that studies have shown an increased accumulation and stabilization of PINK1 at the mitochondria following stress where it recruits other chaperones and proteins to damaged mitochondria (Matsuda et al., 2010), it may be suspected that $p66^{shc}$ is involved in PINK1's recruitment to damaged mitochondria. Finally, the expression levels of CHIP are increased following OGD, suggesting that PINK1 may, in turn, recruit CHIP to damaged mitochondria. Using immunofluorescent analyses, we demonstrate that not only is PINK1 recruited to mitochondria following oxidative stress, but so is CHIP. These data further suggest a relationship between CHIP and the mitochondria. In order to identify the possible mechanisms regarding CHIP's

involvement in governing mitochondrial function, we moved back into our CHIP knockout model system. Using isolated mitochondria from CHIP deficient mice, we demonstrate for the first time that loss of CHIP is associated with accelerated mitochondrial permeability transition activities. The precise mechanism by which CHIP governs mitochondrial transition activities has yet to be elucidated. Yet, we hypothesize that CHIP is recruited to damaged mitochondria following stress where it may interact with the mitochondrial associated protein VDAC, thereby preventing the opening of this channel and the release of pro-apoptotic factors from the mitochondria into the cell. Due to VDAC's location in the outer mitochondrial membrane, it presents a suitable and immediate target for interaction with CHIP. However, we also speculate that CHIP may either interfere at other levels of the mitochondrial permeability complex or aid in sequestering activated caspases and other cell-death proteins.

Taken together, this work reveals a unique mechanism whereby CHIP acts as an essential regulator of redox tone and may be involved in governing mitophagy. Moreover, in combination with our recent data demonstrating that CHIP overexpression is associated with decreased neuronal survival, these data underscore the importance of an exquisite balance of CHIP levels required to maintain cellular health under conditions of protein stress.

CHAPTER V

SUMMARY AND FUTURE DIRECTIONS

In the last decade, over 100 studies have provided evidence that acute overexpression of CHIP has neuroprotective potential in the context of chronic neurodegenerative diseases, including Parkinson's and Alzheimer's disease (Dickey & Kamal et al., 2007, Dickey et al., 2008, Dickey & Patterson et al., 2007, Dikshit et al., 2007, Hohfeld et al., 2001, Imai et al., 2002, Ko et al., 2009, Petrucelli et al., 2004, Sahara et al., 2005, Shimura et al., 2004, Williams et al., 2009). CHIP functions as a HSP70 co-chaperone and an E3 ubiquitin ligase (Qian et al., 2006). These studies afford the protective role of CHIP not only in its ability to influence HSP70's folding activities and expression levels, but also in its ability to ubiquitinate damaged client proteins for their subsequent proteasomal degradation (Arndt et al., 2007, Jiang et al., 2001, Kampinga et al., 2003, Murata et al., 2003, Murata et al., 2001). Despite the benefits associated with acute CHIP overexpression in models of chronic neurodegenerative diseases, CHIP's role in determining neuronal fate in acute neurological injury, including ischemic stroke, has previously not been examined.

We found that CHIP expression is increased in post-mortem tissue samples from patients who suffered TIAs or ischemic stroke (Stankowski & Zeiger et al., 2010). We initially hypothesized that the increase in CHIP expression levels observed in patients who suffered from TIA or stroke was a means of neurons to remove damaged proteins from the cellular environment and to enhance neuronal survival. We observed however,

that the chronic overexpression of CHIP is detrimental to neuronal survival when neural cells were exposed to stroke-like injury (Stankowski & Zeiger et al., 2010). Mechanistically, this effect appears to be dependent upon either the excessive oxidation of protein substrates or the inability of cells to remove damaged proteins from the cellular environment. These studies suggest that long-term changes in CHIP are likely a poor therapeutic target for chronic disease treatment.

Neuronal OGD increases oxidative protein damage and alters proteasome function *in vitro*

Ischemic stroke triggers a multitude of molecular events, all of which contribute to the observed neuronal damage and death. Using our neuronal *in vitro* model system of oxygen glucose deprivation (OGD), we not only found that CHIP expression levels were increased following mild or moderate OGD, but so were the levels of total oxidized proteins. These observations are in keeping with other studies in which we observed that neurons can withstand high levels of oxidative stress as long as the energetic status is maintained (Brown et al., 2010). Moreover, these data confirmed that our *in vitro* model system of OGD presents a pliable platform to capture the earliest molecular events following acute injury (Stankowski & Zeiger et al., 2010, Zeiger et al., 2010). In contrast, exposure to lethal OGD resulted in a robust decrease in total protein oxidation levels, underscoring the swift nature of death following severe stress in which cells experience rapid, unrecoverable damage (Stankowski & Zeiger et al., 2010).

Effects of neuronal OGD on protein oxidation

While measurements of total protein oxidation in our OGD model were obtained 24hr following the insult, the identification of both the specific protein targets of oxidative stress and the temporal profile of protein oxidation following ischemic stroke are areas of intense interest. Defining the relationship between specific oxidative protein modifications and changes will allow for a better understanding of pathways involved in stress signaling and for the potential identification of biomarkers and novel therapeutic targets. These experiments are of high clinical value, as studies aimed at interfering with oxidative protein damaged have failed to recapitulate the successful results obtained using animal models of ischemic stroke (Chacon et al., 2008, Maples et al., 2004, Shuaib et al., 2007).

The best-known antioxidant study is the Stroke-Acute Ischemic NXY Treatment (SAINT) trial in which the effect of the free-radical spin trap disodium 2,4-disulfophenyl-N-tert-butylnitrone (NXY-059) was assessed on outcome following acute ischemic stroke (Chacon et al., 2008, Shuaib et al., 2007). The first phase of the SAINT trials led to positive outcomes as the co-administration of NXY-059 with the thrombolytic t-PA within the first 4hr following symptom onset resulted in decreased rates of intracranial hemorrhage (Chacon et al., 2008). However, during Phase II, there was actually no statistically significant difference between the frequency of intracranial hemorrhage in patients treated with t-PA in combination with NXY-059 or placebo (Shuaib et al., 2007).

NXY-059 acts as a free-radical spin-trap, scavenging highly reactive and unstable radicals (Kubow et al., 1984, Maples et al., 2004). Despite the benefits that were observed in animal models of ischemic stroke and in the first phase of the SAINT clinical

trials (Chacon et al., 2008), it has been hypothesized that the enzymatic products of NXY-095 may be neurotoxic (Chacon et al., 2008). Moreover, it remains to be determined if total levels of ROS actually decrease via the use of spin-traps and if spin-traps have a preference for certain free radical species. This is of particular importance as the biochemistry of oxidative pathobiology is highly complex, implying that each individual disease may require a specific and optimal antioxidant therapy, which may have to be administered early on in chronic neurological disorders or to at-risk patients of acute neurological disorders (Delanty et al., 2000, Singh et al., 2004). These outstanding questions underline the fact that more research regarding the mechanisms of free radical-scavenging by antioxidants is required in an attempt to develop more targeted and ultimately safer antioxidant therapies to narrow the window of oxidative protein damage and to improve outcome.

Effects of neuronal OGD on protein turnover

While identifying specific protein targets of oxidative stress is important, investigating the effects of mild, moderate or lethal OGD on the proper function of a variety of protein clearance systems, including proteasomal degradation and autophagy, are becoming increasingly recognized as alternate means to block neuronal death. Our data demonstrate that mild or moderate OGD does not interfere with proteasome function, yet lethal OGD results in a significant decrease in proteasome activity. While the removal of damaged proteins appears to be fully functional following mild or moderate OGD, it remains unknown at which time point following lethal OGD proteasomes start to fail.

Furthermore, the investigation of the composition and localization of proteasomes not only within different brain regions but also within different subcellular neuronal compartments may provide new insight into regional vulnerability to ischemia and how proteasome expression correlates with E3 ligase expression. Using two-dimensional Blue Native/SDS-PAGE and tandem mass spectrometry analyses, studies have recently identified the presence of different proteasome populations within eukaryotic cells (Shibatani et al., 2006). Specifically, these studies found that in contrast to the traditional notion suggesting that proteasomes always consist of a 20S core and two adjacent regulatory subunits, emerging evidence suggests that proteasomes may be composed of the 20S subunit only, a singly-capped 20S subunit or a doubly-capped 26S proteasome (Brooks et al., 2000, Shibatani et al., 2006, Tai et al., 2010). Using synaptosomal and cytosolic extracts from rat cortices in combination with mass spectrometry, these studies have also shown that doubly-capped 26S proteasomes are predominantly located in the cortex (Tai et al., 2010). This evidence suggests that regions which are at high risk for stroke may be equipped with unique proteasome families that may also be less efficient in removing damaged proteins.

In addition to a different regional distribution of proteasomes, the subcellular localization of proteasomes also changes following neuronal stimulation (Tai et al., 2010). Using *in vitro* model systems of ischemic stroke, protein aggregates were observed in close proximity to nuclei and mitochondria (Hu et al., 2001). One might predict that changes in the subcellular localization of proteasomes occur following acute ischemic injury as a means of neurons to direct this protein clearance machinery towards areas of higher protein damage, such as the nucleus, mitochondrion and ER.

While the ubiquitin proteasome pathway was the initial target of this work due to its close association with the E3 ubiquitin ligase CHIP, it remains unknown if other cellular clearance processes, such as autophagy, can compensate for the loss of proteasome function. Ongoing efforts in the lab have shown that CHIP can translocate to the mitochondria following ischemia where it is suggested to be associated with autophagy-based removal of mitochondria, or mitophagy. Knowing if one clearance pathway is more resistant to an acute lethal insult would allow us to explore if redirecting damaged proteins to a more efficient clearance system could ultimately improve neuronal outcome.

Energetic demands for protein refolding and degradation

The processes underlying protein degradation and refolding are highly dependent on the availability of sufficient energy reserves and recent studies have demonstrated that the energetic status of a cell plays an essential role in determining protein fate (Arndt et al., 2007, Kampinga et al., 2003). That is, while low levels of ATP direct proteins to the refolding machinery, high levels of ATP are associated with increased protein degradation (Arndt et al., 2007, Kampinga et al., 2003). These findings are highly intriguing, as *in vivo* model systems of ischemic stroke have demonstrated that one of the most fundamental changes that occurs following ischemia is the precipitous drop of ATP within 2 minutes following transient ischemia (Doyle et al., 2008). These results coincide with preliminary data from our lab showing decreased levels of total ATP following neuronal exposure to lethal OGD. This would suggest that in the presence of decreased ATP levels, increased protein refolding versus degradation may be detected

following ischemic injury (Kampinga et al., 2003). Yet, *in vivo* rat focal brain ischemia is associated with aggregation of ubiquitinated proteins following the insult (Hu et al., 2001, Hu et al., 2000), suggesting a disconnect between *in vitro* models and *in vivo* observations. Ongoing work in the lab using renilla-luciferase reporter assays in neurons exposed to OGD may allow us to determine if a decrease in protein refolding activities exists and if folding is associated with improved outcome following acute injury.

In addition to the energetic status of cells, Arndt and co-workers have demonstrated that the association of HSP70 with different co-chaperone networks governs protein fate (Arndt et al., 2007). While we found that CHIP expression is increased in neurons following mild or moderate OGD (Stankowski & Zeiger et al., 2010), it remains to be determined if BAG-1 expression is also altered in this paradigm. As described in Chapter I, the association of HSP70 with CHIP and BAG-1 enhances HSP70's degradation activities. While CHIP is involved in tagging damaged proteins for their subsequent proteasomal degradation, BAG-1 has been shown to direct the protein complex to the proteasome via its ubiquitin-like domain (Arndt et al., 2007). It may therefore be speculated that in the presence of decreased levels of BAG-1, ubiquitinated proteins may not be efficiently transported to the proteasome, thus resulting in their intracellular aggregation. Arndt and colleagues also demonstrated that CHIP can associate with HSP70 in the presence of co-chaperones other than BAG-1 (Arndt et al., 2007). In contrast to the degradation-promoting activities of BAG-1, HSP70 binding protein 1 (HSPBP1) and Bcl-2-associated athanogene 2 (BAG-2) have been found to direct the activities of this multi-protein complex toward protein refolding, as HSPBP1 and BAG-2 can inhibit the ubiquitin ligase activity of CHIP or abrogate CHIP's

interaction with E2 conjugating enzymes, respectively (Arndt et al., 2007). If co-chaperones other than BAG-1 associate with HSP70 and CHIP following acute injury, one may predict that damaged client proteins are predominantly directed toward protein refolding. Moreover, given the observed accumulation of protein aggregates in models of ischemic stroke (Hu et al., 2001, Hu et al., 2000), one may also speculate that refolding activities are impaired following acute injury.

Taken together, these results would ultimately provide further insight into the mechanisms underlying protein fate following acute ischemic injury and could allow us to identify novel targets for therapeutic intervention.

CHIP overexpression interferes with proteasome function and decreases neural survival following acute oxidative injury

While a multitude of molecular events are elicited in our neuronal *in vitro* model system of OGD, we were particularly interested in elucidating the effects of a pure oxidative insult on neural survival in cells that chronically overexpress CHIP, as oxidative stress is one of the earliest and most essential events triggered following ischemic stroke. We therefore moved into the HT-22 cell line, as this cell line is not only an excellent and well-described model of neural oxidative injury (Maher, 2005, van Leyen et al., 2005), but it also allowed us to drive CHIP expression at high levels. As presented in Chapter II, chronic CHIP overexpression resulted in the accumulation of polyubiquitinated and oxidized proteins as well as a significant decrease in baseline proteasome activity (Stankowski & Zeiger et al., 2010). Knowing that CHIP overexpressing cells are more prone to accumulate damaged proteins in the form of protein aggregates, a detailed analysis of the composition of these aggregates using

immunoflourescent analyses would provide insight into which proteins associate with damaged substrates in an attempt to govern protein fate. It may be hypothesized that molecular chaperones, CHIP, ubiquitin, subunits of the proteasome as well as CHIP substrates may be present within these aggregates suggesting the involvement of all of these proteins in trying to refold or degrade a given client protein.

In addition to an increased formation of ubiquitin aggregates in CHIP overexpressing cells, our data in **FIGURE 2.7A** also show that these inclusion bodies predominantly accumulate in close proximity to the nucleus. This observation is particularly intriguing as a recent study by Sha and colleagues demonstrated a role of CHIP in the aggresome pathway (Sha et al., 2009). Aggresome formation occurs around the microtubule organizing center in perinuclear location and is now considered to be a normal cytosolic response to aggregated proteins. These so called "holding stations" have been shown to form in response to cellular indigestion, a situation in which the rate of aggregate formation exceeds the rate of aggregate elimination. Such an imbalance is most likely to occur when cells are confronted with an overload of damaged proteins, which overwhelms the proteasome and results in decreased activity of this multicatalytic protease (Sha et al., 2009; Kopito et al., 2000). Given our observation that ubiquitin inclusion bodies form in close proximity to the nucleus (**FIGURE 2.7A**) as well as our finding that chronic CHIP overexpression is associated with decreased proteasome activity (**FIGURE 2.7B**), it may be hypothesized that our observed inclusion bodies are indeed aggresomal holding stations (Sha et al., 2009). To assess if these inclusion bodies are aggresomes, additional immunofluorescence studies probing for the mammalian histone deacetylase HDAC6, which serves as a linker between the dynein motor and the

protein substrate, thereby governing the transport of ubiquitinated protein substrates to aggresomal holding stations (Sha et al., 2009), would be required.

In the context of proteasome function, the mechanism by which CHIP interferes with proteasome activity remains to be elucidated. It may be assumed that the presence of high levels of the E3 ubiquitin ligase CHIP results in excessive protein ubiquitination, thereby overwhelming the proteasome, which in turn responds with a decrease in its activity. Moreover, using multiubiquitin-proteasome binding assays, Urushitani and colleagues have demonstrated that the S5α subunit of the proteasome is a substrate for CHIP (Urushitani et al., 2004). This finding is of interest as preliminary data from our laboratory demonstrated decreased baseline expression levels of the S5α subunit in CHIP overexpressing cells. As a result, it may be speculated that CHIP interferes at the level of proper proteasomal assembly. Similarly, studies have led to the identification of a variety of chaperones that are involved in mediating proteasome assembly (Rosenzweig et al., 2008, Rosenzweig et al., 2008). Knowing if any of these chaperones present potential substrates for CHIP and if the expression levels of these chaperones are decreased in CHIP overexpressing cells would further support the notion that CHIP interferes with proteasome function at the level of proteasome assembly.

While these effects of CHIP on proteasome assembly may be considered to be of direct nature, a recent study demonstrated that the cellular redox status can also interfere with proteasomal function (Silva et al., 2008). Using purified yeast proteasomes that were exposed to hydrogen peroxide and the chelating agent diethylenetriaminepentaacetic acid, Silva and colleagues found that cysteine residues of the 20S proteasomal core are S-glutathionylated by reduced glutathione (GSH) and that

this oxidative modification does indeed decrease the chymotrypsin-like activity of the proteasome (Silva et al., 2008). In preliminary studies, we determined that baseline levels of total GSH are elevated in CHIP overexpressing cells, suggesting that the redox status in our CHIP overexpressing cells may also contribute to the observed decrease in the chymoptrypsin-like activity. Overall, a follow-up on these results would allow for a better understanding of how high levels of CHIP can interfere with proteasome function, which in turn would promote the identification of additional targets for therapeutic intervention.

CHIP's role in governing mitophagy

While CHIP's role in the ubiquitin proteasome pathway became apparent after the discovery that CHIP acts as an E3 ubiquitin ligase (Jiang et al., 2001, Murata et al., 2001), a novel role of E3 ligases recently came to the forefront: the involvement of E3 ligases in governing mitochondrial homeostasis as well as the autophagy-based removal of damaged mitochondria, or mitophagy. Studies in the field of Parkinson's disease demonstrated that the E3 ligase Parkin is recruited to damaged mitochondria where it interacts with the serine/threonine kinase PINK1 in an attempt to remove damaged mitochondria (Poole et al., 2008, Rakovic et al., 2010, Ziviani et al., 2010). Studies using transgenic fly strains for PINK1 and Parkin demonstrated that these proteins act in the same pathway, with PINK1 acting upstream of Parkin (Poole et al., 2008). It is proposed that PINK1 and Parkin govern mitophagy via Parkin's ability to ubiquitinate the pro-fusion protein mitofusin, and mutations in either PINK1 or Parkin resulted not only in

decreased ubiquitination of mitofusin, but also in increased tissue degeneration due to the accumulation of damaged mitochondria (Poole et al., 2008).

In concert with results obtained from transgenic flies in which Parkin is mutated (Poole et al., 2008), studies using Parkin null mice also showed that these animals present with mitochondrial abnormalities, including decreased mitochondrial respiratory capacity, increased oxidative damage, decreased expression of proteins involved in mitochondrial function including subunits of complex I of the ETC, swollen mitochondria and fragmented cristae (Abou-Sleiman et al., 2006, Banerjee et al., 2009, Malkus et al., 2009, Muqit et al., 2006). It remains to be discerned, however, if mitochondrial morphology and dynamics change in CHIP knockout animals. While Parkin has been shown to mediate the ubiquitination of the pro-fusion protein mitofusin, it is unknown if mitofusin is also a substrate for CHIP and if CHIP plays a role in mitochondrial dynamics.

To investigate the relationship between CHIP and mitochondria, we moved into a CHIP knockout mouse model system and found increased levels of total oxidized proteins in the absence of CHIP. These data suggest that CHIP deficient animals either have problems removing damaged proteins from the cellular environment, or generate higher levels of oxidatively damaged proteins. As mitochondria are the major source of endogenous ROS, we sought to further pursue our studies to investigate if CHIP is involved in governing mitochondrial homeostasis and potentially mitophagy. In addition to the increased levels of total oxidized proteins, CHIP deficient animals also have increased expression levels of the stress sensor PINK1 and the autophagic marker LC3. When moving into our neuronal *in vitro* model system of OGD, we found that CHIP

translocates to mitochondria following a lethal insult, leading us to further pursue the potential role of CHIP in mediating mitochondrial health. We found that CHIP deficiency is associated with accelerated stress-induced mitochondrial permeability transition activities. These data support the notion that CHIP is an essential regulator of mitochondrial turnover, yet the exact mechanism remains to be elucidated. We speculate that CHIP controls mitochondrial transition activities at the level of the VDAC channel, preventing its premature opening and subsequent release of pro-apoptotic factors under conditions of stress. Due to VDAC's localization in the outer mitochondrial membrane, this channel provides the most promising and direct target for CHIP's interference with mitochondrial transition activities. It is, however, plausible to speculate that CHIP may also interfere at other levels of the mitochondrial permeability complex. For instance, studies have demonstrated that HSPs can promote cellular survival by sequestering and binding activated caspases and other cell death proteins (Beere, 2005). It is therefore reasonable to hypothesize that CHIP may also interfere with cell death by inhibiting mitochondrial release of cytochrome c, preventing the translocation of Bax to mitochondria following stress or interfering with the assembly of the apoptosome. These results would provide further insight into the relationship between CHIP and the mitochondria and help better understand by which mechanism CHIP interferes with cell death.

Overall, we are still at the beginning of our understanding regarding how CHIP is recruited to the mitochondria. It remains to be elucidated if changes in mitochondrial potential can trigger the translocation of CHIP to the mitochondria, or if CHIP senses the presence of fragmented and damaged mitochondria within cells. It is unknown if CHIP

interacts with PINK1 and if this interaction is required for CHIP's recruitment to damaged mitochondria. While studies have demonstrated that PINK1 does not phosphorylate Parkin, and Parkin does not ubiquitinate PINK1 (Vives-Bauza et al., 2010), it remains to be determined if this same relationship exists between PINK1 and CHIP. Lastly, studies identifying the protein domains of CHIP which govern CHIP's relocalization to damaged mitochondria as well as mitophagy would provide further insights into the mechanism underlying CHIP-mediated mitophagy. Using CHIP mutants in an *in vitro* model system of acute injury would allow us to better understand how CHIP mediates mitochondrial dynamics and turnover.

Summary

In summary, our results provide novel insight into the complexity underlying ischemic stroke. Not only did we uncover previously unappreciated effects of chronic CHIP overexpression on neuronal survival, but we also provided data supporting a novel function of CHIP: namely its involvement in mitophagy. Future studies aimed at identifying how CHIP expression levels are regulated and if the use of small molecule therapies to exogenously modify CHIP expression in an attempt to increase neuronal survival following acute ischemic injury, will allow us to make progress in our quest to identify potential targets for therapeutic intervention. The finding that CHIP is an essential regulator of mitochondrial homeostasis presents exciting new avenues that will allow us to better understand the complexity of the CHIP protein and how CHIP's involvement in a variety of processes can govern cellular outcome.

REFERENCES

Abou-Sleiman, P. M., Muqit, M. M. and Wood, N. W. (2006) Expanding insights of mitochondrial dysfunction in Parkinson's disease. *Nat Rev Neurosci*, **7**, 207-19.

Adachi, H., Waza, M., Tokui, K., Katsuno, M., Minamiyama, M., Tanaka, F., Doyu, M. and Sobue, G. (2007) CHIP overexpression reduces mutant androgen receptor protein and ameliorates phenotypes of the spinal and bulbar muscular atrophy transgenic mouse model. *The Journal of Neuroscience*, **27**, 5115-5126.

Adhami, F., Liao, G., Morozov, Y. M., Schloemer, A., Schmithorst, V. J., Lorenz, J. N., Dunn, R. S., Vorhees, C. V., Wills-Karp, M., Degen, J. L., Davis, R. J., Mizushima, N., Rakic, P., Dardzinski, B. J., Holland, S. K., Sharp, F. R. and Kuan, C.-Y. (2006) Cerebral Ischemia-Hypoxia Induces Intravascular Coagulation and Autophagy. *Am J Pathol*, **169**, 566-583.

Aizenman, E., Stout, A. K., Hartnett, K. A., Dineley, K. E., McLaughlin, B. and Reynolds, I. J. (2000) Induction of neuronal apoptosis by thiol oxidation: putative role of intracellular zinc release. *J Neurochem*, **75**, 1878-1888.

Albers, G. W., Caplan, L. R., Easton, J. D., Fayad, P. B., Mohr, J. P., Saver, J. L. and Sherman, D. G. (2002) Transient Ischemic Attack — Proposal for a New Definition. *New England Journal of Medicine*, **347**, 1713-1716.

Anderson, L. G., Meeker, R. B., Poulton, W. E. and Huang, D. Y. (2009) Brain distribution of carboxy terminus of Hsc70-interacting protein (CHIP) and its nuclear translocation in cultured cortical neurons following heat stress or oxygen-glucose deprivation. *Cell Stress Chaperones*,

Armstead, W. M., Nassar, T., Akkawi, S., Smith, D. H., Chen, X. H., Cines, D. B. and Higazi, A. A. (2006) Neutralizing the neurotoxic effects of exogenous and endogenous tPA. *Nat Neurosci*, **9**, 1150-5.

Arndt, V., Rogon, C. and Höhfeld, J. (2007) To be, or not to be – molecular chaperones in protein degradation. *Cell Mol Life Sci*, **64**, 2525.

Arrington, D. D., Van Vleet, T. R. and Schnellmann, R. G. (2006) Calpain 10: a mitochondrial calpain and its role in calcium-induced mitochondrial dysfunction. *Am J Physiol Cell Physiol*, **291**, C1159-71.

Avila, J., Lucas, J. J., Perez, M. and Hernandez, F. (2004) Role of tau protein in both physiological and pathological conditions. *Physiol Rev*, **84**, 361-84.

Ballinger, C. A., Connell, P., Wu, Y., Hu, Z., Thompson, L. J., Yin, L. Y. and Patterson, C. (1999) Identification of CHIP, a novel tetratricopeptide repeat-containing protein that interacts with heat shock proteins and negatively regulates chaperone functions. *Mol Cell Biol*, **19**, 4535-45.

Banerjee, R., Starkov, A. A., Beal, M. F. and Thomas, B. (2009) Mitochondrial dysfunction in the limelight of Parkinson's disease pathogenesis. *Biochim Biophys Acta*, **1792**, 651-63.

Beere, H. M. (2005) Death versus survival: functional interaction between the apoptotic and stress-inducible heat shock protein pathways. *The Journal of Clinical Investigation*, **115**, 2633-9.

Beere, H. M. and Green, D. R. (2001) Stress management - heat shock protein-70 and the regulation of apoptosis. *Trends Cell Biol*, **11**, 6-10.

Benveniste, H., Drejer, J., Schousboe, A. and Diemer, N. H. (1984) Elevation of the extracellular concentrations of glutamate and aspartate in rat hippocampus during transient cerebral ischemia monitored by intracerebral microdialysis. *J Neurochem*, **43**, 1369-74.

Bolanos, J. P., Moro, M. A., Lizasoain, I. and Almeida, A. (2009) Mitochondria and reactive oxygen and nitrogen species in neurological disorders and stroke: Therapeutic implications. *Adv Drug Deliv Rev*, **61**, 1299-315.

Brooks, P., Fuertes, G., Murray, R. Z., Bose, S., Knecht, E., Rechsteiner, M. C., Hendil, K. B., Tanaka, K., Dyson, J. and Rivett, J. (2000) Subcellular localization of proteasomes and their regulatory complexes in mammalian cells. *Biochem J*, **346 Pt 1**, 155-61.

Brouns, R. and De Deyn, P. P. (2009) The complexity of neurobiological processes in acute ischemic stroke. *Clin Neurol Neurosurg*, **111**, 483-495.

Brown, J. E., Zeiger, S. L. H., Hettinger, J. C., Brooks, J. D., Holt, B., Morrow, J. D., Musiek, E. S., Milne, G. and McLaughlin, B. (2010) Essential Role of the Redox-Sensitive Kinase p66shc in Determining Energetic and Oxidative Status and Cell Fate in Neuronal Preconditioning. *Journal of Neuroscience*, **30**, 5242-5252.

Bukau, B., Weissman, J. and Horwich, A. (2006) Molecular Chaperones and Protein Quality Control. *Cell*, **125**, 443-451.

Chacon, M. R., Jensen, M. B., Sattin, J. A. and Zivin, J. A. (2008) Neuroprotection in cerebral ischemia: emphasis on the SAINT trial. *Curr Cardiol Rep*, **10**, 37-42.

Chan, P. H. (2001) Reactive oxygen radicals in signaling and damage in the ischemic brain. *J Cereb Blood Flow Metab*, **21**, 2-14.

Chen, Y., Stevens, B., Chang, J., Milbrandt, J., Barres, B. A. and Hell, J. W. (2008) NS21: re-defined and modified supplement B27 for neuronal cultures. *J Neurosci Methods*, **171**, 239-47.

Choi, D. W. (1992) Excitotoxic cell death. *J Neurobiol*, **23**, 1261-1276.

Chu, C. T. (2008) Eaten Alive: Autophagy and Neuronal Cell Death after Hypoxia-Ischemia. *Am J Pathol*, **172**, 284-287.

Codreanu, S. G., Zhang, B., Sobecki, S. M., Billheimer, D. D. and Liebler, D. C. (2009) Global analysis of protein damage by the lipid electrophile 4-hydroxy-2-nonenal. *Mol and Cell Proteomics*, **8**, 670-80.

Coux, O., Tanaka, K. and Goldberg, A. L. (1996) Structure and functions of the 20S and 26S proteasomes. *Annu Rev Biochem*, **65**, 801-847.

Cyr, D. M., Hohfeld, J. and Patterson, C. (2002) Protein quality control: U-box-containing E3 ubiquitin ligases join the fold. *Trends Biochem Sci*, **27**, 368-375.

Dai, Q., Zhang, C., Wu, Y., McDonough, H., Whaley, R. A., Godfrey, V., Li, H. H., Madamanchi, N., Xu, W., Neckers, L., Cyr, D. and Patterson, C. (2003) CHIP activates HSF1 and confers protection against apoptosis and cellular stress. *Embo J*, **22**, 5446-58.

Dalle-Donne, I., Rossi, R., Giustarini, D., Milzani, A. and Colombo, R. (2003) Protein carbonyl groups as biomarkers of oxidative stress. *Clin Chim Acta*, **329**, 23.

Das, S. K., Mukherjee, S. and Vasudevan, D. M. (2007) Oxidative Stress is the Primary Event: Effects of Ethanol Consumption in Brain. *Indian Journal of Clinical Biochemistry*, **22**, 99-104.

Davis, J. B. and Maher, P. (1994) Protein kinase C activation inhibits glutamate-induced cytotoxicity in a neuronal cell line. *Brain Res*, **652**, 169-173.

Delanty, N. and Dichter, M. A. (2000) Antioxidant Therapy in Neurologic Disease. *Arch Neurol*, **57**, 1265-1270.

Dennehy, M. K., Richards, K. A. M., Wernke, G. R., Shyr, Y. and Liebler, D. C. (2005) Cytosolic and Nuclear Protein Targets of Thiol-Reactive Electrophiles. *Chem Res Toxicol*, **19**, 20-29.

Dias-Santagata, D., Fulga, T. A., Duttaroy, A. and Feany, M. B. (2007) Oxidative stress mediates tau-induced neurodegeneration in Drosophila. *J Clin Invest*, **117**, 236-45.

Dickey, C. A., Kamal, A., Lundgren, K., Klosak, N., Bailey, R. M., Dunmore, J., Ash, P., Shoraka, S., Zlatkovic, J., Eckman, C. B., Patterson, C., Dickson, D. W., Nahman, N. S., Hutton, M., Burrows, F. and Petrucelli, L. (2007) The high-affinity HSP90-CHIP complex recognizes and selectively degrades phosphorylated tau client proteins. *The Journal of Clinical Investigation*, **117**, 648.

Dickey, C. A., Koren, J., Zhang, Y.-J., Xu, Y.-f., Jinwal, U. K., Birnbaum, M. J., Monks, B., Sun, M., Cheng, J. Q., Patterson, C., Bailey, R. M., Dunmore, J., Soresh, S., Leon, C., Morgan, D. and Petrucelli, L. (2008) Akt and CHIP coregulate tau degradation through coordinated interactions. *Proceedings of the National Academy of Sciences*, **105**, 3622-3627.

Dickey, C. A., Patterson, C., Dickson, D. and Petrucelli, L. (2007) Brain CHIP: removing the culprits in neurodegenerative disease. *Trends Mol Med*, **13**, 32.

Dikshit, P. and Jana, N. R. (2007) The co-chaperone CHIP is induced in various stresses and confers protection to cells. *Biochemical and Biophysical Research Communications*, **357**, 761.

Douglas, P. M. and Dillin, A. (2010) Protein homeostasis and aging in neurodegeneration. *The Journal of Cell Biology*, **190**, 719-729.

Doyle, K. P., Simon, R. P. and Stenzel-Poore, M. P. (2008) Mechanisms of ischemic brain damage. *Neuropharmacology*, **55**, 310-318.

Droge, W. (2002) Free radicals in the physiological control of cell function. *Physiological Reviews*, **82**, 47-95.

Du, S., McLaughlin, B., Pal, S. and Aizenman, E. (2002) In vitro neurotoxicity of methylisothiazolinone, a commonly used industrial and household biocide, proceeds via a zinc and extracellular signal-regulated kinase mitogen-activated protein kinase-dependent pathway. *J Neurosci*, **22**, 7408-7416.

Egana, J. T., Zambrano, C., Nunez, M. T., Gonzalez-Billault, C. and Maccioni, R. B. (2003) Iron-induced oxidative stress modify tau phosphorylation patterns in hippocampal cell cultures. *Biometals*, **16**, 215-23.

Ellis, R. J. and van der Vies, S. M. (1991) Molecular Chaperones. *Annual Review of Biochemistry*, **60**, 321-347.

Erecinska, M. and Silver, I. A. (1994) Ions and energy in mammalian brain. *Progress in Neurobiology*, **43**, 37.

Fabricius, M., Fuhr, S., Bhatia, R., Boutelle, M., Hashemi, P., Strong, A. J. and Lauritzen, M. (2006) Cortical spreading depression and peri-infarct depolarization in acutely injured human cerebral cortex. *Brain*, **129**, 778-790.

Fam, S. S. and Morrow, J. D. (2003) The isoprostanes: unique products of arachidonic acid oxidation-a review. *Current Medicinal Chemistry*, **10**, 1723-40.

Farmer, E. E. and Davoine, C. (2007) Reactive electrophile species. *Current Opinion in Plant Biology*, **10**, 380-386.

Garcia, J. H., Liu, K.-F. and Ho, K.-L. (1995) Neuronal Necrosis After Middle Cerebral Artery Occlusion in Wistar Rats Progresses at Different Time Intervals in the Caudoputamen and the Cortex. *Stroke*, **26**, 636-643.

Gilgun-Sherki, Y., Rosenbaum, Z., Melamed, E. and Offen, D. (2002) Antioxidant Therapy in Acute Central Nervous System Injury: Current State. *Pharmacological Reviews*, **54**, 271-284.

Ginsberg, M. D. (2008) Neuroprotection for ischemic stroke: past, present and future. *Neuropharmacology*, **55**, 363-89.

Goldbaum, O. and Richter-Landsberg, C. (2002) Activation of PP2A-like phosphatase and modulation of tau phosphorylation accompany stress-induced apoptosis in cultured oligodendrocytes. *Glia*, **40**, 271-82.

Goldberg, A. L. (2005) Nobel Committee Tags Ubiquitin for Distinction. *Neuron*, **45**, 339.

Goldberg, A. L. (2003) Protein degradation and protection against misfolded or damaged proteins. *Nature*, **426**, 895.

Goll, D. E., Thompson, V. F., Li, H., Wei, W. and Cong, J. (2003) The calpain system. *Physiol Rev*, **83**, 731-801.

Gonzalez-Zulueta, M., Feldman, A. B., Klesse, L. J., Kalb, R. G., Dillman, J. F., Parada, L. F., Dawson, T. M. and Dawson, V. L. (2000) Requirement for nitric oxide activation of p21(ras)/extracellular regulated kinase in neuronal ischemic preconditioning. *PNAS*, **97**, 436-41.

Gorter, J. A., Petrozzino, J. J., Aronica, E. M., Rosenbaum, D. M., Opitz, T., Bennett, M. V. L., Connor, J. A. and Zukin, R. S. (1997) Global Ischemia Induces Downregulation of Glur2 mRNA and Increases AMPA Receptor-Mediated Ca2+ Influx in Hippocampal CA1 Neurons of Gerbil. *J. Neurosci.*, **17**, 6179-6188.

Greene, J. G. and Greenamyre, J. T. (1996) Bioenergetics and glutamate excitotoxicity. *Progress In Neurobiology*, **48**, 613-634.

Gupta, R., Yonas, H., Gebel, J., Goldstein, S., Horowitz, M., Grahovac, S. Z., Wechsler, L. R., Hammer, M. D., Uchino, K. and Jovin, T. G. (2006) Reduced Pretreatment Ipsilateral Middle Cerebral Artery Cerebral Blood Flow Is Predictive of Symptomatic Hemorrhage Post-Intra-Arterial Thrombolysis in Patients With Middle Cerebral Artery Occlusion. *Stroke*, **37**, 2526-2530.

Halliwell, B. (1992) Reactive oxygen species and the central nervous system. *J Neurochem*, **59**, 1609-23.

Halliwell, B. and Gutteridge, J. Free Radicals in Biology and Medicine. 4th ed. New York: Oxford University Press Inc., 2007

Hancock, J. T., Desikan, R. and Neill, S. J. (2001) Role of reactive oxygen species in cell signalling pathways. *Biochem. Soc. Trans.*, **29**, 345-350.

Hanna, J. and Finley, D. (2007) A proteasome for all occasions. *Federation of European Biochemical Socities Letters*, **581**, 2854-61.

Hegde, A. N. and Upadhya, S. C. (2007) The ubiquitin-proteasome pathway in health and disease of the nervous system. *Trends in Neurosciences*, **30**, 587.

Helton, T. D., Otsuka, T., Lee, M.-C., Mu, Y. and Ehlers, M. D. (2008) Pruning and loss of excitatory synapses by the parkin ubiquitin ligase. *Proceedings of the National Academy of Sciences*, **105**, 19492-19497.

Herrmann, J., Lerman, L. O. and Lerman, A. (2007) Ubiquitin and ubiquitin-like proteins in protein regulation. *Circ Res*, **100**, 1276-91.

Hohfeld, J., Cyr, D. M. and Patterson, C. (2001) From the cradle to the grave: molecular chaperones that may choose between folding and degradation. *EMBO Rep*, **10**, 885-890.

Hoidal, J. R. (2001) Reactive Oxygen Species and Cell Signaling. *Am. J. Respir. Cell Mol. Biol.*, **25**, 661-663.

Hoyt, K. R., McLaughlin, B. A., Higgins, D. S., Jr and Reynolds, I. J. (2000) Inhibition of glutamate-induced mitochondrial depolarization by tamoxifen in cultured neurons. *The Journal of Pharmacology and Experimental Therapeutics*, **293**, 480-486.

Hu, B. R., Janelidze, S., Ginsberg, M. D., Busto, R., Perez-Pinzon, M., Sick, T. J., Siesjo, B. K. and Liu, C. L. (2001) Protein aggregation after focal brain ischemia and reperfusion. *J Cereb Blood Flow Metab*, **21**, 865-75.

Hu, B. R., Martone, M. E., Jones, Y. Z. and Liu, C. L. (2000) Protein aggregation after transient cerebral ischemia. *The Journal of Neuroscience*, **20**, 3191-3199.

Imai, Y., Soda, M., Hatakeyama, S., Akagi, T., Hashikawa, T., Nakayama, K.-I. and Takahashi, R. (2002) CHIP is associated with Parkin, a gene responsible for familial Parkinson's disease, and enhances its ubiquitin ligase activity. *Mol Cell*, **10**, 55-67.

Irving, E. A. and Bamford, M. (2002) Role of mitogen- and stress-activated kinases in ischemic injury. *J Cereb Blood Flow Metab*, **22**, 631-47.

Jana, N. R., Dikshit, P., Goswami, A., Kotliarova, S., Murata, S., Tanaka, K. and Nukina, N. (2005) Co-chaperone CHIP associates with expanded polyglutamine protein and promotes their degradation by proteasomes. *J Biol Chem*, **280**, 11635-11640.

Jarvis, C. R., Anderson, T. R. and Andrew, R. D. (2001) Anoxic Depolarization Mediates Acute Damage Independent of Glutamate in Neocortical Brain Slices. *Cereb. Cortex*, **11**, 249-259.

Jiang, J., Ballinger, C. A., Wu, Y., Dai, Q., Cyr, D. M., Hohfeld, J. and Patterson, C. (2001) CHIP Is a U-box-dependent E3 Ubiquitin Ligase. Identification of HSC70 as a target for ubiquitylation. *The Journal of Biological Chemistry*, **276**, 42938-42944.

Johnston, S. C. (2006) Translation: case study in failure. *Ann Neurol*, **59**, 447-8.

Joshi, I. and Andrew, R. D. (2001) Imaging Anoxic Depolarization During Ischemia-Like Conditions in the Mouse Hemi-Brain Slice. *J Neurophysiol*, **85**, 414-424.

Kaarniranta, K., Oksala, N., Karjalainen, H. M., Suuronen, T., Sistonen, L., Helminen, H. J., Salminen, A. and Lammi, M. J. (2002) Neuronal cells show regulatory differences in the hsp70 gene response. *Brain Res Mol Brain Res*, **101**, 136-40.

Kampinga, H. H., Kanon, B., Salomons, F. A., Kabakov, A. E. and Patterson, C. (2003) Overexpression of the cochaperone CHIP enhances Hsp70-dependent folding activity in mammalian cells. *Mol Cell Biol* **23**, 4948-4958.

Kandel, E. R., Schwartz, J. H. and Jessell, T. M. Principles of neural science. 4th ed. New York: McGraw Hill, 1999

Kanthan, R., Shuaib, A., Griebel, R. and Miyashita, H. (1995) Intracerebral Human Microdialysis : In Vivo Study of an Acute Focal Ischemic Model of the Human Brain. *Stroke*, **26**, 870-873.

Keller, J. N., Huang, F. F., Zhu, H., Yu, J., Ho, Y. S. and Kindy, M. S. (2000) Oxidative stress-associated impairment of proteasome activity during ischemia-reperfusion injury. *J Cereb Blood Flow Metab* **20**, 1467-1473.

Kiang, J. G. and Tsokos, G. C. (1998) Heat shock protein 70 kDa: molecular biology, biochemistry, and physiology. *Pharmacol Ther*, **80**, 183-201.

Kidwell, C. S., Alger, J. R. and Saver, J. L. (2004) Evolving Paradigms in Neuroimaging of the Ischemic Penumbra. *Stroke*, **35**, 2662-2665.

Kim, S.-A., Yoon, J.-H., Kim, D.-K., Kim, S.-G. and Ahn, S.-G. (2005) CHIP interacts with heat shock factor 1 during heat stress. *FEBS Letters*, **579**, 6559.

Kleinhans, H., Mann, O., Schurr, P. G., Kaifi, J. T., Hansen, B., Izbicki, J. R. and Strate, T. (2006) Oxygen radical formation does not have an impact in the treatment of severe acute experimental pancreatitis using free cellular hemoglobin. *World J Gastroenterol*, **12**, 2914-8.

Kleman, A. M., Brown, J. E., Zeiger, S. L., Hettinger, J. C., Brooks, J. D., Holt, B., Morrow, J. D., Musiek, E. S., Milne, G. L. and McLaughlin, B. (2010) p66(shc)'s role as an essential mitophaghic molecule in controlling neuronal redox and energetic tone. *Autophagy*, **6**, 948-9.

Ko, H. S., Bailey, R., Smith, W. W., Liu, Z., Shin, J.-H., Lee, Y.-I., Zhang, Y.-J., Jiang, H., Ross, C. A., Moore, D. J., Patterson, C., Petrucelli, L., Dawson, T. M. and Dawson, V. L. (2009) CHIP regulates leucine-rich repeat kinase-2 ubiquitination, degradation, and toxicity. *Proceedings of the National Academy of Sciences*, **106**, 2897-2902.

Krebiehl, G., Ruckerbauer, S., Burbulla, L. F., Kieper, N., Maurer, B., Waak, J., Wolburg, H., Gizatullina, Z., Gellerich, F. N., Woitalla, D., Riess, O., Kahle, P. J.,

Proikas-Cezanne, T. and Kruger, R. (2010) Reduced basal autophagy and impaired mitochondrial dynamics due to loss of Parkinson's disease-associated protein DJ-1. *PLoS One*, **5**, e9367.

Kubow, S., Janzen, E. G. and Bray, T. M. (1984) Spin-trapping of free radicals formed during in vitro and in vivo metabolism of 3-methylindole. *J Biol Chem*, **259**, 4447-51.

Lambert, A. J. and Brand, M. D. (2009) Reactive oxygen species production by mitochondria. *Methods Mol Biol*, **554**, 165-81.

Lansberg, M. G., Bluhmki, E. and Thijs, V. N. (2009) Efficacy and safety of tissue plasminogen activator 3 to 4.5 hours after acute ischemic stroke: a metaanalysis. *Stroke*, **40**, 2438-41.

Lansberg, M. G., Schrooten, M., Bluhmki, E., Thijs, V. N. and Saver, J. L. (2009) Treatment time-specific number needed to treat estimates for tissue plasminogen activator therapy in acute stroke based on shifts over the entire range of the modified Rankin Scale. *Stroke*, **40**, 2079-84.

Leary, M. C. and Saver, J. L. (2003) Annual incidence of first silent stroke in the United States: a preliminary estimate. *Cerebrovasc Dis*, **16**, 280-5.

Legos, J. J., McLaughlin, B., Skaper, S. D., Strijbos, P. J. L. M., Parsons, A. A., Aizenman, E., Herin, G. A., Barone, F. C. and Erhardt, J. A. (2002) The selective p38 inhibitor SB-239063 protects primary neurons from mild to moderate excitotoxic injury. *Eur J Pharmacol*, **447**, 37-42.

Lenfant, C. (2003) Clinical Research to Clinical Practice — Lost in Translation? *New England Journal of Medicine*, **349**, 868-874.

Lenton, K. J., Therriault, H. and Wagner, J. R. (1999) Analysis of glutathione and glutathione disulfide in whole cells and mitochondria by postcolumn derivatization high-performance liquid chromatography with ortho-phthalaldehyde. *Anal Biochem*, **274**, 125-30.

Levine, R. L., Garland, D., Oliver, C.N., Amici, A., Climent, I., Lenz, A.G., Ahn, B.W., Shaltiel, S. and Stadtman, E.R. (1990) Determination of carbonyl content in oxidatively modified proteins. Methods Enzymol, P. Lester and N.G. Alexander, Editors. Academic Press. p. 464-478.

Levine, R.L., Williams, J.A., Stadtman, E.R. and Shacter, E. (1994) Carbonyl assays for determination of oxidatively modified proteins. Methods Enzymol. P. Lester, Editor. Academic Press. p. 346-357.

Liberatore, G. T., Samson, A., Bladin, C., Schleuning, W.-D. and Medcalf, R. L. (2003) Vampire Bat Salivary Plasminogen Activator (Desmoteplase): A Unique Fibrinolytic Enzyme That Does Not Promote Neurodegeneration. *Stroke*, **34**, 537-543.

Liebler, D. C. (2008) Protein damage by reactive electrophiles: targets and consequences. *Chem Res Toxicol*, **21**, 117-28.

Lipton, P. (1999) Ischemic cell death in brain neurons. *Physiol Rev*, **79**, 1431-568.

Liu, B., Liao, M., Mielke, J. G., Ning, K., Chen, Y., Li, L., El-Hayek, Y. H., Gomez, E., Zukin, R. S., Fehlings, M. G. and Wan, Q. (2006) Ischemic Insults Direct Glutamate Receptor Subunit 2-Lacking AMPA Receptors to Synaptic Sites. *Journal of Neuroscience*, **26**, 5309-5319.

Liu, W., Vives-Bauza, C., Acin-Perez, R., Yamamoto, A., Tan, Y., Li, Y., Magrane, J., Stavarache, M. A., Shaffer, S., Chang, S., Kaplitt, M. G., Huang, X. Y., Beal, M. F., Manfredi, G. and Li, C. (2009) PINK1 defect causes mitochondrial dysfunction, proteasomal deficit and alpha-synuclein aggregation in cell culture models of Parkinson's disease. *PLoS One*, **4**, e4597.

Liu, Y., Fiskum, G. and Schubert, D. (2002) Generation of reactive oxygen species by the mitochondrial electron transport chain. *Journal of Neurochemistry*, **80**, 780-787.

Lloyd-Jones, D., Adams, R., Carnethon, M., De Simone, G., Ferguson, T. B., Flegal, K., Ford, E., Furie, K., Go, A., Greenlund, K., Haase, N., Hailpern, S., Ho, M., Howard, V., Kissela, B., Kittner, S., Lackland, D., Lisabeth, L., Marelli, A., McDermott, M., Meigs, J., Mozaffarian, D., Nichol, G., O'Donnell, C., Roger, V., Rosamond, W., Sacco, R., Sorlie, P., Stafford, R., Steinberger, J., Thom, T., Wasserthiel-Smoller, S., Wong, N., Wylie-Rosett, J., Hong, Y., Committee, f. t. A. H. A. S. and Stroke Statistics Subcommittee. (2009) Heart Disease and Stroke Statistics--2009 Update: A Report From the American Heart Association Statistics Committee and Stroke Statistics Subcommittee. *Circulation*, **119**, e21-181.

Lopez-Atalaya, J. P., Roussel, B. D., Levrat, D., Parcq, J., Nicole, O., Hommet, Y., Benchenane, K., Castel, H., Leprince, J., To Van, D., Bureau, R., Rault, S., Vaudry, H., Petersen, K.-U., Santos, J. S.-d. O., Ali, C. and Vivien, D. (2008) Toward safer thrombolytic agents in stroke: molecular requirements for NMDA receptor-mediated neurotoxicity. *J Cereb Blood Flow Metab*, **28**, 1212-1221.

Luo, Y. and DeFranco, D. B. (2006) Opposing roles for ERK1/2 in neuronal oxidative toxicity: distinct mechanism of ERK1/2 action at early versus late phases of oxidative stress. *J Biol Chem*, **281**, 16436-16442.

Maher, P. (2005) The effects of stress and aging on glutathione metabolism. *Ageing Res Rev*, **4**, 288.

Maisonneuve, E., Ducret, A., Khoueiry, P., Lignon, S., Longhi, S., Talla, E. and Dukan, S. (2009) Rules governing selective protein carbonylation. *PLoS One*, **4**, e7269.

Malkus, K. A., Tsika, E. and Ischiropoulos, H. (2009) Oxidative modifications, mitochondrial dysfunction, and impaired protein degradation in Parkinson's disease: how neurons are lost in the Bermuda triangle. *Mol Neurodegener*, **4**, 24.

Maples, K. R., Green, A. R. and Floyd, R. A. (2004) Nitrone-related therapeutics: potential of NXY-059 for the treatment of acute ischaemic stroke. *CNS Drugs*, **18**, 1071-84.

Marler, J. R. (1995) Tissue Plasminogen Activator for Acute Ischemic Stroke. *New England Journal of Medicine*, **333**, 1581-1588.

Marler, J. R. (2002) NINDS-Sponsored Clinical Trials in Stroke: Past, Present, and Future. *Stroke*, **33**, 311-312.

Martin, L. J., Al-Abdulla, N. A., Brambrink, A. M., Kirsch, J. R., Sieber, F. E. and Portera-Cailliau, C. (1998) Neurodegeneration in excitotoxicity, global cerebral ischemia, and target deprivation: A perspective on the contributions of apoptosis and necrosis. *Brain Res Bull*, **46**, 281-309.

Matsuda, N., Sato, S., Shiba, K., Okatsu, K., Saisho, K., Gautier, C. A., Sou, Y.-s., Saiki, S., Kawajiri, S., Sato, F., Kimura, M., Komatsu, M., Hattori, N. and Tanaka, K. (2010) PINK1 stabilized by mitochondrial depolarization recruits Parkin to damaged mitochondria and activates latent Parkin for mitophagy. *The Journal of Cell Biology*, **189**, 211-221.

Matsumoto, K., Lo, E. H., Pierce, A. R., Halpern, E. F. and Newcomb, R. (1996) Secondary elevation of extracellular neurotransmitter amino acids in the reperfusion phase following focal cerebral ischemia. *J Cereb Blood Flow Metab*, **16**, 114-24.

McDonough, H. and Patterson, C. (2003) CHIP: a link between the chaperone and proteasome systems. *Cell Stress & Chaperones*, **8**, 303-308.

McLaughlin, B., Hartnett, K. A., Erhardt, J. A., Legos, J. J., White, R. F., Barone, F. C. and Aizenman, E. (2003) Caspase 3 activation is essential for neuroprotection in preconditioning. *PNAS*, **100**, 715-720.

McLaughlin, B., Pal, S., Tran, M. P., Parsons, A. A., Barone, F. C., Erhardt, J. A. and Aizenman, E. (2001) p38 activation is required upstream of potassium current enhancement and caspase cleavage in thiol oxidant-induced neuronal apoptosis. *J Neurosci*, **21**, 3303-3311.

McLaughlin, B. A. and DiNapoli, M. (2005) The proteasome ubiquitin system as a drug target in cerebrovascular disease: The therapeutic potential of proteasome inhibitors. *Current Opinion in Investigational Drugs*, **6**, 686-699.

McLaughlin, B. A., Nelson, D., Erecinska, M. and Chesselet, M. F. (1998) Toxicity of dopamine to striatal neurons in vitro and potentiation of cell death by a mitochondrial inhibitor. *J Neurochem*, **70**, 2406-2415.

McLaughlin, B. A., Nelson, D., Silver, I. A., Erecinska, M. and Chesselet, M.-F. (1998) Methylmalonate toxicity in primary neuronal cultures. *Neuroscience*, **86**, 279-290.

McNamara, D. and Dingledine, R. (1990) Dual effect of glycine on NMDA-induced neurotoxicity in rat cortical cultures. *J Neurosci*, **10**, 3970-3976.

Mehta, S. L., Manhas, N. and Raghubir, R. (2007) Molecular targets in cerebral ischemia for developing novel therapeutics. *Brain Res Rev*, **54**, 34-66.

Melov, S., Adlard, P. A., Morten, K., Johnson, F., Golden, T. R., Hinerfeld, D., Schilling, B., Mavros, C., Masters, C. L., Volitakis, I., Li, Q. X., Laughton, K., Hubbard, A., Cherny, R. A., Gibson, B. and Bush, A. I. (2007) Mitochondrial oxidative stress causes hyperphosphorylation of tau. *PLoS One*, **2**, e536.

Michiorri, S., Gelmetti, V., Giarda, E., Lombardi, F., Romano, F., Marongiu, R., Nerini-Molteni, S., Sale, P., Vago, R., Arena, G., Torosantucci, L., Cassina, L., Russo, M. A., Dallapiccola, B., Valente, E. M. and Casari, G. (2010) The Parkinson-associated protein PINK1 interacts with Beclin1 and promotes autophagy. *Cell Death Differ*, **17**, 962-74.

Milne, G. L., Musiek, E. S. and Morrow, J. D. (2005) F2-isoprostanes as markers of oxidative stress in vivo: an overview. *Biomarkers*, **10 Suppl 1**, S10-23.

Min, J.-N., Whaley, R. A., Sharpless, N. E., Lockyer, P., Portbury, A. L. and Patterson, C. (2008) CHIP Deficiency Decreases Longevity, with Accelerated Aging Phenotypes Accompanied by Altered Protein Quality Control. *Mol. Cell. Biol.*, **28**, 4018-4025.

Monaghan, P., Metcalfe, N. B. and Torres, R. (2009) Oxidative stress as a mediator of life history trade-offs: mechanisms, measurements and interpretation. *Ecology Letters*, **12**, 75-92.

Montine, K. S., Quinn, J. F., Zhang, J., Fessel, J. P., Roberts, L. J., 2nd, Morrow, J. D. and Montine, T. J. (2004) Isoprostanes and related products of lipid peroxidation in neurodegenerative diseases. *Chem Phys Lipids*, **128**, 117-24.

Morishima, Y., Wang, A. M., Yu, Z., Pratt, W. B., Osawa, Y. and Lieberman, A. P. (2008) CHIP deletion reveals functional redundancy of E3 ligases in promoting degradation of both signaling proteins and expanded glutamine proteins. *Hum. Mol. Genet.*, **17**, 3942-3952.

Muqit, M. M., Gandhi, S. and Wood, N. W. (2006) Mitochondria in Parkinson disease: back in fashion with a little help from genetics. *Arch Neurol*, **63**, 649-54.

Murata, S., Chiba, T. and Tanaka, K. (2003) CHIP: a quality-control E3 ligase collaborating with molecular chaperones. *The International Journal of Biochemistry & Cell Biology*, **35**, 572-578.

Murata, S., Minami, Y., Minami, M., Chiba, T. and Tanaka, K. (2001) CHIP is a chaperone-dependent E3 ligase that ubiquitylates unfolded protein. *EMBO Rep*, **2**, 1133-8.

Musiek, E. S., Breeding, R. S., Milne, G. L., Zanoni, G., Morrow, J. D. and McLaughlin, B. (2006) Cyclopentenone isoprostanes are novel bioactive products of lipid oxidation which enhance neurodegeneration. *Journal of Neurochemistry*, **97**, 1301-1313.

Nikolay, R., Wiederkehr, T., Rist, W., Kramer, G., Mayer, M. P. and Bukau, B. (2004) Dimerization of the Human E3 Ligase CHIP via a Coiled-coil Domain Is Essential for Its Activity. *J. Biol. Chem.*, **279**, 2673-2678.

Noh, K. M., Yokota, H., Mashiko, T., Castillo, P. E., Zukin, R. S. and Bennett, M. V. (2005) Blockade of calcium-permeable AMPA receptors protects hippocampal neurons against global ischemia-induced death. *Proc Natl Acad Sci U S A*, **102**, 12230-5.

Nollen, E. A. A. and Morimoto, R. I. (2002) Chaperoning signaling pathways: molecular chaperones as stress-sensing `heat shock' proteins. *J Cell Sci*, **115**, 2809-2816.

O'Collins, V., Macleod, M., Donnan, G., Horky, L., Worp, B. and Howells, D. (2006) 1,026 experimental treatments in acute stroke. *Ann Neurol*, **59**, 467 - 477.

Onteniente, B., Rasika, S., Benchoua, A. and Guegan, C. (2003) Molecular pathways in cerebral ischemia - Cues to novel therapeutic strategies. *Molecular Neurobiology*, **27**, 33-72.

Page, M. M., Robb, E. L., Salway, K. D. and Stuart, J. A. (2010) Mitochondrial redox metabolism: Aging, longevity and dietary effects. *Mechanisms of Ageing and Development*, **131**, 242-252.

Pari, L. and Latha, M. (2004) Protective role of Scoparia dulcis plant extract on brain antioxidant status and lipidperoxidation in STZ diabetic male Wistar rats. *BMC Complementary and Alternative Medicine*, **4**, 16.

Pellegrini-Giampietro, D. E., Zukin, R. S., Bennett, M. V., Cho, S. and Pulsinelli, W. A. (1992) Switch in glutamate receptor subunit gene expression in CA1 subfield of hippocampus following global ischemia in rats. *Proc Natl Acad Sci U S A*, **89**, 10499-503.

Petrucelli, L., Dickson, D., Kehoe, K., Taylor, J., Snyder, H., Grover, A., De Lucia, M., McGowan, E., Lewis, J. and Prihar et, a. (2004) CHIP and Hsp70 regulate tau ubiquitination, degradation and aggregation. *Hum Mol Genet*, **13**, 703-714.

Polster, B. M., Basañez, G., Etxebarria, A., Hardwick, J. M. and Nicholls, D. G. (2005) Calpain I Induces Cleavage and Release of Apoptosis-inducing Factor from Isolated Mitochondria. *Journal of Biological Chemistry*, **280**, 6447-6454.

Poole, A. C., Thomas, R. E., Andrews, L. A., McBride, H. M., Whitworth, A. J. and Pallanck, L. J. (2008) The PINK1/Parkin pathway regulates mitochondrial morphology. *Proceedings of the National Academy of Sciences*, **105**, 1638-1643.

Poppek, D., Keck, S., Ermak, G., Jung, T., Stolzing, A., Ullrich, O., Davies, K. J. and Grune, T. (2006) Phosphorylation inhibits turnover of the tau protein by the proteasome: influence of RCAN1 and oxidative stress. *Biochem J*, **400**, 511-20.

Qian, S.-B., McDonough, H., Boellmann, F., Cyr, D. M. and Patterson, C. (2006) CHIP-mediated stress recovery by sequential ubiquitination of substrates and Hsp70. *Nature*, **440**, 551.

Rakovic, A., Grunewald, A., Seibler, P., Ramirez, A., Kock, N., Orolicki, S., Lohmann, K. and Klein, C. (2010) Effect of endogenous mutant and wild-type PINK1 on Parkin in fibroblasts from Parkinson disease patients. *Hum Mol Genet*, **19**, 3124-37.

Ravagnan, L., Gurbuxani, S., Susin, S. A., Maisse, C., Daugas, E., Zamzami, N., Mak, T., Jaattela, M., Penninger, J. M., Garrido, C. and Kroemer, G. (2001) Heat-shock protein 70 antagonizes apoptosis-inducing factor. *Nature Cell Biology*, **3**, 839-43.

Robinson, C. E., Keshavarzian, A., Pasco, D. S., Frommel, T. O., Winship, D. H. and Holmes, E. W. (1999) Determination of Protein Carbonyl Groups by Immunoblotting. *Anal Biochem*, **266**, 48-57.

Rosamond, W., Flegal, K., Furie, K., Go, A., Greenlund, K., Haase, N., Hailpern, S. M., Ho, M., Howard, V., Kissela, B., Kittner, S., Lloyd-Jones, D., McDermott, M., Meigs, J., Moy, C., Nichol, G., O'Donnell, C., Roger, V., Sorlie, P., Steinberger, J., Thom, T., Wilson, M., Hong, Y. and for the American Heart Association Statistics Committee and Stroke Statistics, S. (2008) Heart disease and stroke statistics--2008 update: a report from the American heart association statistics committee and stroke statistics subcommittee. *Circulation*, **117**, e25-146.

Rosenzweig, R. and Glickman, M. H. (2008) Forging a proteasome alpha-ring with dedicated proteasome chaperones. *Nat Struct Mol Biol*, **15**, 218-20.

Rosenzweig, R. and Glickman, M. H. (2008) Chaperone-driven proteasome assembly. *Biochem Soc Trans*, **36**, 807-12.

Rosser, M. F. N., Washburn, E., Muchowski, P. J., Patterson, C. and Cyr, D. M. (2007) Chaperone Functions of the E3 Ubiquitin Ligase CHIP. *J Biol Chem*, **282**, 22267-22277.

Sahara, N., Murayama, M., Mizoroki, T., Urushitani, M., Imai, Y., Takahashi, R., Murata, S., Tanaka, K. and Takashima, A. (2005) In vivo evidence of CHIP up-regulation attenuating tau aggregation. *J Neurochem*, **94**, 1254-63.

Sairanen, T., Karjalainen-Lindsberg, M.-L., Paetau, A., Ijäs, P. and Lindsberg, P. J. (2006) Apoptosis dominant in the periinfarct area of human ischaemic stroke—a possible target of antiapoptotic treatments. *Brain*, **129**, 189-199.

Savitz, S. I. and Fisher, M. (2007) Future of neuroprotection for acute stroke: In the aftermath of the SAINT trials. *Annals of Neurology*, **61**, 396-402.

Sha, Y., Pandit, L., Zeng, S. and Eissa, N. T. (2009) A Critical Role for CHIP in the Aggresome Pathway. *Mol. Cell. Biol.*, **29**, 116-128.

Shacter, E., Williams, J. A., Lim, M. and Levine, R. L. (1994) Differential susceptibility of plasma proteins to oxidative modification: Examination by western blot immunoassay. *Free Radic Biol Med*, **17**, 429-437.

Sharp, F. R., Massa, S. M. and Swanson, R. A. (1999) Heat-shock protein protection. *Trends Neurosci*, **22**, 97-99.

Shibatani, T., Carlson, E. J., Larabee, F., McCormack, A. L., Fruh, K. and Skach, W. R. (2006) Global organization and function of mammalian cytosolic proteasome pools: Implications for PA28 and 19S regulatory complexes. *Mol Biol Cell*, **17**, 4962-71.

Shimura, H., Schwartz, D., Gygi, S. P. and Kosik, K. S. (2004) CHIP-Hsc70 complex ubiquitinates phosphorylated tau and enhances cell survival. *The Journal of Biological Chemistry*, **279**, 4869-4876.

Shuaib, A., Lees, K., Lyden, P., Grotta, J., Davalos, A., Davis, S., Diener, H., Ashwood, T., Wasiewski, W., Emeribe, U. and Investigators, S. I. T. (2007) NXY-059 for treatment of acute ischemic stroke. *N Engl J Med*, **357**, 562 - 571.

Silva, G. M., Netto, L. E., Discola, K. F., Piassa-Filho, G. M., Pimenta, D. C., Barcena, J. A. and Demasi, M. (2008) Role of glutaredoxin 2 and cytosolic thioredoxins in cysteinyl-based redox modification of the 20S proteasome. *FEBS J*, **275**, 2942-55.

Singh, R. P., Sharad, S. and Kapur, S. (2004) Free Radicals and Oxidative Stress in Neurodegenerative Diseases: Relevance of Dietary Antioxidants. *JIACM*, **5**, 218-225.

Snoeckx, L. H. E. H., Cornelussen, R. N., Van Nieuwenhoven, F. A., Reneman, R. S. and Van der Vusse, G. J. (2001) Heat Shock Proteins and Cardiovascular Pathophysiology. *Physiol. Rev.*, **81**, 1461-1497.

Stadtman, E. R. (2006) Protein oxidation and aging. *Free Radic Res*, **40**, 1250-8.

Stanciu, M., Wang, Y., Kentor, R., Burke, N., Watkins, S., Kress, G., Reynolds, I., Klann, E., Angiolieri, M. R. and Johnson et, a. (2000) Persistent activation of ERK contributes to glutamate-induced oxidative toxicity in a neuronal cell line and primary cortical neuron cultures. *The Journal of Biological Chemistry*, **275**, 12200-12206.

Stankowski, J. N., Codreanu, S. G., Liebler, D. C. and McLaughlin, B. (2010) Analysis of Protein Targets by Oxidative Stress using the OxyBlot and Biotin-Avidin-Capture Methodology. *Cell Culture Techniques: Neuromethods.* , [In Press].

Stankowski, J. N., Zeiger, S. L., Cohen, E. L., Defranco, D. B., Cai, J. and McLaughlin, B. M. (2010) C-Terminus of HSC70 Interacting Protein Increases Following Stroke and Impairs Survival Against Acute Oxidative Stress. *Antioxid Redox Signal*,

Sykes, M. C., Mowbray, A. L. and Jo, H. (2007) Reversible Glutathiolation of Caspase-3 by Glutaredoxin as a Novel Redox Signaling Mechanism in Tumor Necrosis Factor-alpha-Induced Cell Death. *Circ Res.*, **100**, 152-154.

Szeto, H. H. (2006) Cell-permeable, mitochondrial-targeted, peptide antioxidants. *AAPS J*, **8**, E277-83.

Tai, H.-C., Besche, H., Goldberg, A. L. and Schuman, E. M. (2010) Characterization of the brain 26S proteasome and its interacting proteins. *Frontiers in Molecular Neuroscience*, **3**,

Unal-Cevik, I., Kilinc, M., Can, A., Gursoy-Ozdemir, Y. and Dalkara, T. (2004) Apoptotic and Necrotic Death Mechanisms Are Concomitantly Activated in the Same Cell After Cerebral Ischemia. *Stroke*, **35**, 2189-2194.

Urushitani, M., Kurisu, J., Tateno, M., Hatakeyama, S., Nakayama, K., Kato, S. and Takahashi, R. (2004) CHIP promotes proteasomal degradation of familial ALS-linked mutant SOD1 by ubiquitinating Hsp/Hsc70. *J Neurochem*, **90**, 231-44.

van Leyen, K., Siddiq, A., Ratan, R. R. and Lo, E. H. (2005) Proteasome inhibition protects HT22 neuronal cells from oxidative glutamate toxicity. *J Neurochem*, **92**, 824-830.

Vanhelmont, T., Vandebroek, T., De Vos, A., Terwel, D., Lemaire, K., Anandhakumar, J., Franssens, V., Swinnen, E., Van Leuven, F. and Winderickx, J. (2010) Serine-409 phosphorylation and oxidative damage define aggregation of human protein tau in yeast. *FEMS Yeast Res*, **10**, 992-1005.

Vives-Bauza, C., Zhou, C., Huang, Y., Cui, M., de Vries, R. L., Kim, J., May, J., Tocilescu, M. A., Liu, W., Ko, H. S., Magrane, J., Moore, D. J., Dawson, V. L., Grailhe, R., Dawson, T. M., Li, C., Tieu, K. and Przedborski, S. (2010) PINK1-dependent recruitment of Parkin to mitochondria in mitophagy. *Proc Natl Acad Sci U S A*, **107**, 378-83.

Voisine, C., Pedersen, J. S. and Morimoto, R. I. (2010) Chaperone networks: tipping the balance in protein folding diseases. *Neurobiol Dis*, **40**, 12-20.

von Engelhardt, J., Coserea, I., Pawlak, V., Fuchs, E. C., Köhr, G., Seeburg, P. H. and Monyer, H. (2007) Excitotoxicity in vitro by NR2A- and NR2B-containing NMDA receptors. *Neuropharmacology*, **53**, 10-17.

Wang, L., Chen, Y., Sternberg, P. and Cai, J. (2008) Essential roles of the PI3 kinase/Akt pathway in regulating Nrf2-dependent antioxidant functions in the RPE. *Invest Ophthalmol Vis Sci*, **49**, 1671-1678.

Wang, X. and Defranco, D. B. (2005) Alternative effects of the ubiquitin-proteasome pathway on glucocorticoid receptor down-regulation and transactivation are mediated by CHIP, an E3 ligase. *Mol Endocrinol*, **19**, 1474.

Williams, A. J., Knutson, T. M., Colomer Gould, V. F. and Paulson, H. L. (2009) In vivo suppression of polyglutamine neurotoxicity by C-terminus of Hsp70-interacting protein (CHIP) supports an aggregation model of pathogenesis. *Neurobiol Dis*, **33**, 342-53.

Winkler, D. T., Bondolfi, L., Herzig, M. C., Jann, L., Calhoun, M. E., Wiederhold, K.-H., Tolnay, M., Staufenbiel, M. and Jucker, M. (2001) Spontaneous Hemorrhagic Stroke in a Mouse Model of Cerebral Amyloid Angiopathy. *J. Neurosci.*, **21**, 1619-1627.

Yenari, M. A. (2002) Heat shock proteins and neuroprotection. *Adv Exp Med Biol* **513**, 281-299.

Ying, J., Clavreul, N., Sethuraman, M., Adachi, T. and Cohen, R. A. (2007) Thiol oxidation in signaling and response to stress: Detection and quantification of physiological and pathophysiological thiol modifications. *Free Radic Biol Med*, **43**, 1099-1108.

Zeiger, S. L., McKenzie, J. R., Stankowski, J. N., Martin, J. A., Cliffel, D. E. and McLaughlin, B. (2010) Neuron specific metabolic adaptations following multi-day exposures to oxygen glucose deprivation. *Biochim Biophys Acta*, **1802**, 1095-104.

Zeiger, S. L., Musiek, E. S., Zanoni, G., Vidari, G., Morrow, J. D., Milne, G. J. and McLaughlin, B. (2009) Neurotoxic lipid peroxidation species formed by ischemic stroke increase injury. *Free Radic Biol Med*, **47**, 1422-31.

Zhu, X., Rottkamp, C. A., Boux, H., Takeda, A., Perry, G. and Smith, M. A. (2000) Activation of p38 kinase links tau phosphorylation, oxidative stress, and cell cycle-related events in Alzheimer disease. *J Neuropathol Exp Neurol*, **59**, 880-8.

Ziviani, E. and Whitworth, A. J. (2010) How could Parkin-mediated ubiquitination of mitofusin promote mitophagy? *Autophagy*, **6**,